doi : 10.17596/0003681

R/V MIRAI Cruise Report

MR02-K06 Leg-1

November 13 – December 16, 2002

Japan Marine Science and Technology Center

(JAMSTEC)

R/V Mirai Cruise Report
MR02-K06 Leg-1

[Contents]

1. Introduction

Air-sea interaction is a key factor to understand the atmospheric and oceanic phenomena over the tropical western Pacific warm pool region. Since the huge amount of latent heat released from active convections developed over the warm pool drives meridional (Hadley) and zonal (Walker) circulations, this tropical western Pacific region is often called "heat engine of the globe".

From the past studies, it is well known that atmospheric features over the warm pool are frequently modulated by the 30-60-day intraseasonal oscillation (Madden-Julian Oscillation, Madden and Julian, 1971,1972, J.Atmos.Sci.). This MJO is very attractive phenomenon in terms of El Nino, because many authors have found the relationship between the occurrence /termination of El Nino and the MJO (M.McPhaden, 1999, Science ; Y.Takayabu et al. 1999, Nature). Furthermore, Nakazawa (1988, J.Meteor.Soc.Japan) found the hierarchy of convective systems within the MJO. It stresses the importance of cloud clusters (several 100km horizontal scale, a couple of day life cycle) and super cloud clusters (several 1,000km scale with 7-10 days period) in this region. Based on these past studies, in the current cruise, atmospheric and oceanic variation associated with the MJO was the main target to be studied.

For the purpose above mentioned, stationary observation was conducted at (2N, 138.5E) from November 22 through December 12, 2002. During the intensive observation period, 5cm Doppler weather radar, atmospheric sounding by radiosonde, surface meteorological measurement, CTD casting down to 500m, and ADCP current measurement were carried out as main missions. In addition, turbulent flux measurement, solar radiation measurement, Mie-scattering LIDAR, greenhouse effect gases measurement, and other many observations were intensively conducted.

This cruise report summarizes the observation items and preliminary results are also included. In the first several sections, basic information such as cruise track, onboard personnel list are described. Details of each observation are stated in Section 6. We also attached useful information as Appendix.

Finally it should be noted that since the TRITON buoy which was deployed at (5N, 130E) in last July had started drifting from November 11, we needed to recover it as soon as possible. Because of this emergency, we passed over the area where we had no clearance for scientific observation from relevant countries. Therefore, it was quitted to get data from 1200 UTC on November 19 through 0800 UTC on November 21.

2. Cruise Summary

2.1 Ship

Name	Research Vessel MIRAI
L x B x D	128.6m x 19.0m x 13.2m
Gross Tonnage	8,672 tons
Call Sign	JNSR
Home Port	Mutsu, Aomori Prefecture

2.2 Cruise Code

MR02-K06 (Leg 1)

2.3 Project Name

The Study of the Air-Sea Interaction in the Tropics

2.4 Undertaking Institute

Japan Marine Science and Te chnology Center (JAMSTEC)
2-15, Natsushima, Yokosuka, Kanagawa 237-0061, JAPAN

2.5 Chief Scientist

Kunio YONEYAMA (Ocean Observation and Research Department / JAMSTEC)

2.6 Periods and Ports of Call

Nov. 13, 2002	departed Sekinehama, Japan
Nov. 14, 2002	called at Hachinohe, Japan
Dec. 16, 2002	arrived at Guam, USA

2.7 Observation Summary

5GHz Doppler radar	continuously (1 volume scan=10 min)
Radiosonde	180 times (every 3 hours Nov.22 to Dec.12)
Radiosonde with Snow White hygrometer	15 times
Ceilometer	continuously (every 1 min)
Total Sky Imager	continuously (every 5 min)
Surface Meteorology	continuously
CTD	172 times (every 3 hours Nov.22 to Dec.12)
Water sampling for greenhouse gas measurement	18 times
ADCP	continuously (every 5 min)
Sea surface water monitoring	continuously (every 1 min)
Mie-scattering LIDAR	continuously
Microwave radiometer	continuously
Disdrometer	continuously
23GHz vertical pointing rain radar	continuously
rain sampling	continuously
Ocean colors / solar radiation	occasionally
Turbulent flux	continuously
Gravity / magnetic force / sea bottom depth	continuously in open seas

PCO_2/pCO_2 measurement	continuously
N_2O,NOx,SOx measurement	continuously
ARGO float	3 times

2.8 Overview

First of all, we must mention that TRITON buoy, which was deployed at 5N, 130E in last July, drifted just before this cruise on November 11, so we were requested to recover this drifting buoy. For this reason, we were urged to go to 5N, 135E. Since we had no permission to obtain the data within the EEZ of the Republic of Palau, we quitted to take data from 1200 UTC on November 19 to 0800 UTC on November 21.

At 0000 UTC on November 22, we started the stationary observation at (2N, 138.5E) in order to investigate precipitation mechanism caused by the cloud clusters that are accompanied with MJO (Madden-Julian Oscillation). The stationary observation continued until 1500 UTC on December 12. According to the analysis done by National Oceanic and Atmospheric Administration / Climate Diagnostic Center (http://www.cdc.noaa.gov), the active phase of MJO passed over the observational area in late November. However, we had no significant precipitation cloud systems during this period. It was apparent that this observational period corresponded to convectively suppressed period. Westerly wind dominated in the lower troposphere during the entire cruise period. Sea surface temperature decreased. Since this year corresponds to El Nino year, it is possible that the large-scale environment may result in this inactivity of clouds.

2.9 Acknowledgments

We would like to express our sincere thanks to Captain M.Akamine and his crew for their skillful ship operation. Thanks are extended to technical staff of Global Ocean Development Inc. and Marine Works Japan, Co.Ltd. for their continuous support.

3. List of Instruments

3.1 Atmospheric Profiles

(a) JAMSTEC / Vaisala Radiosonde System
GPS radiosonde: RS-80-GH, Vaisala
Receiver: DigiCORA MW11, Vaisala

(b) JAMSTEC / "SnowWhite" Radiosonde System
Hygrometer: "SnowWhite", Meteolabor AG
GPS radiosonde: RS-80-G, Vaisala
Antenna: Logperiodic antenna, CLP-5130-2, Create
Discorn antenna, D190, Diamond
Pre-Amplifier: LNX-0720, JACOM
Receiver: IC-R8500, ICOM
Recorder: DTC-790, Sony
Modem: KAM98, Kantronix

(c) HyARC, Nagoya Univ.
Microwave Radiometer: TP/WVP-3000, Radiometrics Co.

(d) NASDA / EORC
Microwave Radiometer: WVR26, Radiometrics Co.

(e) JAMSTEC
Ceilometer: CT-25K, Vaisala

(a) NIES / Tohoku Institute of Technology
Compact Mie Scattering Lidar

3.2 RainClouds and RainWater

(a) JAMSTEC
C-band Doppler Radar: RC-52B, Mitsubishi Electric Co.
Signal Processor: RVP-7, Sigmet Inc.
Antenna Controller: RCP-02, Sigmet Inc.
Control and Processing Software: IRIS/Open, Sigmet Inc.
Inertial Navigation Unit: DRUH, Honeywell

(b) NASDA / EORC
Micro Rain Radar: MRR-2, METEK GmbH

(c) HyARC, Nagoya Univ.
Disdrometer: RD-69, Disdromet

3.3 Solar Radiation and Aerosols

(a) Osaka Univ, Kinki Univ and MUK
Polarization spercral radiometer: PSR-1000, Opto Research Corp.

(b) ILTS, Hokkaido Univ.
Sky Radiometer: POM-01MK2, Prede

3.4 Surface Atmospheric Turbulent Flux

(a) FORSGC and Okayama Univ.
Supersonic Thermoanemometer: DA-600, Kaijo Co.
Infrared Hygrometer: AH-300, Kaijo Co.
Inclinometer: MD-900-T, Appied Geomechanics
Accelerometer: OA700-020, Applied Signal Inc.
Rate Gyros: QRS-0050-100, Sytron Donner
CO2/H2O turbulence sensor: LI-7500, LICOR
Data Logging System: Labview, National Intsruments Co.

3.5 Surface Meteorological Parameters

(a) JAMSTEC / Mirai Met System
Anemometer: KE-500, Koshin Denki
Thermometer: FT, Koshin Denki
Dewpoint Meter DW-1, Koshin Denki
Barometer: F-451, Yokogawa Co.
Rain Gauge: 50202, R.M. Young
Optical Rain Gauge: ORG-115DR, SCTI
Shortwave Radiometer: MS-801, Eiko Seiki
Longwave Radiometer: MS-200, Eiko Seiki
Wave Height Meter: MW-2, Tsurumi-seiki

(b) JAMSTEC / SOAR system
Anemometer: 05106, R. M. Young
Thermometer / Hygrometer: HMP45A, Vaisala
(with 43408 Gill aspirated radiation shield, R.M.Young)
Barometer: 61201, R. M. Young
Rain Gauge: 50202, R. M. Young
Optical Rain Gauge: ORG-115DA, ScTi
Sea Surface Skin Tempreature Sensor: SST-100, Brookhaven National Lab.
TRFN1-0, Koshin Denki, Japan
FT, Koshin Denki, Japan
Shortwave Radiometer: PSP, Eppley Labs.
Longwave Radiometer: PIR, Eppley Labs.
Fast Rotating Shadowband Radiometer: Yankee Engineering Systems
Shortwave Radiometer (upwelling radiation): MS-801, Eiko Seiki
Longwave Radiometer (upwelling radiation): MS-202, Eiko Seiki

(c) JAMSTEC / Total Sky Imager System
Total Sky Imager: Yankee Engineering System

3.6 Greenhouse Effect Gases

(a) MUK
N_2O analyzer: Model 46C, Thermo Environmental Instruments Inc.
CO_2 analyzer: Model VIA-510, HORIBA Ltd.
NOx analyzer: Model 42C-TL, Thermo Environmental Instruments Inc.
N_2O analyzer: Model 43C, Thermo Environmental Instruments Inc.

(b) MRI
Infrared Gas Analyzer: model 4.1, BINOS
CO_2 Coulometer: Model 5012, UIC Inc.

(c) OUS
CO_2 analyzer: Model LI-6252 LI-COR, INC.
Gas mixing unit: Model SO96NL-T, S-ONE, INC.
Equilibrumeter: Model SO96NL-T, S-ONE, INC.
Coulometer: Model5012, UIC Inc.
Titration Manager: TIM900, Radiometer
Auto-Burette: ABU901, Radiometer
pH glass electrode: pHG201-7, Radiometer
Reference operating software: Tim Talk9, Lab Soft

3.7 Ocean Color

(a) MUK, Okayama Univ, Toba-CMT and Kinki Univ.
Polarization Spectral Radiometer: PSR1000, Opto Research Co.
Spectroradiometer: GER1500, Geophysical & Environmental Research Co.
Thermalinfrared Radiometer: CE312, CIMEL Electronique

3.8 Sea Surface Water Monitoring

(a) JAMSTEC
Thermosalinograph: SBE-21, Sea-Bird Electronics, Inc.
Thermometer: SBE3S, Sea-Bird Electronics, Inc.
Dissolved Oxygen Sensor: 2127, Oubisufair Laboratories
Fluorometer: 10-AU-005, Turner Designs
Particle Size Sensor: P-05, Nippon Kaiyo Ltd.
Flowmeter: EMARG2W, Aichi Watch Electronics Ltd.

3.9 Ocean Profiling

(a) JAMSTEC / CTD casts
CTD system: CTD 9plus, Sea-Bird
Temperature Sensor: SBE3-04F, Sea-Bird Electronics, Inc.
Conductivity Sensor: SBE4-04/0, Sea-Bird Electronics, Inc.
Dissolved Oxygen Sensor: SBE43, Sea-Bird Electronics, Inc.
Deck Unit: SBE11, Sea-Bird Electronics, Inc.
Carousel water sampler: SBE32, Sea-Bird Electronics, Inc.

(b) JAMSTEC / Analyses of sampled water
Guildline Autosal salinometer:model 8400B
Software: SEASOFT ver. 4.232, Sea-Bird Electronics, Inc.
Titrator: Metrohm Model 716 DMS Titrino / 10 ml of titration vessel
Metrohm Pt Electrode / 6.0403.100 (NC)
Software: "The Brinkmann Titrino Workcell"

(b) MUK
Shallow-water measurement unit: Chlorothec ACL-220-RS, Alec Electronics Co.

(c) JAMSTEC / Shipboard Acoustic Doppler Current Profiler
Broad-Band ADCP: VM-75, RD Instrument.
GPS Naviation Receiver: MX9400, Leica

(d) JAMSTEC and FORSGC
ARGO float: APEX, Webb Research Ltd.

3.10 Underway geophysics

(a) JAMSTEC
Onboard Gravity Meter: S-116, LaCoste-Romberg
Three-Axes Fluxgate Magnetometer: Tierra Tecnica
Multi-Narrow beam echo sounding system: SeaBeam 2100, SeaBeam Inc.

3.11 Miscellaneous

(a) JAMSTEC
Navigation System: SAINS19, Sena Co.
GMS Receiving System: Nippon Hakuyo
HRPT Receiving System: Terascan
Observation Data Acquisition System: SCS (Scientific Computer System), NOAA

4. Cruise Track and Log

4.1 Cruise Track

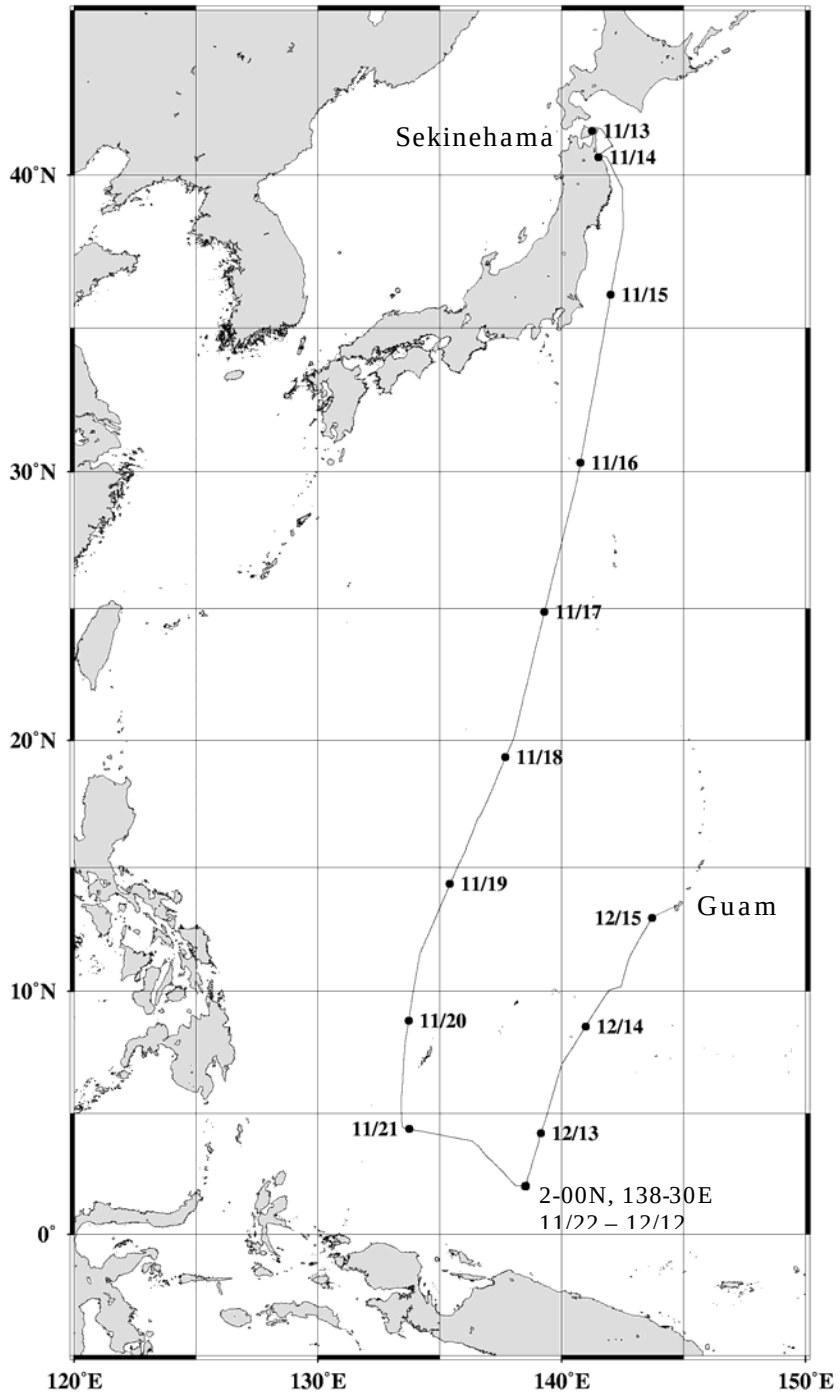

Fig. 4.1-1: MR02-K06 Leg-1 ship track. Labeled position is at 0000UTC of each day.

4.2 Cruise Log

Date	start (LST)	finish	Event	Lat.(deg.)	Lon. (deg.)
13-Nov	14:00		depart Sekinehama		
14-Nov	09:00		arrive Hachinohe		
	13:30		depart Hachinohe		
	18:20		start surface water monitoring		
15-Nov	21:00		start Doppler radar observation		
16-Nov	10:22	11:18	CTD-001 [1000m]	30.00 N	140.68 E
17-Nov	07:25	08:18	CTD-002 [1000m]	25.00 N	139.32 E
18-Nov	05:03	05:56	CTD-003 [1000m]	20.00 N	137.99 E
	08:29		launch radiosonde (RS -001)	19.46 N	137.74 E
	14:29		RS-002	18.09 N	137.14 E
	20:26		launch "SnowWhite" radiosonde (SW-01)	17.00 N	136.63 E
	20:29		RS-003	16.98 N	136.58 E
19-Nov	02:39		RS-004	15.71 N	136.07 E
	08:40		RS-005	14.41 N	135.43 E
	14:29		RS-006	13.09 N	134.86 E
	20:30		RS-007	11.72 N	134.26 E
	21:00		pause all observation		
20-Nov					
21-Nov	08:00	09:00	recover drifting TRITON buoy	4.39 N	133.57 E
	17:00		restart observation		
	20:30		RS-008	3.67 N	136.53 E
	23:40		RS-009	3.08 N	137.08 E
22-Nov	02:29		RS-010	2.58 N	137.59 E
	05:30		RS-011	2.06 N	138.07 E
	05:41		check TRITON buoy	2.00 N	138.11 E
	08:00		arrive stationary observation point (2N, 138.5E)	2.00 N	138.50 E
			start stationary observation		
	08:29		RS-012		
	08:31	09:50	CTD-004 [2000m]		
	09:58	10:11	shallow-water CTD casting to 200m depth (CT-001)		
	10:14		deploy ARGO float	1.98 N	138.52 E
	10:30	11:20	turbulent flux observation		
	11:29		RS-013		
	11:27	11:54	CTD-005 [500m]		
	11:58	12:14	CT-002		
	12:14	14:20	turbulent flux observation		
	14:29		RS-014		
	14:26	14:54	CTD-006 [500m]		
	14:58	15:12	CT-003		
	15:12	16:20	turbulent flux observation		
	17:29		RS-015		
	17:29	17:55	CTD-007 [500m]		
	18:00	18:14	CT-004		
	18:15	19:23	turbulent flux observation		
	20:15		SW-02		
	20:28	21:28	CTD-008 [1500m]		
	20:50		RS-016		
	21:32	21:46	CT-005		
	21:55	23:00	turbulent flux observation		
	23:31		RS-017		
	23:30	00:00	CTD-009 [500m]		

23-Nov	00:06	00:21	CT-006
	00:21	02:25	turbulent flux observation
	02:30		RS-018
	02:32	02:56	CTD-010 [500m]
	03:00	03:15	CT-007
	03:15	05:20	turbulent flux observation
	05:29		RS-019
	05:31	05:54	CTD-011 [500m]
	05:58	06:12	CT-008
	06:12	07:40	turbulent flux observation
	08:29		RS-020
	08:30	08:53	CTD-012 [500m]
	08:56	09:11	CT-009
	09:11	10:40	turbulent flux observation
	11:29		RS-021
	11:28	11:52	CTD-013 [500m]
	11:56	12:10	CT-010
	12:10	13:35	turbulent flux observation
	14:29		RS-022
	14:25	14:54	CTD-014 [500m]
	14:55	15:10	CT-011
	15:10	16:48	turbulent flux observation
	17:24	17:49	CTD-015 [500m]
	17:50		RS-023
	17:53	18:10	CT-012
	18:10	19:32	turbulent flux observation
	20:20		SW-03
	20:29		RS-024
	20:30	21:27	CTD-016 [1000m]
	21:29	21:44	CT-013
	21:44	22:40	turbulent flux observation
	23:29		RS-025
	23:30	23:57	CTD-017 [500m]
24-Nov	00:00	00:14	CT-014
	00:14	01:40	turbulent flux observation
	02:30		RS-026
	02:30	02:55	CTD-018 [500m]
	02:58	03:13	CT-015
	03:13	04:55	turbulent flux observation
	05:29		RS-027
	05:30	05:54	CTD-019 [500m]
	05:58	06:12	CT-016
	06:12	07:48	turbulent flux observation
	08:29		RS-028
	08:30	09:32	CTD-020 [1000m]
	09:35	09:50	CT-017
	09:50	10:50	turbulent flux observation
	11:29		RS-029
	11:25	11:50	CTD-021 [500m]
	11:53	12:09	CT-018
	12:09	13:43	turbulent flux observation
	14:29		RS-030
	14:30	14:52	CTD-022 [500m]
	14:55	15:11	CT-019
	15:11	16:48	turbulent flux observation
	17:29		RS-031
	17:30	17:53	CTD-023 [500m]
	17:55	18:10	CT-020
	18:10	19:41	turbulent flux observation
	20:29		RS-032
	20:31		SW-04
	20:32	21:26	CTD-024 [1000m]
	21:29	21:45	CT-021
	21:45	22:50	turbulent flux observation
	23:49		RS-033

	23:27	23:55	CTD-025 [500m]
	23:59	00:15	CT-022
25-Nov	00:15	01:55	turbulent flux observation
	02:29		RS-034
	02:30	02:56	CTD-026 [500m]
	03:00	03:15	CT-023
	03:15	04:54	turbulent flux observation
	05:29		RS-035
	05:30	05:55	CTD-027 [500m]
	05:59	06:13	CT-024
	06:13	07:50	turbulent flux observation
	08:29		RS-036
	08:29	08:53	CTD-028 [500m]
	08:55	09:10	CT-025
	09:10	10:50	turbulent flux observation
	11:29		RS-037
	11:27	11:51	CTD-029 [500m]
	11:55	12:10	CT-026
	12:10	13:42	turbulent flux observation
	14:29		RS-038
	14:27	14:55	CTD-030 [500m]
	14:56	15:14	CT-027
	15:14	16:33	turbulent flux observation
	17:29		RS-039
	17:27	17:53	CTD-031 [500m]
	17:55	18:12	CT-028
	18:12	19:40	turbulent flux observation
	20:30		RS-040
	20:28	21:13	CTD-032 [1000m]
	21:16	21:32	CT-029
	21:32	22:55	turbulent flux observation
	23:29		RS-041
	23:28	23:58	CTD-033 [500m]
26-Nov	00:00	00:17	CT-030
	00:17	01:53	turbulent flux observation
	02:32	03:00	CTD-034 [500m]
	02:59		RS-042
	03:04	03:20	CT-031
	03:20	04:44	turbulent flux observation
	05:29		RS-043
	05:30	05:56	CTD-035 [500m]
	06:00	06:15	CT-032
	06:15	07:40	turbulent flux observation
	08:29		RS-044
	08:27	09:08	CTD-036 [500m]
	09:11	09:26	CT-033
	09:26	10:40	turbulent flux observation
	11:29		RS-045
	11:28	11:53	CTD-037 [500m]
	11:55	12:11	CT-034
	12:11	13:43	turbulent flux observation
	14:29		RS-046
	14:27	14:54	CTD-038 [500m]
	15:00	15:15	CT-035
	15:15	16:40	turbulent flux observation
	17:29		RS-047
	17:27	17:52	CTD-039 [500m]
	17:54	18:10	CT-036
	18:10	19:35	turbulent flux observation
	20:35		SW-05
	20:36	21:26	CTD-040 [1000m]
	21:01		RS-048
	21:29	21:44	CT-037
	21:44	22:50	turbulent flux observation
	23:29		RS-049
	23:30	23:56	CTD-041 [500m]

	23:59	00:15	CT-038
27-Nov	00:15	01:45	turbulent flux observation
	02:49		RS-049
	02:30	02:54	CTD-042 [500m]
	02:57	03:13	CT-039
	03:13	04:43	turbulent flux observation
	05:39		RS-050
	05:32	05:58	CTD-043 [500m]
	06:02	06:16	CT-040
	06:16	07:40	turbulent flux observation
	08:30		RS-051
	08:30	09:10	CTD-044 [500m]
	09:13	09:32	CT-041
	09:32	10:40	turbulent flux observation
	11:29		RS-052
	11:27	11:52	CTD-045 [500m]
	11:55	12:11	CT-042
	12:11	13:35	turbulent flux observation
	14:29		RS-053
	14:27	14:52	CTD-046 [500m]
	14:54	15:10	CT-043
	15:10	16:40	turbulent flux observation
	17:30		RS-054
	17:27	17:53	CTD-047 [500m]
	17:55	18:10	CT-044
	18:10	19:40	turbulent flux observation
	20:18		SW-06
	20:29		RS-055
	20:27	21:08	CTD-048 [1000m]
	21:10	21:26	CT-045
	21:26	22:50	turbulent flux observation
	23:29		RS-056
	23:28	23:55	CTD-049 [500m]
28-Nov	00:00	00:16	CT-046
	00:16	01:50	turbulent flux observation
	02:29		RS-057
	02:30	02:55	CTD-050 [500m]
	02:59	03:14	CT-047
	03:14	04:50	turbulent flux observation
	05:29		RS-058
	05:30	05:55	CTD-051 [500m]
	05:58	06:14	CT-048
	06:14	07:45	turbulent flux observation
	08:29		RS-059
	08:27	09:25	CTD-052 [1000m]
	09:27	09:43	CT-049
	09:43	10:46	turbulent flux observation
	11:29		RS-060
	11:27	11:52	CTD-053 [500m]
	11:54	12:11	CT-050
	12:11	13:40	turbulent flux observation
	14:29		RS-061
	14:32	14:56	CTD-054 [500m]
	14:59	15:15	CT-051
	15:15	16:40	turbulent flux observation
	17:29		RS-062
	17:28	17:52	CTD-055 [500m]
	17:55	18:14	CT-052
	18:14	19:42	turbulent flux observation
	20:25		SW-07
	20:29		RS-063
	20:30	21:25	CTD-056 [1000m]
	21:28	21:44	CT-053
	21:44	22:50	turbulent flux observation
	23:29		RS-064
	23:30	23:57	CTD-057 [500m]

29-Nov	00:00	00:16	CT-054
	00:16	01:45	turbulent flux observation
	02:29		RS-065
	02:30	02:55	CTD-058 [500m]
	02:58	03:13	CT-055
	03:13	04:45	turbulent flux observation
	05:29		RS-066
	05:29	05:55	CTD-059 [500m]
	05:58	06:14	CT-056
	06:14	07:45	turbulent flux observation
	08:29		RS-067
	08:28	08:52	CTD-060 [500m]
	08:54	09:09	CT-057
	09:09	10:46	turbulent flux observation
	11:29		RS-068
	11:27	11:52	CTD-061 [500m]
	11:55	12:10	CT-058
	12:10	12:55	turbulent flux observation
	14:29		RS-069
	14:27	14:54	CTD-062 [500m]
	14:58	15:13	CT-059
	15:13	16:48	turbulent flux observation
	17:29		RS-070
	17:27	17:53	CTD-063 [500m]
	17:56	18:13	CT-060
	18:13	19:30	turbulent flux observation
	20:21		SW-08
	20:30		RS-071
	20:27	21:09	CTD-064 [1000m]
	21:11	21:26	CT-061
	21:26	22:50	turbulent flux observation
	23:29		RS-072
	23:29	23:55	CTD-065 [500m]
	23:57	00:14	CT-062
30-Nov	00:14	01:43	turbulent flux observation
	02:29		RS-073
	02:30	02:54	CTD-066 [500m]
	02:57	03:12	CT-063
	03:12	04:36	turbulent flux observation
	05:29		RS-074
	05:30	05:54	CTD-067 [500m]
	05:57	06:13	CT-064
	06:13	07:46	turbulent flux observation
	08:29		RS-075
	08:28	09:07	CTD-068 [500m]
	09:10	09:25	CT-065
	09:25	10:50	turbulent flux observation
	11:29		RS-076
	11:27	11:54	CTD-069 [500m]
	11:56	12:12	CT-066
	12:12	13:47	turbulent flux observation
	14:29		RS-077
	14:27	14:52	CTD-070 [500m]
	14:54	15:11	CT-067
	15:11	16:45	turbulent flux observation
	17:29		RS-078
	17:27	17:52	CTD-071 [500m]
	17:55	18:10	CT-068
	18:10	19:40	turbulent flux observation
	20:20		SW-09
	20:29		RS-079
	20:27	21:20	CTD-072 [1000m]
	21:23	21:39	CT-069
	21:39	22:45	turbulent flux observation
	23:29		RS-080
	23:30	23:57	CTD-073 [500m]

1-Dec	00:00	00:16	CT-070
	00:16	01:40	turbulent flux observation
	02:29		RS-081
	02:30	02:56	CTD-074 [500m]
	03:00	03:16	CT-071
	03:16	04:40	turbulent flux observation
	05:29		RS-082
	05:30	05:55	CTD-075 [500m]
	05:58	06:14	CT-072
	06:14	07:40	turbulent flux observation
	08:30		RS-083
	08:27	09:06	CTD-076 [500m]
	09:09	09:25	CT-073
	09:25	10:30	turbulent flux observation
	11:29		RS-084
	11:27	11:52	CTD-077 [500m]
	11:55	12:12	CT-074
	12:12	13:40	turbulent flux observation
	14:29		RS-085
	14:27	14:52	CTD-078 [500m]
	14:55	15:10	CT-075
	15:10	16:45	turbulent flux observation
	17:29		RS-086
	17:27	17:52	CTD-079 [500m]
	17:55	18:10	CT-076
	18:10	19:37	turbulent flux observation
	20:16		SW-10
	20:29		RS-087
	20:30	21:10	CTD-080 [1000m]
	21:13	21:28	CT-077
	21:28	22:50	turbulent flux observation
	23:29		RS-088
	23:30	23:54	CTD-081 [500m]
	23:57	00:13	CT-078
2-Dec	00:13	01:40	turbulent flux observation
	02:29		RS-089
	02:30	02:55	CTD-082 [500m]
	02:58	03:14	CT-079
	03:14	04:45	turbulent flux observation
	05:31		RS-090
	05:27	05:54	CTD-083 [500m]
	05:57	06:12	CT-080
	06:12	07:45	turbulent flux observation
	08:29		RS-091
	08:27	09:23	CTD-084 [1000m]
	09:26	09:41	CT-081
	09:41	10:35	turbulent flux observation
	11:29		RS-092
	11:27	11:53	CTD-085 [500m]
	11:56	12:12	CT-082
	12:12	13:40	turbulent flux observation
	14:29		RS-093
	14:27	14:51	CTD-086 [500m]
	14:53	15:08	CT-083
	15:08	16:46	turbulent flux observation
	17:29		RS-094
	17:27	17:53	CTD-087 [500m]
	17:57	18:12	CT-084
	18:12	19:38	turbulent flux observation
	20:29		RS-095
	20:39		SW-11
	20:40	21:33	CTD-088 [1000m]
	21:36	21:52	CT-085
	21:52	22:48	turbulent flux observation
	23:29		RS-096
	23:30	23:54	CTD-089 [500m]

	23:57	00:12	CT-086
3-Dec	00:12	01:40	turbulent flux observation
	02:29		RS-097
	02:30	02:55	CTD-090 [500m]
	02:58	03:12	CT-087
	03:12	04:45	turbulent flux observation
	05:29		RS-098
	05:27	05:52	CTD-091 [500m]
	05:54	06:10	CT-088
	06:10	07:45	turbulent flux observation
	08:29		RS-099
	08:27	08:51	CTD-092 [500m]
	08:54	09:10	CT-089
	09:10	10:40	turbulent flux observation
	11:29		RS-100
	11:27	11:51	CTD-093 [500m]
	11:54	12:10	CT-090
	12:10	13:30	turbulent flux observation
	14:29		RS-101
	14:27	14:54	CTD-094 [500m]
	14:57	15:11	CT-091
	15:11	16:43	turbulent flux observation
	17:29		RS-102
	17:27	17:52	CTD-095 [500m]
	17:55	18:10	CT-092
	18:10	19:38	turbulent flux observation
	20:17		SW-12
	20:29		RS-103
	20:30	21:17	CTD-096 [1000m]
	21:20	21:35	CT-093
	21:35	22:47	turbulent flux observation
	23:29		RS-104
	23:50	23:54	CTD-097 [500m]
	23:56	00:12	CT-094
4-Dec	00:12	01:43	turbulent flux observation
	02:29		RS-105
	02:30	02:55	CTD-098 [500m]
	02:58	03:12	CT-095
	03:12	04:44	turbulent flux observation
	05:29		RS-106
	05:27	05:52	CTD-099 [500m]
	05:55	06:10	CT-096
	06:10	07:42	turbulent flux observation
	08:29		RS-107
	08:27	09:05	CTD-100 [500m]
	09:08	09:26	CT-097
	09:26	10:40	turbulent flux observation
	11:30		RS-108
	11:27	11:52	CTD-101 [500m]
	11:54	12:10	CT-098
	12:10	13:43	turbulent flux observation
	14:29		RS-109
	14:27	14:52	CTD-102 [500m]
	14:54	15:08	CT-099
	15:08	16:44	turbulent flux observation
	17:30		RS-110
	17:27	17:53	CTD-103 [500m]
	17:55	18:10	CT-100
	18:10	19:40	turbulent flux observation
	20:29		RS-111
	20:45		SW-13
	20:31	21:26	CTD-104 [1000m]
	21:29	21:45	CT-101
	21:45	22:40	turbulent flux observation
	23:29		RS-112
	23:30	23:55	CTD-105 [500m]

	23:58	00:14	CT-102
5-Dec	00:14	01:44	turbulent flux observation
	02:29		RS-113
	02:30	02:54	CTD-106 [500m]
	02:57	03:11	CT-103
	03:11	04:38	turbulent flux observation
	05:29		RS-114
	05:27	05:53	CTD-107 [500m]
	05:55	06:10	CT-104
	06:10	07:37	turbulent flux observation
	08:29		RS-115
	08:27	09:07	CTD-108 [500m]
	09:10	09:25	CT-105
	09:25	10:40	turbulent flux observation
	11:29		RS-116
	11:27	11:52	CTD-109 [500m]
	11:54	12:10	CT-106
	12:10	13:43	turbulent flux observation
	14:27	14:51	CTD-110 [500m]
	15:00		RS-117
	14:54	15:10	CT-107
	15:10	16:40	turbulent flux observation
	17:29		RS-118
	17:27	17:41	CTD-111 [500m]
	17:58	18:13	CT-108
	18:13	19:38	turbulent flux observation
	20:29		SW-14
	20:29		RS-119
	20:44	20:59	CT-109
	21:07	21:37	CTD-112 [500m]
	21:37	22:50	turbulent flux observation
	23:29		RS-120
	23:30	23:54	CTD-113 [500m]
	23:57	00:11	CT-110
6-Dec	00:11	01:43	turbulent flux observation
	02:29		RS-121
	02:30	02:56	CTD-114 [500m]
	02:58	03:14	CT-111
	03:14	04:40	turbulent flux observation
	05:29		RS-122
	05:27	05:52	CTD-115 [500m]
	05:54	06:12	CT-112
	06:12	07:42	turbulent flux observation
	08:29		RS-123
	08:27	09:22	CTD-116 [1000m]
	09:25	09:40	CT-113
	09:40	10:42	turbulent flux observation
	11:29		RS-124
	11:27	11:51	CTD-117 [500m]
	11:53	12:08	CT-114
	12:08	13:44	turbulent flux observation
	14:29		RS-125
	14:27	14:53	CTD-118 [500m]
	14:55	15:10	CT-115
	15:10	16:20	turbulent flux observation
	17:29		RS-126
	17:27	17:52	CTD-119 [500m]
	17:55	18:09	CT-116
	18:09	19:37	turbulent flux observation
	20:29		RS-127
	20:32		SW-15
	20:35	21:29	CTD-120 [1000m]
	21:32	21:47	CT-117
	21:47	22:47	turbulent flux observation
	23:29		RS-128
	23:30	23:54	CTD-121 [500m]

	23:56	00:11	CT-118
7-Dec	00:11	01:46	turbulent flux observation
	02:29		RS-129
	02:30	02:53	CTD-122 [500m]
	02:56	03:10	CT-119
	02:10	04:38	turbulent flux observation
	05:29		RS-130
	05:27	05:52	CTD-123 [500m]
	05:55	06:10	CT-120
	06:10	07:35	turbulent flux observation
	08:30		RS-131
	08:27	08:52	CTD-124 [500m]
	08:54	09:09	CT-121
	09:09	10:23	turbulent flux observation
	11:29		RS-132
	11:27	11:51	CTD-125 [500m]
	11:55	12:09	CT-122
	12:09	13:41	turbulent flux observation
	14:29		RS-133
	14:27	14:53	CTD-126 [500m]
	14:55	15:09	CT-123
	15:09	16:48	turbulent flux observation
	17:29		RS-134
	17:29	17:52	CTD-127 [500m]
	17:55	18:11	CT-124
	18:11	19:45	turbulent flux observation
	20:29		RS-135
	20:30	21:13	CTD-128 [1000m]
	21:16	21:31	CT-125
	21:31	22:47	turbulent flux observation
	23:29		RS-136
	23:30	23:54	CTD-129 [500m]
	23:57	00:13	CT-126
8-Dec	00:13	01:43	turbulent flux observation
	02:29		RS-137
	02:30	02:55	CTD-130 [500m]
	02:59	03:14	CT-127
	03:14	04:40	turbulent flux observation
	05:29		RS-138
	05:27	05:52	CTD-131 [500m]
	05:56	06:11	CT-128
	06:11	07:40	turbulent flux observation
	08:29		RS-139
	08:27	09:07	CTD-132 [500m]
	09:10	09:26	CT-129
	09:26	10:41	turbulent flux observation
	11:29		RS-140
	11:27	11:53	CTD-133 [500m]
	11:56	12:10	CT-130
	12:10	13:40	turbulent flux observation
	14:29		RS-141
	14:27	14:55	CTD-134 [500m]
	14:57	15:12	CT-131
	15:12	16:40	turbulent flux observation
	17:29		RS-142
	17:27	17:54	CTD-135 [500m]
	17:56	18:12	CT-132
	18:12	19:37	turbulent flux observation
	20:29		RS-143
	20:30	21:27	CTD-136 [1000m]
	21:30	21:45	CT-133
	21:45	22:50	turbulent flux observation
	23:29		RS-144
	23:30	23:59	CTD-137 [500m]
9-Dec	00:02	00:17	CT-134
	00:17	01:40	turbulent flux observation

	02:50		RS-145
	02:30	02:32	CTD-138 [500m]
	02:59	03:13	CT-135
	03:13	04:38	turbulent flux observation
	05:29		RS-146
	05:27	05:54	CTD-139 [500m]
	05:56	06:11	CT-136
	06:11	07:45	turbulent flux observation
	08:39		RS-147
	08:27	09:05	CTD-140 [500m]
	09:07	09:22	CT-137
	09:22	10:47	turbulent flux observation
	11:29		RS-148
	11:27	11:52	CTD-141 [500m]
	11:54	12:10	CT-138
	12:10	13:43	turbulent flux observation
	14:29		RS-149
	14:27	14:53	CTD-142 [500m]
	14:56	15:10	CT-139
	15:10	16:40	turbulent flux observation
	17:29		RS-150
	17:27	17:52	CTD-143 [500m]
	17:54	18:10	CT-140
	18:10	19:30	turbulent flux observation
	20:29		RS-151
	20:30	21:14	CTD-144 [1000m]
	21:17	21:32	CT-141
	21:32	22:45	turbulent flux observation
	23:29		RS-152
	23:30	23:54	CTD-145 [500m]
	23:57	00:12	CT-142
10-Dec	00:12	01:45	turbulent flux observation
	02:29		RS-153
	02:30	02:54	CTD-146 [500m]
	02:57	03:12	CT-143
	03:12	04:35	turbulent flux observation
	05:29		RS-154
	05:27	05:52	CTD-147 [500m]
	05:55	06:10	CT-144
	06:10	07:45	turbulent flux observation
	08:29		RS-155
	08:27	09:22	CTD-148 [1000m]
	09:24	09:39	CT-145
	09:39	10:52	turbulent flux observation
	11:41		RS-156
	11:27	11:51	CTD-149 [500m]
	11:54	12:10	CT-146
	12:10	13:38	turbulent flux observation
	14:27	14:52	CTD-150 [500m]
	15:00		RS-157
	14:55	15:10	CT-147
	15:10	16:37	turbulent flux observation
	17:29		RS-158
	17:27	17:52	CTD-151 [500m]
	17:55	18:10	CT-148
	18:10	19:45	turbulent flux observation
	20:29		RS-159
	20:30	21:29	CTD-152 [1000m]
	21:32	21:48	CT-149
	21:48	22:55	turbulent flux observation
	23:29		RS-160
	23:30	23:56	CTD-153 [500m]
	23:58	00:15	CT-150
11-Dec	00:15	01:45	turbulent flux observation
	02:29		RS-161
	02:30	02:43	CTD-154 [500m]

	03:00	03:15	CT-151					
	03:15	04:40	turbulent flux observation					
	05:29		RS-162					
	05:27	05:53	CTD-155 [500m]					
	05:57	06:11	CT-152					
	06:11	07:43	turbulent flux observation					
	08:29		RS-163					
	09:06	09:34	CTD-156 [500m]					
	09:37	09:51	CT-153					
	09:51	10:32	turbulent flux observation					
	11:29		RS-164					
	11:27	11:52	CTD-157 [500m]					
	11:55	12:10	CT-154					
	12:10	13:45	turbulent flux observation					
	14:30		RS-165					
	14:27	14:55	CTD-158 [500m]					
	14:57	15:11	CT-155					
	15:11	16:40	turbulent flux observation					
	17:29		RS-166					
	17:27	17:52	CTD-159 [500m]					
	17:56	18:10	CT-156					
	18:10	19:45	turbulent flux observation					
	20:29		RS-167					
	20:30	21:14	CTD-160 [1000m]					
	21:17	21:32	CT-157					
	21:32	22:46	turbulent flux observation					
	23:29		RS-168					
	23:30	23:55	CTD-161 [500m]					
	23:58	00:13	CT-158					
12-Dec	00:13	01:45	turbulent flux observation					
	02:30		RS-169					
	02:30	02:55	CTD-162 [500m]					
	02:58	03:14	CT-151					
	03:14	04:40	turbulent flux observation					
	05:29		RS-170					
	05:27	05:52	CTD-163 [500m]					
	05:54	06:09	CT-152					
	06:09	07:40	turbulent flux observation					
	08:30		RS-171					
	08:27	08:53	CTD-164 [500m]					
	08:55	09:10	CT-153					
	09:10	10:40	turbulent flux observation					
	11:29		RS-172					
	11:27	11:52	CTD-165 [500m]					
	11:55	12:10	CT-154					
	12:10	13:33	turbulent flux observation					
	14:29		RS-173					
	14:27	14:52	CTD-166 [500m]					
	14:54	15:10	CT-155					
	15:10	16:37	turbulent flux observation					
	17:29		RS-174					
	17:27	17:41	CTD-167 [500m]					
	17:55	18:10	CT-156					
	18:10	19:42	turbulent flux observation					
	20:29		RS-175					
	20:27	21:27	CTD-168 [1000m]					
	21:29		CT-157					
	21:44	22:45	turbulent flux observation					
	23:30		RS-176					
	23:30	23:55	CTD-169 [500m]					
	23:58	00:13	CT-158					
13-Dec			finish stationary observation					
	02:30		RS-177	2.50	N	138.67	E	
	05:29		RS-178	3.24	N	138.88	E	
	08:29		RS-179	4.02	N	139.09	E	
	12:27	13:43	CTD-170 [2000m]	5.00	N	139.42	E	

	13:43		deploy ARGO float	5.01	N	139.41	E
	22:08	23:02	CTD-171 [1000m]	7.00	N	140.00	E
	23:58	01:22	CTD-172 [2000m]	7.01	N	139.99	E
14-Dec	01:27		deploy ARGO float	7.01	N	139.99	E
	09:10		finish Doppler radar observation				
	22:00		adjust LST ([UTC+9h] to [UTC+10h])				
15-Dec			finish sea surface water monitoring				
16-Dec	08:30		arrive Guam				

5. Participants List

5.1 On Board Scientists / Engineer / Technical Staff

Name	Affiliation
Yoneyama, Kunio	JAMSTEC
Katsumata, Masaki	JAMSTEC
Chuda, Takashi	FORSGC
Shinoda, Taro	HyARC, Nagoya Univ.
Takahashi, Chiharu	HyARC, Nagoya Univ.
Matsui, Ichiro	NIES
Takemi, Tetsuya	Osaka Univ.
Inoue, Jun	Osaka Univ.
Tanaka, Masatsugu	Osaka Univ.
Shibuya, Takehiro	Osaka Univ.
Hayashi, Mitsuru	MUK
Miyake, Jun	MUK
Nakagawa, Masakazu	MUK
Sanjiki, Ryutaro	Kinki Univ.
Shiozaki, Takuhei	Osaka Pref. Univ.
Takahashi, Satoshi	Okayama Univ.
Kouno, Takehiko	Okayama Univ.
Harada, Kyoko	Okayama Univ.
Takami, Jinsuke	Okayama Univ.
Taniguchi, Daisuke	Okayama Univ.
Yamashita, Eiji	Okayama Univ. of Sci.
Machida, Tomohiko	Okayama Univ. of Sci.
Goto, Koichi	KEEC
Hanyu, Masaki	GODI
Sueyoshi, Souichiro	GODI
Nagahama, Norio	GODI
Sagishima, Katsunori	MWJ
Ozawa, Satoshi	MWJ
Inoue, Asako	MWJ
Takahashi, Naoko	MWJ
Sugiyama, Tomohiko	MWJ
Moro, Masaki	MWJ
Umetsu, Nozomi	MWJ
Hisatsune, Yoshiyuki	MWJ

Japan Marine Science and Technology Center (JAMSTEC)
Frontier Observational Research System for Global Change (FORSGC)
Natsushima-cho 2-15, Yokosuka 237-0061 JAPAN
TEL: +81-46-866-3811

Hydrospheric Atmospheric Research Center (HyARC), Nagoya Univ.
Furo-cho, Chigusa-ward, Nagoya 464-8601 JAPAN

National Institute of Environmental Studies (NIES)
16-2, Onogawa, Tsukuba, Ibaraki 305-0053 JAPAN

Osaka University
2-1, Yamadaoka, Suita-ward, Osaka 565-0871 JAPAN

Maritime University of Kobe (MUK)
5-1-1, Fukae-Minami, Higashi-Nada-ward, Kobe 658-0022 JAPAN

Kinki University
3-4-1, Kowakae, Higashi-Osaka, Osaka 577-8502 JAPAN
TEL: +81-6-6721-2332

Osaka Prefecture University
1-1, Gakuen-cho, Sakai, Osaka 599-8531 JAPAN

Okayama University
3-1-1, Tsushimanaka, Okayama 700-8530 JAPAN

Okayama University of Science (OUS)
1-1, Ridai-cho, Okayama 700-0005 JAPAN

Environmental Chemistry Department,
Kansai Environmental Engineering Center CO.,LTD. (KEEC)
1-3-5, Azuchimachi, Chuo-ward, Osaka 541-0052 JAPAN

Global Ocean Development Inc. (GODI)
Kami-oooka-nishi 1-13-8, Kounan-ward, Yokohama 233-0002 JAPAN

Marine Works Japan Ltd. (MWJ)
1-1-7, Mutsuura, Kanazawa-ward, Yokohama 236-0031 JAPAN

5.2 Ship Crew

Master	Akamine, Masaharu
Chief Officer	Hashimoto, Takaaki
1st Officer	Inoue, Haruhiko
2nd Officer	Fujita, Shingo
3rd Officer	Fukaura, Nobuo
Chief Engineer	Ohno, Akiteru
1st Engineer	Araki, Nobuya
2nd Engineer	Masuno, Koji
3rd Engineer	Machino, Takahiro
Chief Radio Officer	Nakabayashi, Shuji
2nd Radio Officer	Shishido, Keiichiro
Boatswain	Kinoshita, Hirokazu
Able Seaman	Naruo, Hisashi
Able Seaman	Yamauchi, Keiji
Able Seaman	Kawata, Seiichiro
Able Seaman	Omote, Kunihiko
Able Seaman	Oguni, Hisao
Able Seaman	Suzuki, Masaru
Able Seaman	Kudo, Kazuyoshi
Able Seaman	Sato, Tsuyoshi
Able Seaman	Aisaka, Takeharu
Able Seaman	Okada, Masashige
Able Seaman	Komata, Shuji
No.1 Oiler	Honda, Sadanori
Oiler	Tsukamoto, Kiyoharu
Oiler	Sugimoto, Yoshihiro
Oiler	Miyazaki, Takashi
Oiler	Matsuo, Toshio
Oiler	Taniguchi, Daisuke
Chief Steward	Koga, Yasuaki
Steward	Kurita, Yasutaka
Steward	Hiraishi, Hatsuji
Steward	Ota, Hitoshi
Steward	Uemura, Kozo
Steward	Sasaki, Wataru

6. Summary of Observations

6.1 Atmospheric Profiles

6.1.1 Radiosonde

(1) Personnel

Kunio Yoneyama	(JAMSTEC) Principal Investigator
Masaki Katsumata	(JAMSTEC)
Masaki Hanyu	(GODI)
Souichoro Sueyoshi	(GODI)
Norio Nagahama	(GODI)
Takashi Chuda	(FORSGC)
Taro Shinoda	(HyARC, Nagoya University)
Chiharu Takahashi	(HyARC, Nagoya University)

(2) Objective

The radiosonde observations are carried out to obtain atmospheric soundings of temperature, humidity, wind speed / direction, and their temporal variation, as the basic dataset to understand atmospheric environment.

(3) Method

Atmospheric sounding by radiosonde was carried out every 3 hours at (2N,138.5E) from November 22 through December 12, 2002. In total, 180 soundings were carried out (Table 6.1-1). The main system consists of processor (Vaisala, DigiCORA MW11), GPS antenna (GA20), UHF antenna (RB21), balloon launcher (ASAP), and GPS radiosonde sensor (RS80-15GH).

Prior to launch, humidity and temperature sensors were calibrated using humidity calibrator (Digilog Instruments, Vaporpak H-31) and pressure sensor was calibrated using Vaisala barometer (PTB220). Calibrator humidity was set at 70%.

(4) Preliminary results

Time-height cross sections of equivalent potential temperature, mixing ratio, zonal and meridional wind components are shown in Fig.6.1.1-1, respectively. Several basic parameters are calculated from sounding data. They include convective available potential energy (CAPE), total precipitable water (TPW), lifted condensation level (LCL), and 1000-700 hPa layer-mean zonal and meridional wind components. Those are depicted in Fig.6.1.1-2. Vertical profiles of temperature and dew point temperature are plotted on the thermodynamic chart with wind profiles. These figures can be found in Appendix-C. During the whole observational period, westerly winds were prevailed in the lower troposphere. One of the most significant features is that this observation period corresponds to the convectively suppressed period. CAPE and TPW decrease with time. Especially, it became very dry in the mid-troposphere on December 7-8, as TPW shows the values less than 40 mm.

(5) Data archive

Data were sent to the world meteorological community by Global Telecommunication System through the Japan Meteorological Agency, immediately after the each observation. Raw data is recorded as ASCII format every 2 seconds during ascent. The raw datasets will be submitted to JAMSTEC Data Management Office. Corrected and projected onto every 5hPa level datasets are available from K.Yoneyama of JAMSTEC.

Table 6.1.1-1 Radiosonde launch log.

Date	Lat.	Long.	Surface Conditions					Max Altitude		Cloud	
YYYYMMDDHH	degN	degE	hPa	degC	%	deg	m/s	hPa	m	Amount	Type
2002111800	19.52	137.77	1014.3	27.0	93	66	8.4	27.6	24276	6	Ac,Sc,Cu,As
2002111806	18.17	137.18	1009.6	29.2	74	65	10.5	33.1	23113	4	Cu
2002111812	16.98	136.60	1011.0	29.0	74	52	8.2	37.7	22348	4	Sc,Cu
2002111818	15.80	136.08	1010.0	25.4	93	335	4.3	802.3	2025	10	Cb
2002111900	14.42	135.45	1009.3	29.2	81	73	11.6	32.8	23213	3	Cu,As
2002111906	13.16	134.90	1006.2	29.2	79	61	9.2	30.1	23700	4	Cu,As,Cs
2002111912	11.79	134.29	1006.3	28.9	82	75	12.2	367.3	8246	8	As,Sc,Cu
2002112112	3.72	136.45	1003.5	29.1	79	270	11.4	40.5	21871	8	Ac,As,Sc
2002112115	3.11	137.02	1003.7	27.7	94	270	6.7	45.2	21211	10	Cs,Cu
2002112118	2.63	137.53	1003.2	28.6	81	254	11.9	44.5	21286	4	Ci,Cs,Cu
2002112121	2.09	138.02	1003.6	28.5	84	245	8.0	150.4	14247	9	Sc,As,Cu
2002112200	2.00	138.50	1006.3	28.4	85	232	5.0	23.6	25244	10	Cu,Sc
2002112203	1.94	138.50	1004.9	28.7	87	213	4.9	24.5	24952	9	Cu,As
2002112206	1.90	138.58	1003.2	28.8	81	142	7.4	153.8	14116	8	Cu,As
2002112209	1.95	138.55	1004.1	28.6	78	178	4.0	33.4	23040	8	Sc,As
2002112212	1.92	138.43	1006.2	28.2	83	43	1.8	60.9	19452	6	Sc,Cu
2002112215	1.95	138.51	1006.2	28.1	77	119	5.2	69.1	18695	6	Cs,Cu
2002112218	1.98	138.53	1004.8	26.2	96	112	6.3	24.4	25010	4	Cb,Sc,Cs
2002112221	2.00	138.52	1006.4	27.4	83	42	3.6	26.9	24416	9	Cu,Sc,Ac
2002112300	2.01	138.54	1008.2	28.2	83	73	4.7	38.7	22144	7	Cu,Sc,Ac
2002112303	2.00	138.54	1007.0	28.6	76	85	3.1	26.3	24536	8	Sc,Ac,Cu
2002112306	1.99	138.52	1005.3	29.0	80	36	1.6	25.7	24658	10	As,Cu
2002112309	2.00	138.51	1006.2	29.3	77	74	1.4	36.0	22590	9	Ci,Sc,Cu,As
2002112312	2.00	138.50	1007.2	28.1	82	38	2.5	40.9	21846	4	St
2002112315	2.01	138.53	1007.2	28.0	72	4	0.7	32.1	23319	2	Ci,Sc
2002112318	2.01	138.51	1005.6	27.8	80	180	0.2	37.6	22307	4	As
2002112321	2.01	138.48	1006.2	27.5	84	242	1.7	25.3	24801	4	Ac
2002112400	2.01	138.48	1007.7	28.5	84	252	3.5	25.3	24780	6	Ci,Cu
2002112403	1.98	138.50	1007.0	29.0	78	196	1.1	25.0	24862	6	Cu,Sc,Cs,Ci
2002112406	1.96	138.47	1005.9	28.7	75	266	0.4	27.7	24203	8	Cu
2002112409	2.03	138.48	1006.2	28.7	74	305	1.7	49.9	20607	9	unknown
2002112412	1.99	138.51	1008.0	28.5	78	316	2.6	32.3	23293	2	unknown
2002112415	1.99	138.51	1008.0	28.4	77	296	3.5	55.5	19975	3	Sc,Cs,Ac
2002112418	2.01	138.47	1007.0	28.1	80	295	5.4	66.3	18908	2	Cu,Sc
2002112421	2.00	138.49	1008.5	28.4	75	291	4.3	29.5	23824	2	Ac,Sc
2002112500	2.01	138.48	1009.8	28.7	81	290	2.7	21.0	25976	2	Cu
2002112503	2.01	138.48	1008.4	29.1	77	284	3.6	20.1	26211	4	Cu,Ac,As
2002112506	1.96	138.50	1007.1	29.1	74	256	7.3	26.4	24500	5	Cu,Ac
2002112509	1.95	138.50	1007.1	28.1	76	268	7.5	35.1	22752	5	As,Sc,Ci
2002112512	2.00	138.49	1008.7	28.0	83	325	6.3	31.9	23367	1	unknown
2002112515	2.00	138.44	1009.1	28.2	83	305	6.7	24.9	24876	6	Cu
2002112518	1.99	138.50	1007.9	28.9	82	285	6.2	39.2	22046	6	Cu
2002112521	2.00	138.50	1008.7	27.9	79	280	6.5	25.2	24772	7	Ac,Cu
2002112600	1.98	138.48	1010.3	28.4	81	257	7.2	22.5	25524	3	Ci,Cu
2002112603	1.97	138.49	1009.1	28.7	78	262	7.6	47.9	20864	9	Sc,Cu,Ci
2002112606	1.96	138.48	1007.0	28.6	77	275	7.1	31.7	23325	8	Ci,Sc,Cb
2002112609	1.99	138.48	1007.3	28.2	79	291	6.6	28.4	24047	8	Ci
2002112612	2.00	138.51	1009.5	28.4	81	286	5.6	49.8	20634	-	unknown
2002112615	2.00	138.49	1009.7	28.4	79	317	4.9	36.4	22539	9	unknown
2002112618	1.99	138.50	1007.4	28.3	74	325	4.6	28.6	24002	6	Cu,Ac,Cs
2002112621	2.00	138.50	1009.4	28.9	96	285	12.8	206.0	12267	10	St
2002112700	2.05	138.46	1011.1	26.3	96	37	1.0	45.7	21159	8	As,Ns
2002112703	2.03	138.51	1009.1	28.1	87	244	4.7	22.7	25496	7	Ci,As,Cb,Cu
2002112706	1.98	138.49	1007.6	28.6	78	270	6.2	81.7	17718	8	Sc,Cu,As
2002112709	1.98	138.46	1008.4	28.4	75	295	5.6	44.1	21350	10	Sc,St
2002112712	1.99	138.48	1009.7	28.4	77	301	5.9	44.6	21323	-	unknown
2002112715	2.02	138.47	1009.2	28.4	75	294	4.7	26.5	24529	7	unknown
2002112718	1.99	138.43	1007.7	28.0	74	278	6.9	23.8	25198	1	Cu

Date	Lat.	Long.	Surface Conditions					Max Altitude		Cloud	
YYYYMMDDHH	degN	degE	hPa	degC	%	deg	m/s	hPa	m	Amount	Type
2002112721	1.98	138.45	1008.8	28.0	78	284	6.3	22.5	25541	5	Cu,Sc
2002112800	1.99	138.46	1010.4	28.5	76	294	6.3	25.2	24839	7	Cc,Cs,Cu
2002112803	1.98	138.47	1007.8	28.5	75	292	7.8	22.8	25426	7	Ac,Sc
2002112806	1.98	138.48	1006.7	28.6	72	295	7.2	26.7	24428	6	Ac,Sc
2002112809	2.00	138.48	1008.0	28.9	77	301	5.7	28.7	24016	9	Ac,Cu
2002112812	2.00	138.50	1010.2	28.4	78	295	5.0	33.4	23078	-	unknown
2002112815	2.02	138.49	1009.5	28.0	83	311	6.1	26.0	24658	-	unknown
2002112818	2.03	138.49	1007.2	27.9	83	306	6.1	40.2	21907	-	unknown
2002112821	2.01	138.49	1009.1	28.0	84	294	6.8	29.5	23826	10	Ac,Cu
2002112900	2.03	138.47	1010.9	28.6	82	292	5.1	38.6	22183	4	Ac,Cu
2002112903	2.02	138.47	1009.0	28.9	80	307	5.6	20.1	26246	2	Cb,Ci,As,Sc
2002112906	2.01	138.52	1007.1	28.5	79	315	5.9	25.4	24803	2	Cb,As,Ci
2002112909	2.00	138.47	1008.5	27.2	86	209	4.4	51.6	20409	9	Ac
2002112912	2.00	138.50	1010.0	28.3	78	320	5.7	33.5	23029	-	unknown
2002112915	2.04	138.49	1008.5	28.0	81	321	6.6	35.1	22756	-	unknown
2002112918	2.03	138.51	1006.9	27.9	79	318	8.9	28.0	24114	-	unknown
2002112921	2.00	138.50	1007.6	27.9	80	313	6.4	20.8	26038	8	Ac,Cu
2002113000	2.03	138.49	1009.5	28.4	82	319	6.2	26.4	24558	2	Cu
2002113003	2.02	138.50	1008.0	28.5	83	309	5.7	197.8	12524	2	Cb,Cu,Sc,As
2002113006	2.01	138.50	1006.1	28.7	81	320	4.1	21.7	25700	2	As,Cb,Sc
2002113009	2.02	138.50	1006.9	28.4	79	320	4.2	31.6	23367	3	As,Ci,Cu
2002113012	2.00	138.50	1008.3	28.4	78	336	4.9	26.2	24550	-	unknown
2002113015	2.00	138.49	1008.3	28.1	81	320	4.3	30.8	23527	-	unknown
2002113018	2.01	138.51	1006.5	27.9	80	337	4.2	28.3	24030	-	unknown
2002113021	2.01	138.51	1007.5	27.9	82	339	5.1	21.8	25726	1	Cu
2002120100	2.04	138.51	1009.3	28.4	83	355	3.9	24.6	24977	1-	Ci,Cu
2002120103	1.99	138.49	1007.9	28.6	79	283	3.7	22.5	25508	2	Ci,As,Cb,Sc
2002120106	1.97	138.50	1006.4	28.6	77	267	3.0	21.8	25697	6	As,Cu,Cb,Sc
2002120109	2.01	138.47	1006.6	28.4	78	289	2.7	116.3	15721	6	As,Cu
2002120112	2.00	138.50	1008.3	28.5	76	336	3.3	35.8	22623	-	unknown
2002120115	2.04	138.48	1008.7	28.4	79	327	4.2	24.8	24928	7	As
2002120118	2.01	138.50	1007.3	28.3	76	299	4.4	23.7	25207	6	unknown
2002120121	2.03	138.48	1008.3	27.9	81	301	3.5	37.7	22295	4	Cu,As,Cb
2002120200	2.03	138.48	1010.2	28.8	79	299	4.0	26.6	24495	3	Cu,Ci
2002120203	2.00	138.50	1010.8	28.5	76	288	5.3	22.5	25536	1	Cu,Cb,Ci
2002120206	1.99	138.50	1007.4	28.5	77	291	4.8	22.2	25569	2	Cu,Cb,Sc
2002120209	2.00	138.49	1007.3	28.2	78	303	5.2	25.7	24662	1-	Cu
2002120212	2.00	138.49	1009.3	28.2	79	301	5.2	27.2	24335	0	-
2002120215	2.01	138.50	1009.6	28.0	83	301	4.7	27.9	24153	0	-
2002120218	2.01	138.50	1007.7	27.7	84	280	4.0	25.1	24806	2	unknown
2002120221	2.02	138.48	1008.5	27.8	73	306	4.6	43.6	21430	5	Cu,Cb,As,St
2002120300	2.04	138.47	1010.7	28.2	80	316	3.8	20.5	26132	5	Cb,Cu
2002120303	1.99	138.49	1009.7	28.3	82	312	3.0	26.2	24548	2	Cu
2002120306	1.99	138.50	1007.6	28.8	78	278	3.1	29.1	23822	2	Cu
2002120309	2.00	138.50	1008.5	28.6	76	299	3.5	27.8	24168	1+	Cu,Cb
2002120312	2.00	138.50	1010.3	28.4	78	338	1.4	22.6	25519	1-	unknown
2002120315	2.00	138.50	1009.9	28.0	81	321	2.6	28.5	24027	1	unknown
2002120318	2.03	138.52	1008.3	27.8	83	333	2.4	25.9	24611	2	Cu
2002120321	2.04	138.50	1008.7	27.7	83	14	2.0	23.1	25346	4	Ci,As,Cu
2002120400	2.03	138.50	1010.0	28.4	81	19	3.2	22.1	25634	5	As,Cu
2002120403	2.02	138.51	1009.4	28.8	80	0	1.2	34.1	22902	4	Cu,Sc
2002120406	2.01	138.50	1007.5	29.0	77	285	1.4	24.7	24874	4	As,Cu,Cb,Sc,Ci
2002120409	2.00	138.50	1007.9	28.5	76	25	1.0	26.4	24499	3	Cb,Cu
2002120412	2.00	138.50	1009.3	28.5	78	338	2.5	28.2	24112	1	Sc
2002120415	2.00	138.51	1009.3	28.5	74	348	2.7	24.5	24980	1	unknown
2002120418	2.03	138.50	1007.8	27.4	82	38	3.8	31.9	23301	4	unknown
2002120421	2.02	138.51	1008.5	28.2	77	327	3.1	29.9	23698	8	Cu,Ac
2002120500	2.03	138.51	1010.2	28.4	78	338	4.0	26.2	24557	4	As,Cu,Cb,Ci
2002120503	2.00	138.50	1009.0	28.5	78	302	4.9	27.1	24317	3	Ci,Cu,Ac
2002120506	2.00	138.50	1007.0	28.9	76	317	5.0	40.6	21789	2	Cu,Sc,Ci
2002120509	2.00	138.49	1007.4	28.5	76	322	7.0	31.8	23338	2	Cu,Ci

Date	Lat.	Long.	Surface Conditions					Max Altitude		Cloud	
YYYYMMDDHH	degN	degE	hPa	degC	%	deg	m/s	hPa	m	Amount	Type
2002120512	2.00	138.50	1008.7	28.5	80	338	5.4	26.5	24518	3	Sc
2002120515	2.01	138.49	1008.3	28.4	78	333	5.8	34.7	22801	5	As
2002120518	2.02	138.51	1006.7	28.2	81	332	7.6	30.3	23606	-	unknown
2002120521	2.02	138.51	1006.9	28.2	79	331	6.9	22.8	25438	7	Cu,As
2002120600	2.03	138.50	1008.5	28.5	78	338	6.4	26.5	24495	7	Ci,Ac,Cu
2002120603	2.00	138.50	1007.9	28.7	77	319	5.7	20.5	26112	7	Cu
2002120606	2.02	138.50	1006.2	28.7	79	296	6.2	26.5	24441	2	Cu
2002120609	2.01	138.50	1006.6	28.1	87	318	6.3	27.5	24250	2	Cu,Cb,Sc
2002120612	2.01	138.50	1007.9	28.4	78	334	5.5	25.8	24670	2	Sc
2002120615	2.00	138.51	1007.4	28.2	77	331	7.6	27.6	24237	5	As
2002120618	2.04	138.51	1006.4	28.0	81	304	6.2	27.9	24141	-	unknown
2002120621	2.01	138.49	1007.0	28.1	78	324	6.6	28.7	24000	4	Cu,As,Ci
2002120700	2.03	138.54	1008.6	28.2	80	321	6.1	46.2	21035	4	Ci
2002120703	2.01	138.51	1007.0	28.3	85	291	7.5	26.4	24481	3	Cu,Ci
2002120706	2.00	138.51	1005.1	28.4	82	289	8.3	23.6	25160	4	Cu,Cb
2002120709	1.98	138.47	1005.3	27.9	84	295	8.1	28.9	23923	1-	Cu
2002120712	2.00	138.49	1007.2	28.0	83	307	5.5	28.4	24051	2	unknown
2002120715	2.01	138.50	1007.0	27.8	84	292	6.5	24.4	24969	3	unknown
2002120718	2.00	138.49	1005.2	27.6	84	297	7.7	28.3	24038	2	unknown
2002120721	1.99	138.49	1006.7	27.5	83	298	7.1	24.9	24822	1	Cb
2002120800	2.00	138.50	1008.2	28.0	82	281	7.7	28.4	24043	2	Cb
2002120803	2.00	138.49	1006.9	28.1	80	275	7.3	25.6	24657	5	Cu
2002120806	1.97	138.48	1005.2	28.3	80	284	8.8	869.6	1285	1	Cu
2002120809	1.99	138.49	1006.1	28.2	81	293	7.5	30.3	23609	1	Cu
2002120812	1.99	138.49	1007.6	28.1	81	292	7.3	27.4	24257	1	Cu
2002120815	1.99	138.49	1007.8	28.1	78	305	8.5	95.8	16881	1	unknown
2002120818	2.00	138.51	1005.9	27.9	77	310	6.9	24.3	24987	1	unknown
2002120821	1.99	138.49	1006.8	27.6	82	298	6.5	25.0	24823	1	Cu
2002120900	2.00	138.50	1009.1	27.1	79	314	4.5	20.0	26267	2	Cu
2002120903	2.00	138.49	1007.7	28.5	78	315	6.2	40.7	21809	1-	Cu
2002120906	1.99	138.48	1006.2	28.3	77	313	6.0	35.7	22593	2	Cu
2002120909	2.00	138.50	1007.4	28.2	76	305	6.2	27.2	24316	1	Cu,Cs
2002120912	1.99	138.48	1009.5	28.1	76	298	6.4	33.8	22976	1	unknown
2002120915	2.00	138.50	1008.4	27.7	77	310	5.6	28.4	24058	1	unknown
2002120918	2.00	138.50	1006.6	27.4	80	305	7.5	32.3	23227	2	unknown
2002120921	2.00	138.50	1008.2	27.4	81	321	7.2	26.5	24465	2	Ac,Cc
2002121000	2.00	138.49	1010.6	27.9	81	317	5.6	25.1	24821	1	Ac,Ci,Cb
2002121003	2.00	138.50	1010.0	27.8	80	307	3.7	19.6	26394	6	Cu,Ci,As,Cs
2002121006	1.99	138.51	1008.3	28.3	72	271	4.5	26.7	24459	6	As,Cu,Cs
2002121009	2.00	138.50	1008.5	28.1	73	304	4.9	30.1	23691	4	Cs,Ci
2002121012	2.00	138.50	1010.0	27.9	78	324	3.8	30.2	23683	3	Ac
2002121015	2.01	138.50	1010.2	27.6	78	332	4.0	29.2	23893	2	unknown
2002121018	2.00	138.51	1009.5	27.3	80	332	4.0	26.2	24565	1	unknown
2002121021	2.01	138.50	1010.6	27.2	79	312	3.6	34.4	22866	1	Cu
2002121100	2.00	138.50	1011.6	27.6	79	323	3.9	21.9	25692	0	-
2002121103	2.00	138.50	1010.6	27.7	79	329	2.7	35.3	22703	0	-
2002121106	2.02	138.47	1008.7	27.8	77	337	3.2	55.1	19994	4	Cu
2002121109	2.01	138.50	1009.8	27.6	78	299	2.5	27.2	24309	3	Cu
2002121112	2.00	138.48	1011.6	27.7	77	295	1.5	24.7	24924	1	Cu
2002121115	2.00	138.47	1011.1	27.3	80	323	1.3	30.8	23562	0+	unknown
2002121118	2.01	138.46	1010.5	27.2	81	3	1.8	28.4	24036	0+	unknown
2002121121	2.02	138.50	1011.4	27.0	80	121	0.4	25.5	24727	1	Cu,As,Ci
2002121200	2.00	138.50	1013.2	27.6	80	120	0.3	22.6	25476	0	-
2002121203	2.01	138.48	1012.7	27.9	77	339	0.8	21.2	25875	1	Cu
2002121206	1.98	138.48	1010.1	28.6	72	189	1.2	74.6	18226	0+	Cu
2002121209	2.01	138.48	1010.8	28.5	72	122	0.2	34.3	22900	1-	Ac,Ci
2002121212	2.01	138.47	1012.3	28.0	74	323	1.0	34.4	22888	1	Ac
2002121215	2.00	138.49	1011.8	27.8	73	319	1.8	37.1	22408	0+	unknown
2002121218	2.46	138.64	1010.0	27.4	75	323	1.5	27.9	24135	0+	Sc
2002121221	3.18	138.86	1011.3	27.1	77	235	0.2	24.0	25079	0+	Ci,Cu
2002121300	3.98	139.07	1012.9	27.7	78	253	1.7	91.6	17108	2	Ac,Cu

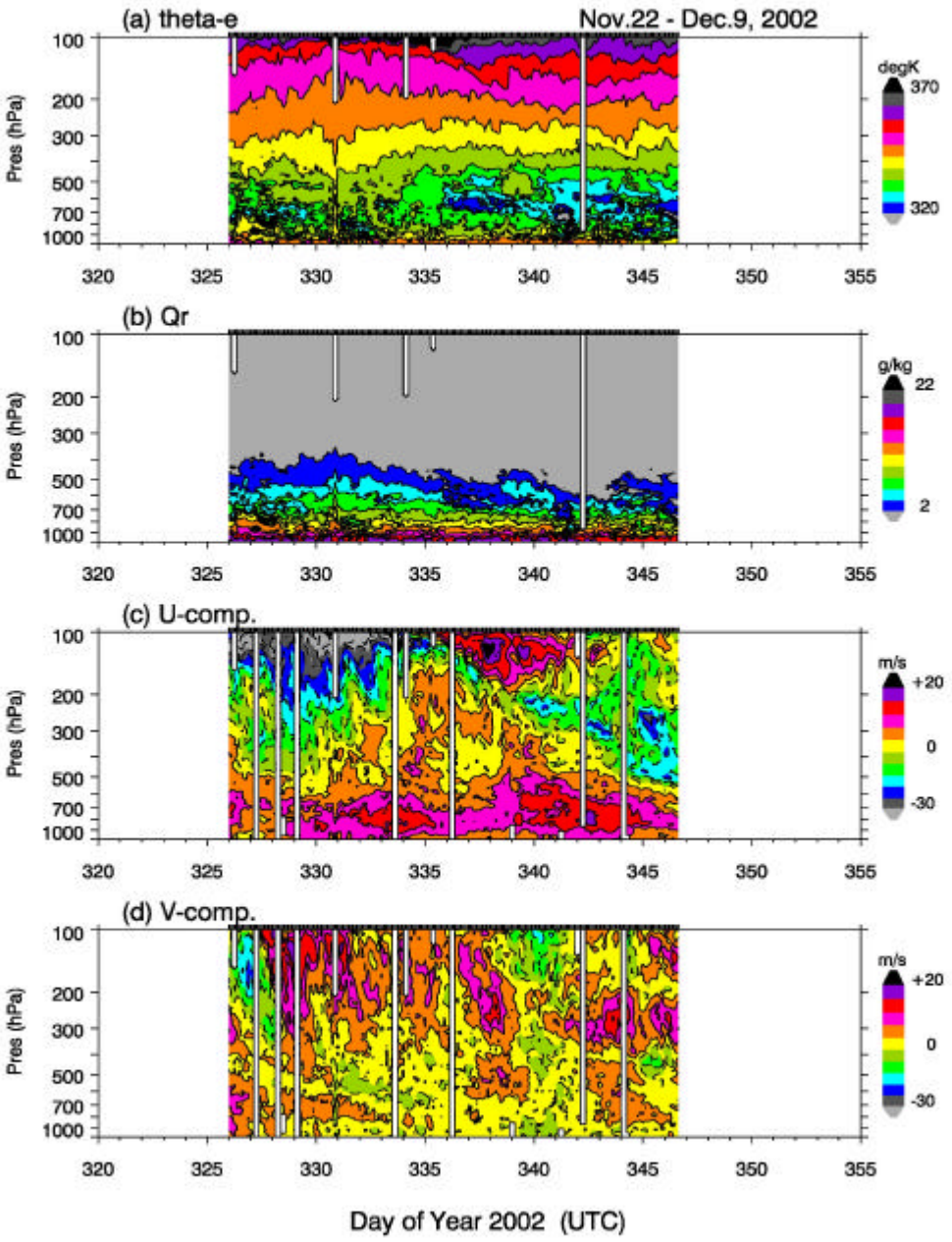

Fig. 6.1.1-1 Time-height cross sections of (a) equivalent potential temperature (degK), (b) mixing ratio (g/kg), (c) zonal wind component (m/s), and (d) meridional wind component (m/s). DAY326 corresponds November 22, 2002.

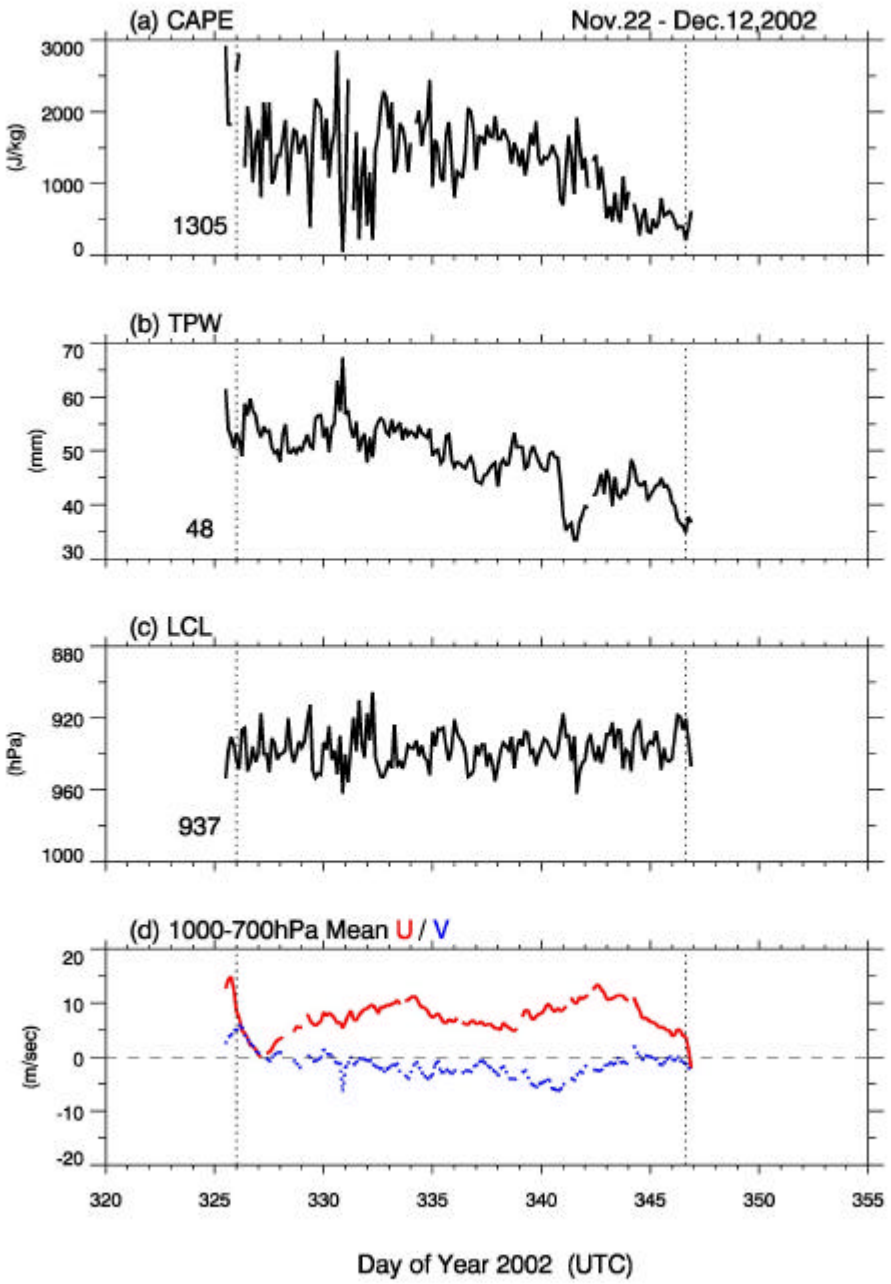

Fig. 6.1.1-2 Time series of (a) convective available potential energy, (b) total precipitable water, (c) lifted condensation level, and (d) 1000-700 hPa layer-mean zonal (red) and meridional (blue) wind components. Dashed lines indicate start/end time of stationary observation at (2N, 138.5E).

6.1.2 Radiosonde with Snow White Hygrometer

(1) Personnel

Kunio Yoneyama	(JAMSTEC)	: Principal Investigator
Masaki Katsumata	(JAMSTEC)	
Masaki Hanyu	(GODI)	: Operation Leader
Souichoro Sueyoshi	(GODI)	
Norio Nagahama	(GODI)	
Masatomo Fujiwara	(Kyoto University)	

(2) Objective

Accurate humidity measurement and data comparison with Vaisala radiosonde

(3) Method

"Snow White" hygrometer that is developed by Meteolabor AG in Switzerland can measure the humidity accurately with electrically chilled mirror dew-point sensor. We launched Vaisala RS80-15 radiosonde with this hygrometer 15 times during the cruise. Block diagram of receiving system is depicted in Fig. 6.1.2-1.

(4) Preliminary results

Since current model does not support the correction of solar radiation, we had to launch them at night. Launch dates and surface conditions are listed in Table 6.1.2-1. An example of sounding results is shown in Fig. 6.1.2-2.

(5) Data archive

ASCII raw data will be submitted to JAMSTEC Data Management Office. Correction will be done by K.Yoneyama of JAMSTEC.

Table 6.1.2-1: Snow White launch log.

	Launch time	Lat.	Long.	Surface Conditions					Snow White	Vaisala RS80-15
No.	YYYYMMDDHHMM	degN	degE	hPa	degC	%	deg	m/s	Serial No.	Serial No.
1	200211181124	16.98	136.61	1013.1	28.9	74	58	8.8	ASW35-2N-00607	233208808
2	200211221114	1.94	138.44	1008.1	28.2	82	123	3.8	ASW35-2N-00606	233209214
3	200211231119	2.00	138.51	1009.2	28.1	82	36	1.5	ASW35-2N-00602	233208702
4	200211241130	1.59	138.50	1010.3	28.4	78	291	1.7	ASW35-2N-00591	233208813
5	200211261134	2.00	138.47	1010.0	28.1	81	294	6.2	ASW35-2N-00592	233209415
6	200211271118	2.00	138.50	1011.6	28.3	81	318	4.8	ASW35-2N-00593	233209410
7	200211281125	2.00	138.50	1012.2	28.2	80	301	5.1	ASW35-2N-00596	233209411
8	200211291121	2.00	138.50	1012.1	28.3	75	326	5.0	ASW35-2N-00599	233209406
9	200211301119	2.00	138.52	1010.5	28.3	80	344	5.1	ASW35-2N-00608	233208803
10	200212011116	2.00	138.50	1010.2	28.4	76	335	3.8	ASW35-2N-00605	233209200
11	200212021139	2.00	138.50	1011.6	28.2	80	320	4.6	ASW35-2N-00603	233208809
12	200212031117	2.00	138.50	1012.4	28.3	78	328	1.7	ASW35-2N-00595	233208814
13	200212041145	2.03	138.48	1011.1	28.4	79	338	2.6	ASW35-2N-00601	233209210
14	200212051129	2.00	138.49	1010.5	28.3	80	333	5.5	ASW35-2N-00594	233209215
15	200212061132	2.00	138.51	1010.0	28.4	78	327	5.7	ASW35-2N-00604	233208703

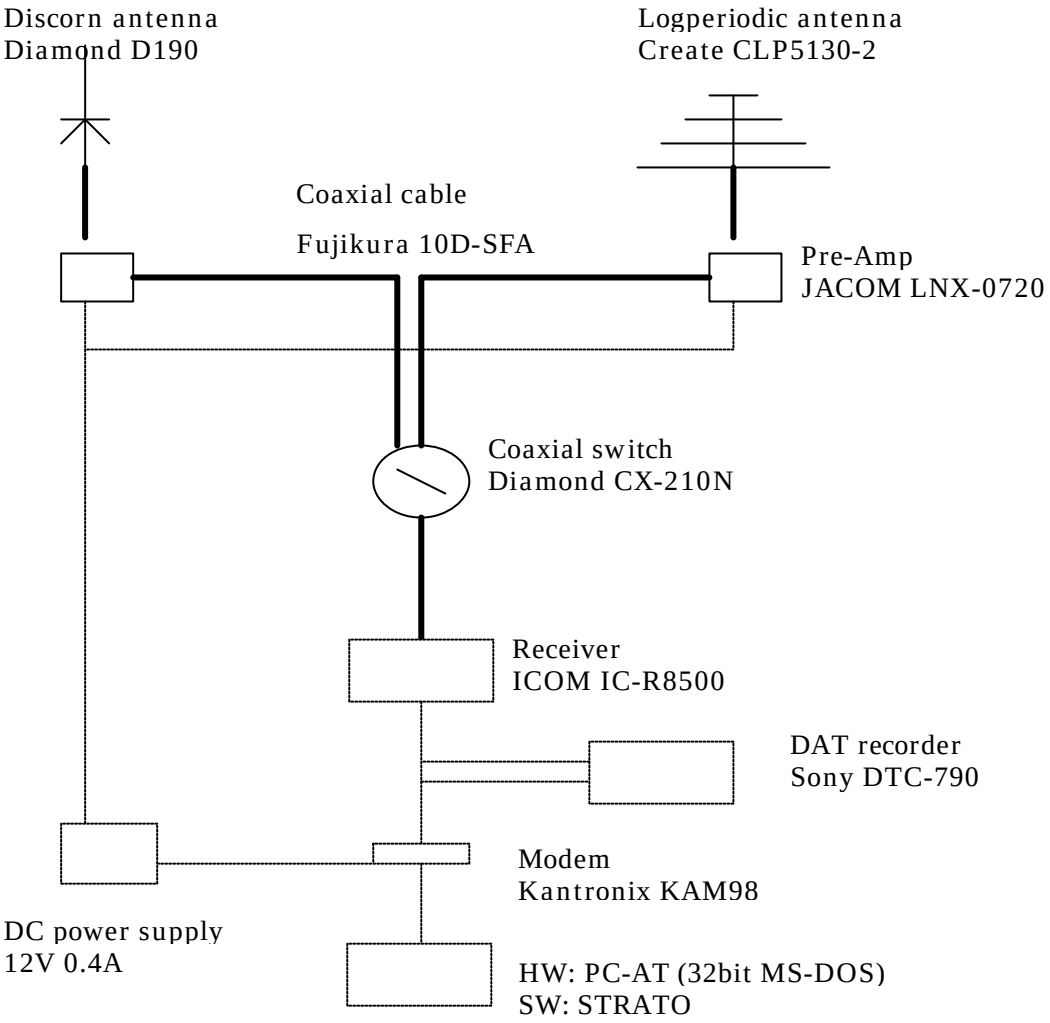

Fig. 6.1.2-1: Block diagram of Snow White telemetry receiving system.

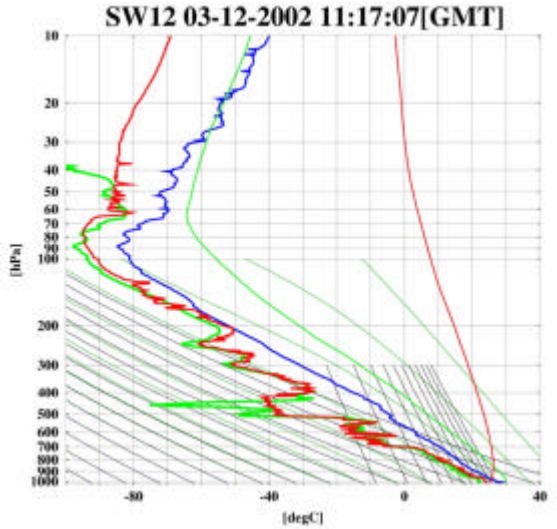

Fig. 6.1.2-2: Profiles of dew(frost)-point by Snow White(green) / Vaisala (red) and temperature by Vaisala RS80-15 (blue) taken on December 3, 2002.

6.1.3 Microwave Radiometers

6.1.3.1 Water Vapor / Temperature Profiler

(1) Personnel

Taro Shinoda (HyARC, Nagoya Univ.): Principle Investigator
Chiharu Takahashi (HyARC, Nagoya Univ.)

(2) Objectives

The microwave radiometer TP/WVP-3000 can obtain temperature, water vapor and cloud liquid water profiles from the surface to 10 km in height every about 15 minutes. The objective of the observation by using this instrument is to research the temperature and water vapor profile around the precipitating systems, and to research diurnal variation of structure of the atmospheric boundary layer over the ocean.

(3) Methods

The radiometer includes two separate subsystems. The temperature profiling subsystem utilizes at selected 7 frequencies between 51 and 59 GHz (51.250, 52.280, 53.850, 54.940, 56.660, 57.290, 58.800 GHz). The water vapor profiling subsystem receives at selected 5 frequencies between 22 and 30 GHz (22.235, 23.035, 23.835, 26.235, 30.000 GHz). Surface meteorological sensors measure air temperature, barometric pressure, and relative humidity. To improve measurement of water vapor and cloud liquid water density profiles, cloud base altitude information is obtained with an infrared thermometer.

The receiver gain is measured using a calibrated noise diode as a gain standard. It uses the mathematical inversion method for retrieving temperature, water vapor, and cloud liquid water profiles by utilizing artificial neural networking analysis (the Stuttgart Neural Network System). The profiles of these parameters are output in 100 meters up to 1 km and 250 meters from 1 to 10 km. The accuracy of temperature profiles is 0.5 K.

The observation is performed continuously from 12 November to 16 December 2002, except for the daytime on 15 November (from 0810 to 1530 JST), from 19 November (2100 JST) to 21 November (1630 JST) by passing the Palawan and/or Indonesian EEZ, and from 23 November (1630 JST) to 24 November (1600 JST). During the observation, the profiles of temperature, water vapor and cloud liquid water are obtained every about 15 minutes.

(4) Preliminary Results

The receiver gain values on the selected frequencies are obtained during the observation period, but all the retrieving profiles of temperature, water vapor, and cloud liquid water are impractical values because of the error of the standard data or the neural network analysis. The profile of these parameters will have to be retrieved (recalculated) by utilizing the correct standard data (radio sounding dataset) and correctly tuned neural network system. This procedure is the future work. The diurnal variation of the atmospheric boundary layer and moist layer around the sea surface by using the microwave radiometer dataset will be analyzed after the profile of these parameters will be retrieved.

(5) Data Archive

The inventory information will be submitted to JAMSTEC DMO (Data Management Office). The original data will be archived at and available from Hyrdoshperic Atmospheric Research Center, Nagoya University (contact Taro Shinoda) and also will be submitted to JAMSTEC.

6.1.3.2 Vertically Integrated Water Vapor / Cloud Liquid Water

(1) Personnel

Masayuki Sasaki (NASDA/EORC*): Principle Investigator (not on board)
Satoshi Takahashi (Okayama Univ.): On-board P.I.

(2) Objectives

The satellite-borne microwave radiometers are the powerful device to obtain the spatial and temporal variation of the water vapor, cloud liquid water, etc, especially over the ocean where the ground-based observation is poor. To validate the products of AMSR (Advanced Mircowave Radiometer) / ADEOS-II, brand-new satellite-borne microwave radiometer, the ground-based microwave radiometer is installed on the vessel and continuous observation is carried out.

(3) Methods

The microwave radiometer WVR26 (Radiometrics Co.) is used for this observation.

The radiometer obtained brightness temperature data for the two frequency, 23GHz and 31GHz. The brightness temperature data is converted to the vertically integrated water vapor amount and cloud liquid water amount.

The observation is performed continuously from 12 November to 16 December 2002, except over the Palawan and/or Indonesian EEZ.

(4) Preliminary Results

The observed data will be checked and analyzed after the cruise.

(5) Data Archive

The original data will be archived at NASDA/EORC, and will be submitted to JAMSTEC.

*NASDA/EORC: National Space Development Agency of JAPAN / Earch Observation Research Center.

6.1.4 Ceilometer

(1) Personnel

Masaki Katsumata	(JAMSTEC):	Principal Investigator
Kunio Yoneyama	(JAMSTEC)	
Masaki Hanyu	(GODI):	Operation Leader
Souichiro Sueyoshi	(GODI)	
Norio Nagahama	(GODI)	

(2) Objective

The information of the cloud base height and the liquid water amount around cloud base is important to understand the processes on the formation of the cloud. As one of the methods to measure them, the ceilometer observation was carried out.

(3) Methods

We measured cloud base height and backscatter profile using CT-25K (VAISALA, Finland) ceilometer throughout MR02-K06 leg1 cruise from the departure of Sekinehama on 13 November 2002 to the arrival of Guam on 16 December 2002, except EEZ of the Republics of Palau and Indonesia.

Major parameters for the measurement configuration are as follows;

Laser source:	Indium Gallium Arsenide (InGaAs) Diode
Transmitting wave length:	905±5 nm at 25 deg-C
Transmitting average power:	8.9 mW
Repetition rate:	5.57kHz
Detector:	Silicon avalanche photodiode (APD)
Responsibility at 905 nm:	65 A/W
Measurement range:	0～7.5 km
Resolution:	50 ft in full range
Sampling rate:	60 sec

On the archived dataset, three cloud base height and backscatter profile are recorded with the resolution of 30 m (100 ft.). If the apparent cloud base height could not be determined, vertical visibility and the height of detected highest signal are calculated instead of the cloud base height.

(4) Preliminary results

The first, second and third lowest cloud base height which the ceilometer detected during the stationary observation are plotted in Fig. 6.1.4-1. This figure implies that the cloud base height in the observation range (to 7.5km height) have bimodal distribution; around 500m height (near lowest condensation level) and 4 to 6 km height (near zero-degree-C temperature level). The further analyses are the future work.

(5) Data archives

Ceilometer data obtained during this cruise will be submitted to and archived by the DMO (Data Management Office) of JAMSTEC.

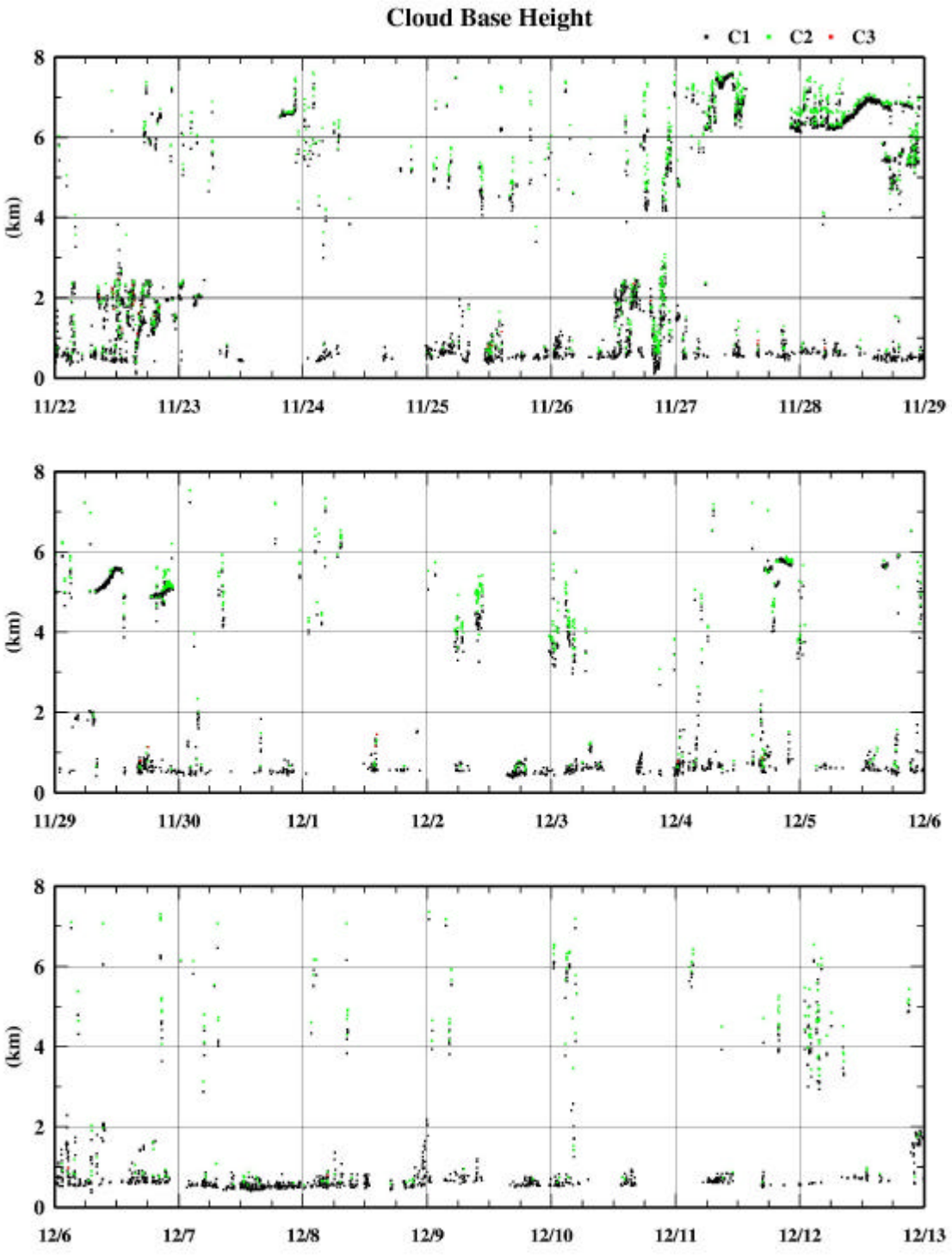

Figure 6.1.4-1: 1st, 2nd and 3rd lowest cloud base height during the stationary observation

6.1.5 Mie Scattering Lidar

(1) Personnel

Ichiro Matsui (National Institute for Environmental Studies) On board personnel
Atsushi Shimizu (National Institute for Environmental Studies)
Nobuo Sugimoto (National Institute for Environmental Studies)

(2) Objectives

Objectives of the observations and experiments during this cruise are to study distribution and optical characteristics of aerosols and clouds using a two-wavelength dual polarization lidar.

(3) Method

Vertical profiles of aerosols and clouds were measured with a two-wavelength dual polarization lidar. The lidar employs a Nd:YAG laser as a light source which generates the fundamental output at 1064 nm and the second harmonic at 532 nm. Transmitted laser energy is typically 100 mJ per pulse at 1064 nm and 50 mJ per pulse at 532 nm. The pulse repetition rate is 10 Hz. The receiver telescope has a diameter of 25 cm. The receiver has three detection channels to receive the lidar signals at 1064 nm and the parallel and perpendicular polarization components at 532 nm. An analog-mode avalanche photo diode (APD) is used as a detector for 1064 nm, and photomultiplier tubes (PMTs) are used for 532 nm. The detected signals are recorded with a digital oscilloscope and stored on a hard disk with a computer. The lidar system was installed in a 20-ft container with the cloud profiling radar (CPR) of the Communications Research Laboratory (CRL). The container has a glass window on the roof, and the lidar was operated continuously regardless of weather.

(4) Results

Figure 6.5-1 shows the quick-look time-height indications of the range-corrected signal during of this cruise. The lower clouds at 600 m are continuously observed over western Pacific Ocean. Cirrus clouds are also frequently observed in an altitude range of 10 to 18km.

(5) Data archive

- Raw data
  lidar signal at 532 nm (parallel polarization), lidar signal at 532 nm (perpendicular polarization)
  lidar signal at 1064 nm, temporal resolution 10 sec., vertical resolution 6 m
- Processed data
  cloud base height, apparent cloud top height, cloud phase, cloud fraction
  boundary layer height (aerosol layer upper boundary height)
  backscatter coefficient of aerosols, depolarization ratio

All data will be archived at National Institute for Environmental Studies, and submitted to JAMSTEC within 3-years.

(7) Remarks

We did not observe the atmosphere in the EEZ of Republic of Palau from 12:00-19-November to 12:00-21-November 2002 (UTC).

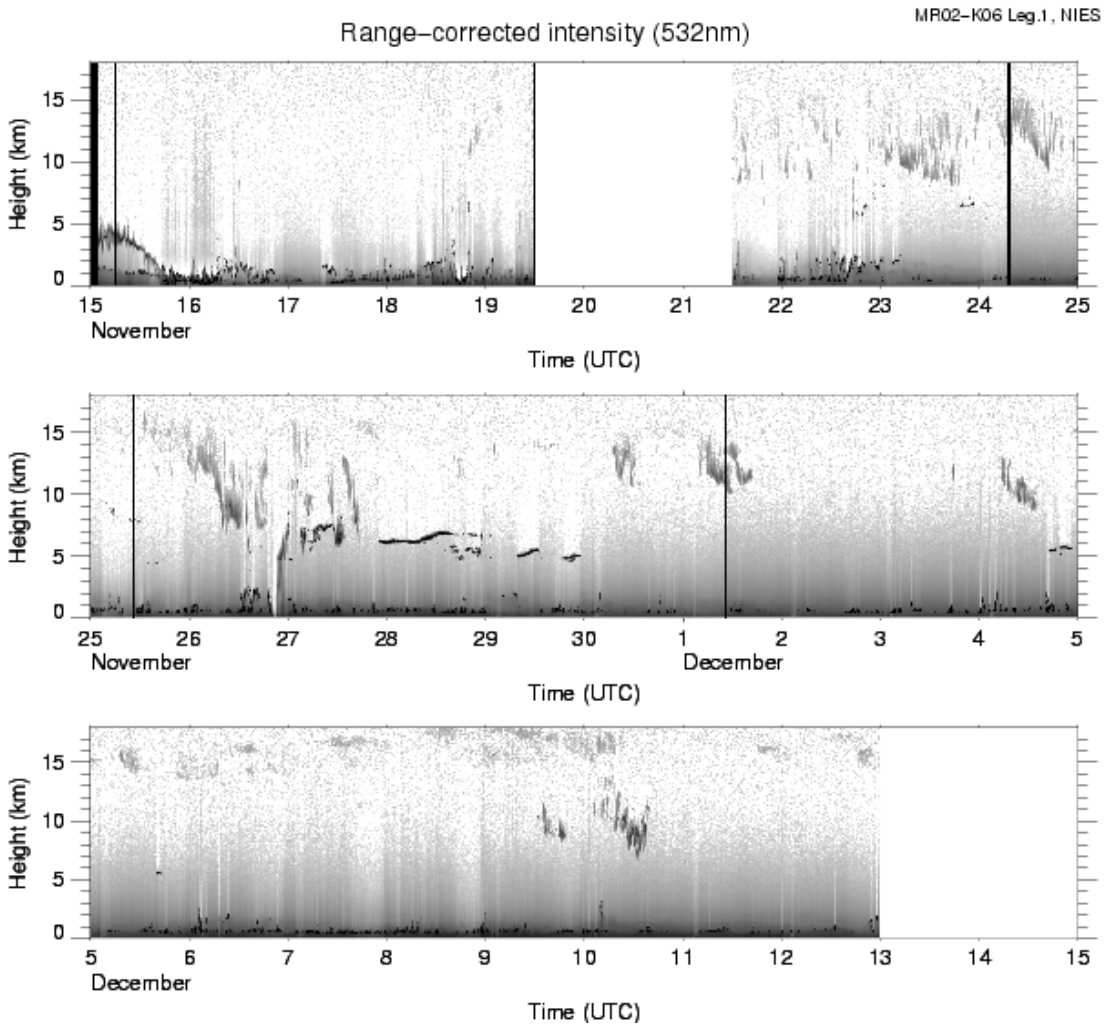

Fig. 6.1.5-1: Range-corrected signal at 532 nm

6.2 Rain Cloud and Rain Water

6.2.1 Doppler Radar

(1) Personnel

Masaki Katsumata	(JAMSTEC):	Principal Investigator
Masaki Hanyu	(GODI):	Operation Leader
Kunio Yoneyama	(JAMSTEC)	
Takashi Chuda	(FORSGC)	
Taro Shinoda	(HyARC, Nagoya Univ.)	
Chiharu Takahashi	(HyARC, Nagoya Univ.)	
Souichiro Sueyoshi	(GODI)	
Norio Nagahama	(GODI)	

(2) Objective

The Doppler radar is operated to obtain spatial and temporal distribution of rainfall amount, and structure of precipitating cloud systems. The objective of this observation is to investigate the mechanism, role and impact of the precipitating systems in the climate system.

(3) Methods

The hardware specification of this shipboard Doppler radar (RC-52B, manufactured by Mitsubishi Electric Co. Ltd., Japan) is:

Frequency:	5290 MHz
Beam Width:	better than 1.5 degrees
Output Power:	250 kW (Peak Power)
Signal Processor:	RVP-7 (Sigmet Inc., U.S.A.)
Inertial Navigation Unit:	DRUH (Honeywell Inc., U.S.A.)
Application Software:	IRIS/Open (Sigmet Inc., U.S.A.).

The hardware is calibrated by checking (1) frequency, (2) mean power output, (3) pulse repetition frequency (PRF) for once a day, and (4) transmitting pulse width and (5) receiver linearity at the beginning and the end of the intensive (stationary) observation period.

The observation is performed continuously from 15 November to 14 December 2002, except in the EEZ of the Republic of Palau and the Republic of Indonesia. During the observation, the programmed "tasks" are repeated every 10 minutes. One cycle consists of one "volume scan" (consists of PPIs for 21 elevations) with Doppler-mode (160-km range for reflectivity and Doppler velocity), and one-elevation "Surveillance" PPI with Intensity-mode (300-km range for reflectivity). In the interval of the cycles, RHI (Range Height Indicator) scans were operated to obtain detailed vertical cross sections with Doppler-mode. The Doppler velocity is unfolded automatically by dualPRF unfolding algorithm for the volume scan for volume scan (not for RHIs). The parameters for the above three tasks are listed in Table 6.2.1-1.

Table 6.2.1-1: Parameters for each task.

	Surveillance PPI	Volume Scan	RHI
Pulse Width	2 [microsec]	0.5 [microsec]	
Scan Speed	18 [deg./sec.]		Automatically determined
PRF	260 [Hz]	900 / 720 [Hz] (Dual PRF)	900 [Hz]
Sweep Integration	32 samples		
Ray Spacing	1.0 [deg.]		0.2 [deg.]
Bin Spacing	250 [m]	125 [m]	
Elevations	0.5	0.5, 1.2, 2.0, 3.0, 4.0, 5.0, 6.0, 7.0, 8.0, 9.0, 10.1, 11.3, 12.8, 14.6, 16.6, 18.9, 21.6, 25.0, 29.0, 34.0, 40.0	0.0 to 70.0
Azimuths	Full Circle		Optional
Range	300 [km]	160 [km]	

(4) Preliminary Results

The temporal variation of the radar-derived precipitating area is shown in Fig.6.2.1-1. As shown, the radar detected very few amount of rain within the range through the stationary observation period, while the active phase of the MJO seemed to pass over the observation point. Most of the large echo is in the south of the range and further than 100-km in the range distance.

The further analyses are future work.

(5) Data Archive

The inventory information of the Doppler radar data will be submitted to JAMSTEC DMO. The original data will be archived at and available from Ocean Observation and Research Department of JAMSTEC (contact Masaki Katsumata).

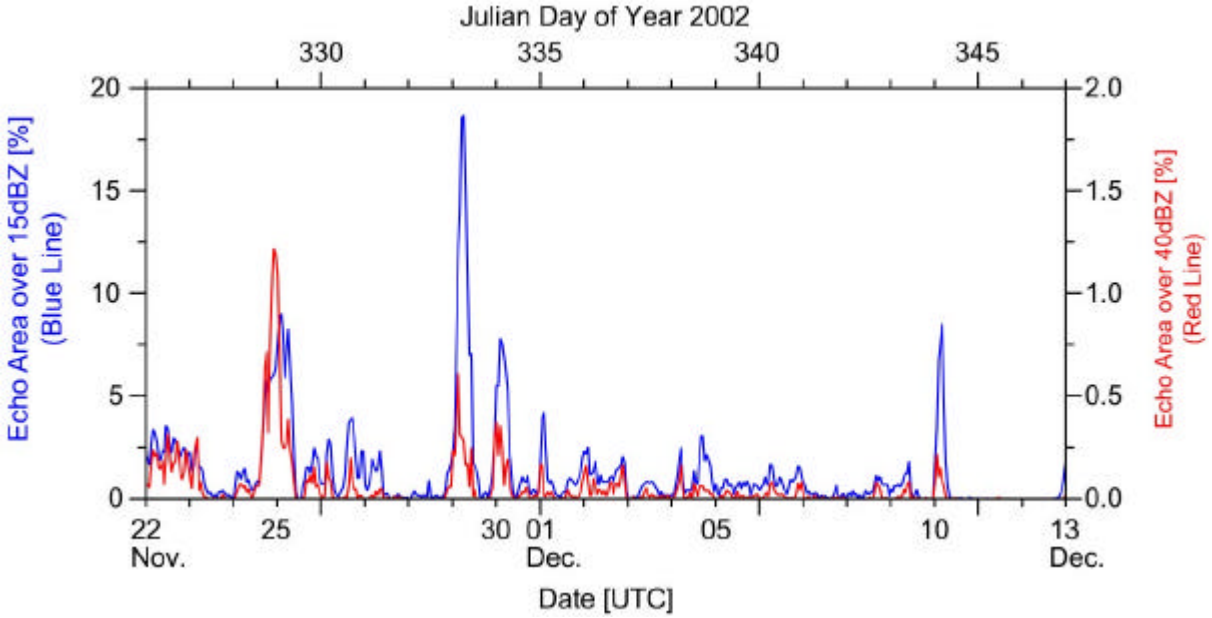

Fig. 6.2.1-1: Temporal variation of the echo area over 15dBZ (blue) and over 40dBZ (red), by the ratio to the radar observation area within 200-km, obtained by surveillance PPI.

6.2.2 Micro Rain Radar

(1) Personnel

Masayuki Sasaki (NASDA/EORC*): Principle Investigator (not on board)
Satoshi Takahashi (Okayama Univ.): On-board P.I.

(2) Objectives

The satellite-borne microwave radiometers are the powerful device to obtain the spatial and temporal variation of the water vapor, cloud liquid water, etc, especially over the ocean where the ground-based observation is poor. To validate the products of AMSR (Advanced Mircowave Radiometer) / ADEOS-II, brand-new satellite-borne microwave radiometer, the ground-based vertically-pointed rain radar is installed on the vessel and continuous observation is carried out.

(3) Methods

The micro rain radar MRR-2 (METEK GmbH) is used for this observation.

The radar is a compact 24 GHz FM-CW-radar for the measurement of profiles of drip size distribution and rain rates, liquid water content and characteristic falling velocity of the raindrops. The transmitter power is 50 mW.

In this observation, the data is obtained every 60 seconds, at every 200-m range gate to 6000-m height. The observation is performed continuously from 12 November to 16 December 2002, except over the Palawan and/or Indonesian EEZ.

(4) Preliminary Results

The observed data will be checked and analyzed after the cruise.

(5) Data Archive

The original data will be archived at NASDA/EORC, and will be submitted to JAMSTEC.

*NASDA/EORC: National Space Development Agency of JAPAN / Earch Observation Research Center.

6.2.3 Disdrometer

(1) Personnel

Taro Shinoda (HyARC, Nagoya Univ.)
Chiharu Takahashi (HyARC, Nagoya Univ.)

(2) Objectives

The disdrometer can obtain both number of size distribution of raindrops (20 categories) and rainfall intensity in every minute. We can dstinguish the type of cloud brought about rainfall events (convective or stratiform clouds) by utilizing the size distribution of raindrops.

(3) Methods

A microphone is installed in the top of the disdrometer. When raindrops hit this microphone, the magnitude and the times of sound are transferred to the size distribution and number of raindrops. There are 20 categories of the size distribution and the sum of raindrops is calculated as the rainfall intensity. The time resolution is one minute.

(4) Preliminary Results

During the observation period, there are few rainfall events. By using the Doppler radar observation, rainfall events break out on November 26, December 6 and 10. We could obtain the size distribution of raindrops and rainfall intensity of these rainfall events.

(5) Data Archive

The inventory information of the disdrometer data obtained during this cruise will be submitted to JAMSTEC DMO (Data Management Office). The original data will be archived at and available from Hyrdoshperic Atmospheric Research Center, Nagoya University (contact person is Taro Shinoda) and also will be submitted to JAMSTEC.

(6) Remarks

(a) The categories of the size distribution are as follows:

1:	0.313 --- 0.405 mm,	11:	1.747 --- 2.077 mm,
2:	0.405 --- 0.506 mm,	12:	2.077 --- 2.441 mm,
3:	0.506 --- 0.597 mm,	13:	2.441 --- 2.727 mm,
4:	0.597 --- 0.715 mm,	14:	2.727 --- 3.011 mm,
5:	0.715 --- 0.827 mm,	15:	3.011 --- 3.385 mm,
6:	0.827 --- 1.000 mm,	16:	3.385 --- 3.705 mm,
7:	1.000 --- 1.232 mm,	17:	3.705 --- 4.127 mm,
8:	1.232 --- 1.430 mm,	18:	4.127 --- 4.573 mm,
9:	1.430 --- 1.582 mm,	19:	4.573 --- 5.101 mm,
10:	1.582 --- 1.747 mm,	20:	larger than 5.101 mm.

(b) The size distribution dataset are very noisy because of the vibration of the ship or the noise of wind. We recommend to exclude or ignore the size distribution from category 1 to 4, when you use this dataset.

6.2.4 Sampling of the Stable Isotopes in Precipitation

(1) Personnel

Takashi Chuda (Frontier Observation Research System for Global Change)
Kimpei Ichiyanagi (Frontier Observation Research System for Global Change)
Naoyuki Kurita (Frontier Observation Research System for Global Change)

(2) Objectives

The samples of precipitation are collected to obtain temporal variation of stable isotopes in Tropical rainfall and special distributions of stable isotopes in precipitation all over the Asia.

(3) Methods

The samples of precipitation are collected by the 250 ml plastic bottle with plastic cap (see Fig. 1). Stable isotopic composition for hydrogen and oxygen in water is determined by the isotope ratio mass spectrometry (IRMS). The IRMS used in this study is Finnigan MAT 252 (Thermo Quest K. K.) with CO_2 & H_2 equilibration device

Fig. 6.2.4-1: The sample of precipitation at 8:00 (LT), 27 November, 2002.

(4) Data Archives

We collected only one sample of precipitation for a period from 21 November to 12 December 2002 (Table 1). The original sample will be preserved at Frontier Observation Research System for Global Change. The inventory information will be submitted to JAMSTEC DMO. The analyzed dataset will be submitted to JAMSTEC DMO.

Table 6.2.4-1: List of samples of rain in MR02K06.

Date (LT)	Sample No.
02/11/27 8:00	#1

6.3 Solar Radiation and Aerosols

6.3.1 Solar Radiation

(1) Personnel

Tetsuya Takemi (Osaka University): On-board leader
Ryutaro Sanjiki (Kinki University)

On-shore scientist:
Katsutoshi Kozai (Kobe University of Mercantile Marine): Principal Investigator

(2) Objective

Atmospheric aerosols have been recognized as having a profound effect on the global climate change by interacting shortwave and longwave radiation transfer in the atmosphere. The purpose of the present observation is to elucidate the characteristics of aerosols in a maritime area by measuring direct solar radiation and scattering radiation in clear conditions.

(3) Methods

Polarization spectral radiometer (Opto Research Corp., PSR1000, see Fig. 6.3.1-1) measures the atmospheric absorption of the solar radiation and the polarization degree at six different angles (45, 60, 75, 90, 105, and 120 degrees) from the solar direction at six wavelengths (443, 490, 565, 670, 765, and 865 nm). The six wavelengths correspond to those of the POLDER sensor installed on ADEOS. Thus, the present observation provides the ground-truth data for the satellite. Fig.6.3.1-2 demonstrates the schematic figure of the observation method. The aerosol optical thickness and angstrom coefficient are derived from the data obtained by measuring the direct solar radiation, while the aerosol chemical properties can be derived from the measurement of the scattering radiation.

Table 6.3.1-1 summarizes the observation schedule during the present cruise. On November 20th and 21st, no observations were conducted because Mirai was within the EEZs of Palau and Indonesia.

Fig.6.3.1-1: PSR-1000.

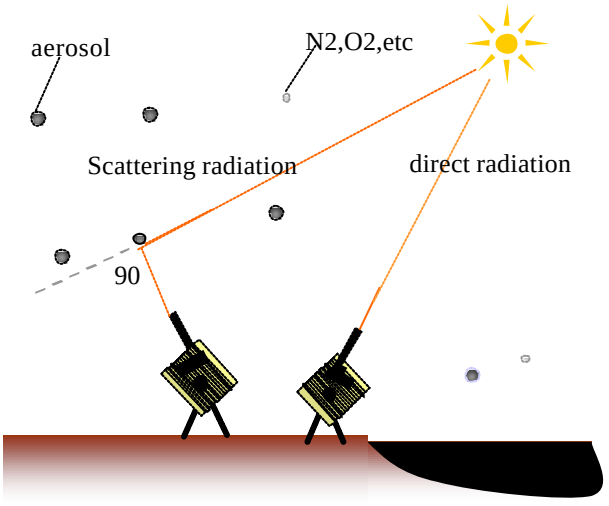

Fig.6.3.1-2: Observation Schema

Table 6.3.1-1: List of observed parameters and schedule.

	PSR-1000		Time	Remarks
day	direct	scat		
13-Nov				
14-Nov				
15-Nov				
16-Nov				
17-Nov	○	○	9:00-11:15 , 13:15-15:00	No Clouds
18-Nov				
19-Nov	○	○	13:00-15:00	
20-Nov				No observation in the Palau and Indonesia EEZ
21-Nov				
22-Nov				
23-Nov				
24-Nov	○		10:00 , 14:00	
25-Nov	○	○	9:00-12:00	
26-Nov				
27-Nov				
28-Nov				
29-Nov	○	○	11:00-15:30	No Clouds
30-Nov	○	○	9:00-12:30 , 13:30-15:00	No Clouds
1-Dec	○	○	9:30-12:30	No Clouds
2-Dec	○	○	9:15-12:15 , 13:15-1500	No Clouds
3-Dec	○	○	9:30-12:00 , 13:20-13:30	No Clouds
4-Dec	○	○	10:30-12:30 , 13:30-1400	No Clouds
5-Dec	○	○	10:00-12:30 , 13:45-15:30	No Clouds
6-Dec				
7-Dec	○	○	12:15-15:30	No Clouds
8-Dec	○		12:30-15:00	
9-Dec	○	○	11:00-12:30	
10-Dec				
11-Dec	○	○	11:30-14:30	No Clouds
12-Dec	○	○	10:30-12:30 , 13:30-15:00	No Clouds
13-Dec				
14-Dec				
15-Dec				
16-Dec				

(4) Results

Fig 6.3.1-3 shows the temporal variation of optical thickness of aerosols at 865 nm. Data obtained on two clear days are chosen as a preliminary result. On 2 December the aerosol optical thickness has small variations at around 0.04, while on 3 December the aerosol optical thickness has small variations at around 0.03.

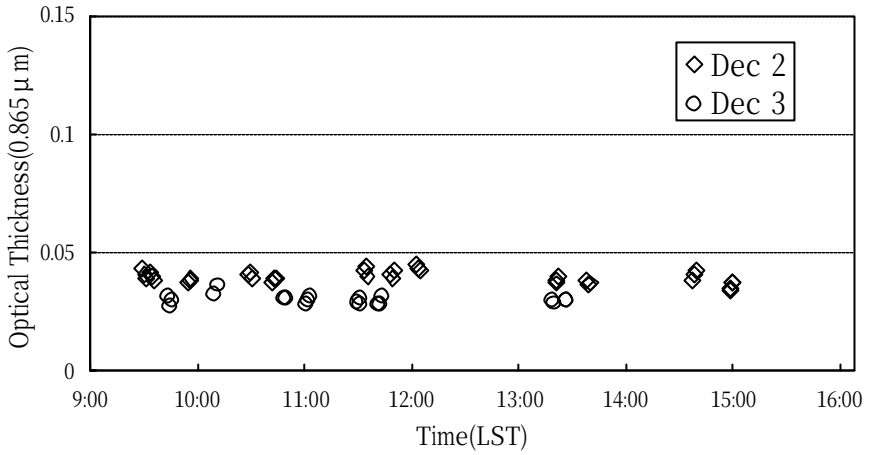

Fig. 6.3.1-3: Time variation of aerosol optical thickness at 865 nm.

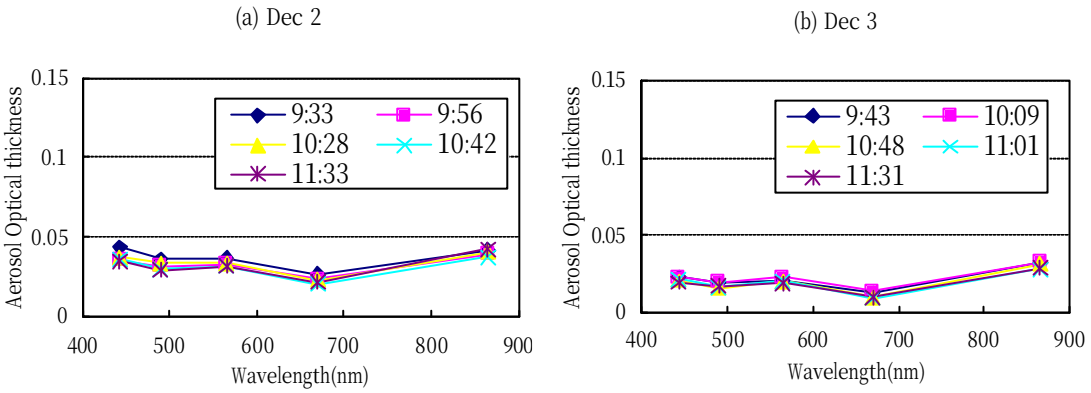

Fig. 6.3.1-4: Spectral aerosol optical thickness on (a) 2 December, and (b) 3 December.

Fig 6.3.1-4 (a) and (b) show the wavelength dependence of the aerosol optical thickness at the same days of Fig. 6.3.1-3. There is a small dependence of the optical thickness on wavelength. The wavelength dependence can be related to the size distribution of aerosols (e.g. small variations for large natural originated aerosols while large variations for small anthropogenic aerosols). From the preliminary results shown in Fig 6.3.1-4, the distribution of large naturally originated aerosols (like oceanic aerosols) can be identified.

Fig 6.3.1-5 (a) and (b) show the degrees of polarization with wavelengths. These polarization measurements can be utilized for the retrieval of aerosol parameters, which cannot be retrieved only with radiance data (direct sunlight measurements).

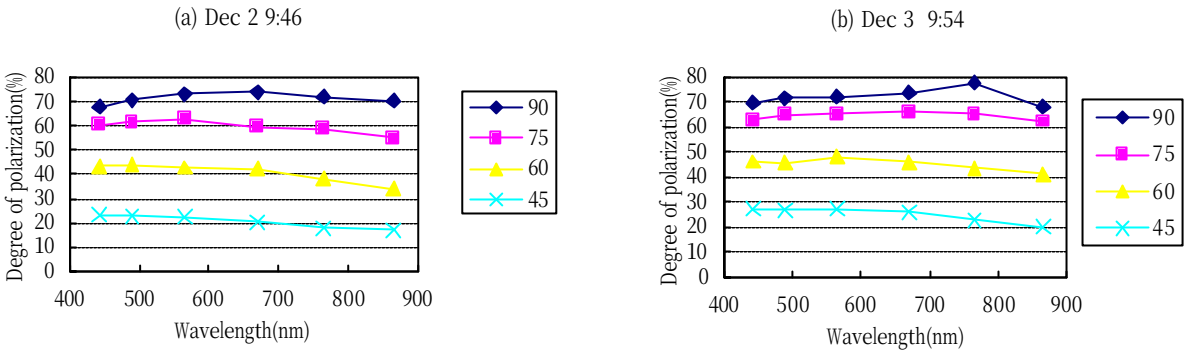

Fig. 6.3.1-5: Degree of polarization with different observed angles on (a) 2 December, and (b) 3 December (Legends show the degree from the sun direction).

(5) Data Archive

All the data obtained during this cruise are archived at Kinki University and Kobe University of Mercantile Marine, and will be open to public after quality checks and required corrections. The corrected data will be submitted to JAMSTEC Data Management Office.

6.3.2 Sky Radiometer

(1) Personnel

Tatsuo ENDOH (Institute of Low Temperature Science, Hokkaido University)

(2) Objectives

One of the most important objects is the collection of calibration and validation data from the surface (Nakajima et al.1996, 1997 and 1999). It may be considered for the observation over the widely opening of the huge ocean to be desired ideally because of horizontal homogeneity. Furthermore, the back ground values of aerosol concentration are easily obtained over there (Ohta et al.1996, Miura et al. 1997 and Takahashi et al. 1996) and vertical profile of aerosol concentration are obtained by means of extrapolation up to the scale height. It is desired to compare the integrated value of these profiles of aerosol concentration with optical thickness observed by the optical and radiative measurement (Hayasaka et al. 1998, Takamura et al.1994). Facing this object, the optical and radiative observations were carried out by mean of the Sky Radiometer providing more precise radiation data as the radiative forcing for global warming.

(3) Methods

The instruments used in this work are shown as following in Table 6.3.2-1.

Sky Radiometer was measuring irradiating intensities of solar radiation through seven different filters with the scanning angle of 2-140 degree. These data will provide finally optical thickness, Ångström exponent, single scattering albado and size distribution of atmospheric aerosols with a kind of retrieval method.

Optical Particle Counter was measuring the size of large aerosol particle and counting the number concentration with laser light scattering method and providing the size distribution in 0.3,0.5,1.0,2.0 and 5.0 micron of diameter with real time series display graphically.

(4) Results

Information of data and sample obtained are summarized in Table 6.3.2-2. The sky radiometer has been going well owing to more calm and silent condition and circumstances about shivering problems provided by the R/V Mirai whose engines are supported by well defined cushions. Therefore, measured values will be expected to be considerably stable and provide good calculated parameters in higher quality. However, some noise waves were found to interfere the 16,13 and 12channel marine bands of VHF from sky radiometer. Fortunately the origin and source were identified by using a VHF wide band receiver and the interference waves were kept by fairly separating from two VHF antennae and decreased to recovery of 100%.

Aerosols size distribution of number concentration have been measured by the Particle Counter and data obtained are displayed in real time by a kind of time series *in situ* with 5stages of size range of 0.3, 0.5, 1.0, 2.0, and 5.0 micron in diameter.

(6) Data archive

This aerosol data by the Particle Counter will be able to be archived soon and anytime. However, the data of other kind of aerosol measurements are not archived so soon and developed, examined ,

arranged and finally provided as available data after a certain duration. All data will archived at ILTS (Endoh), Hokkaido University, CCSR(Nakajima), University of Tokyo and CEReS (Takamura), Chiba University. The quality-checked dataset will be submitted to JAMSTEC within 3-year.

(7) References

Takamura, T., et al., 1994: Tropospheric aerosol optical properties derived from lidar, sun photometer and optical particle counter measurements. Applied Optics, Vol. 33, No. 30,7132-7140.

Hayasaka, T., T. Takamura, et al., 1998: Stratification and size distribution of aerosols retrieved from simultaneous measurements with lidar, a sunphotometer, and an aureolemeter. Applied Optics, 37(1998), No 6, 961-970.

Nakajima, T., T. Endoh and others(7 parsons) 1999: Early phase analysis of OCTS radiance data for aerosol remote sensing., IEEE Transactions on Geoscience and Remote Sensing, Vol. 37, No. 2, 1575-1585.

Nakajima, T., et al., 1997: The current status of the ADEOS-II/GLI mission. Advanced and Next-generation Satellites, eds. H. Fujisada, G . Calamai, M. N. Sweeting, SPIE 2957, 183-190.

Nakajima, T., and A. Higurashi, 1996: AVHRR remote sensing of aerosol optical properties in the Persian Gulf region, the summer 1991. J . Geophys. Res., 102, 16935-16946.

Ohta, S., et al., 1997: Variation of atmospheric turbidity in the area around Japan. Journal of Global Environment Engineering, Vol.3, 9-21.

Ohta, S., et al., 1996: Chemical and optical properties of lower tropospheric aerosols measured at Mt. Lemmon in Arizona, Journal of Global Environment Engineering,Vol.2,67-78.

Takahashi, T., T. Endoh, et al., 1996: Influence of the growth mechanism of snow particles on their chemical composition. Atmospheric Environment, Vol.30, No. 10/11, 1683-1692.

Miura, K., S. Nakae, et al.,: Optical properties of aerosol particles over the Western Pacific Ocean, Proc. Int. Sym. Remote Sensing, 275-280, 1997.

Table 6.3.2-1: Information of obtained data inventory (Method)

Item, No.data	Name	Instrument	Site position
Optical thickness Ångström exponent.	Endoh	Sky Radiometer (Prede,POM-01MK2)	roof of stabilizer
Aerosol Size distribution	Endoh	Particle Counter (Rion,KC-01C)	compass deck(inlet) & environmental research laboratory

Table 6.3.2-2: Data and Sample inventory

Data/Sample	rate	site	object	name	state	remarks
Sun & Sky Light	1/5min (fine& daytime)	roof of stabilizer	optical thickness Ångström expt.	Endoh	land analysis	11/13'02-11/19'01
Size distribution of aerosols	1/2.5min	compass deck	concentration of aerosols	Endoh	on board	11/13'01-11/19'01

6.4 Surface Atmospheric Turbulent Flux

(1) Personnel

Tetsuya Takemi (Osaka University): On-board leader
Satoshi Takahashi (Okayama University)
Kyoko Harada (Okayama University)
Daisuke Taniguchi (Okayama University)

On-shore scientists:
Osamu Tsukamoto (Okayama University): Principal Investigator
Hiroshi Ishida (Kobe University of Mercantile Marine/
Frontier Observational Research System for Global Change)

(2) Objective

For the understanding of air-sea interaction, accurate measurements of surface heat and fresh water budgets are necessary as well as momentum exchange through the sea surface. In addition to these exchanges, the evaluation of carbon dioxide surface flux is also indispensable for the study of global warming. Sea surface turbulent fluxes of momentum, sensible heat, latent heat (water vapor), and carbon dioxide were measured by using the eddy correlation method that is believed to be most accurate and free from assumptions. These surface heat flux data are combined with radiation fluxes and water temperature profiles to derive the surface energy budget.

(3) Methods

The surface turbulent flux system consists of turbulence instruments (Kaijo Co., Ltd.) and ship motion sensors (Kanto Aircraft Instrument Co., Ltd.). The turbulence sensors are installed at the top of the foremast. A three-dimensional sonic anemometer-thermometer (Kaijo, DA-600) has been in operation since June 2000 (MR00-K04), and an infrared hygrometer (LICOR, LI-7500) (which replaced a Kaijo's AH-300) since May 2002. The sonic anemometer measures three-dimensional wind components relative to the ship including apparent wind velocity due to ship motion. The ship motions are independently measured by ship motion sensors, including a two-axis inclinometer (Applied Geomechanics, MD-900-T), a three-axis accelerometer (Applied Signal Inc., QA-700-020), and a three-axis rate gyro (Systron Donner, QRS-0050-100). LI7500 is a CO2/H2O turbulence sensor that measures turbulent signals of carbon dioxide and water vapor simultaneously. Fig. 6.4-1 shows the installation of the instruments at the top of the foremast.

These turbulence and ship motion signals are sampled at 10 Hz by a PC-based data logging system (Labview, National Instruments Co., Ltd.). This PC system is connected to the Mirai network system to obtain ship speed and heading data that are used to derive absolute wind components relative to the ground. Combining these wind data with the turbulence measurements, turbulent fluxes and statistics are calculated in a real-time basis and displayed on the PC. During the cruise, we have upgraded the Labview software to be more robust against network failures. After this upgrade, the processing software has been running successfully without any system errors.

During the stationary observation period, a ship maneuvering suitable for the turbulence measurements (i.e., Mirai runs against wind direction at 5-8 knot) was operated every three hour for about 1-1.5 hour (after CTD casting). This special maneuvering is quite important for the ship-borne flux evaluation systems since without the maneuvering the dynamical and thermal

effects of the ship's body would work unfavorably for the accurate flux evaluations.

On 20 and 21 November no observations were conducted because Mirai was in the EEZs of Palau and Indonesia.

(4) Preliminary Results

The continuous measurements of turbulent fluctuations were carried out throughout the present cruise. Three-hourly ship operations for turbulent flux measurements during the stationary observation period were performed as listed in Table 6.4-1. Fig.6.4-2 shows the three-hourly surface fluxes of sensible heat and latent heat, and Fig.6.4-3 shows the carbon dioxide surface fluxes. The latent heat fluxes are much larger than the sensible heat fluxes, which is consistent with the previous studies over oceanic areas. The carbon dioxide fluxes are generally negative (downward flux), which means that the present location in the tropical western Pacific is a CO2 sink.

(5) Data Archive

All the data obtained during this cruise are archived at Okayama University, and will be open to public after quality checks and corrections. Interested scientists should contact Prof. Osamu Tsukamoto at Okayama University. The corrected data and inventory information will be submitted to JAMSTEC Data Management Office.

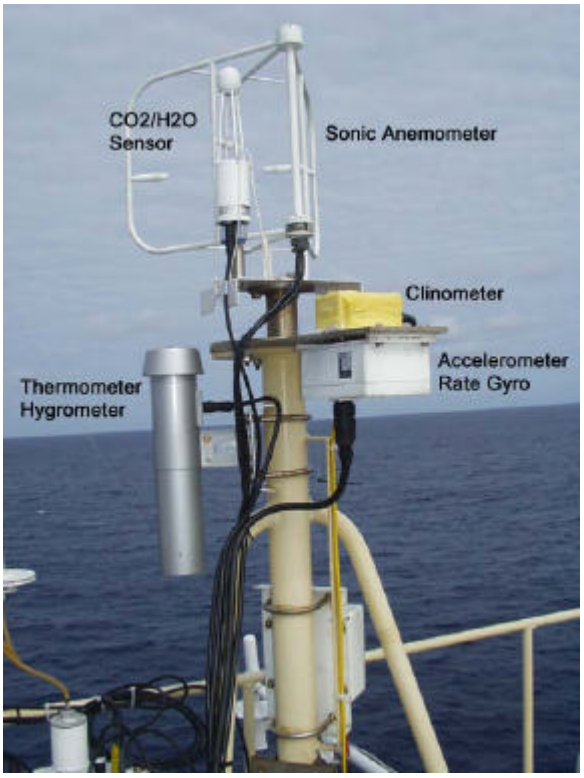

Fig.6.4-1: The installation of the turbulence measurements sensors at the top of the foremast.

Table 6.4-1: List of flux measurements. All the times are Japan Standard Time.

28-Nov	0:16	1:50	1:34	cloudy
	3:14	4:50	1:36	
	6:14	7:45	1:31	fine
	9:43	10:40	0:57	cloudy
	12:11	13:40	1:29	fine
	15:15	16:40	1:25	cloudy
	18:14	19:42	1:28	cloudy
	21:44	22:50	1:06	cloudy
29-Nov	0:16	1:45	1:29	fine
	3:13	4:45	1:32	
	6:14	7:45	1:31	cloudy
	9:09	10:46	1:37	fine
	12:10	12:55	0:45	fine
	15:13	16:48	1:35	fine
	18:13	19:30	1:17	cloudy
	21:26	22:50	1:24	fine
30-Nov	0:14	1:43	1:29	fine
	3:12	4:36	1:24	
	6:13	7:46	1:33	fine
	9:25	10:50	1:25	fine
	12:12	13:47	1:35	fine
	15:11	16:45	1:34	fine
	18:10	19:40	1:30	fine
	21:39	22:45	1:06	fine
1-Dec	0:16	1:40	1:24	fine
	3:16	4:40	1:24	
	6:14	7:40	1:26	fine
	9:25	10:30	1:05	fine
	12:12	13:40	1:28	fine
	15:10	16:45	1:35	fine
	18:10	19:37	1:27	fine
	21:28	22:50	1:22	fine
2-Dec	0:13	1:40	1:27	fine
	3:14	4:45	1:31	
	6:12	7:45	1:33	fine
	9:41	10:35	0:54	fine
	12:12	13:40	1:28	fine
	15:08	16:46	1:38	fine
	18:12	19:38	1:26	fine
	21:52	22:48	0:56	fine
3-Dec	0:12	1:40	1:28	fine
	3:12	4:45	1:33	fine
	6:10	7:45	1:35	fine
	9:10	10:40	1:30	fine
	12:10	13:30	1:20	fine
	15:11	16:43	1:32	fine
	18:10	19:38	1:28	fine
	21:35	22:47	1:12	fine

28-Nov	0:16	1:50	1:34	cloudy
	3:14	4:50	1:36	
	6:14	7:45	1:31	fine
	9:43	10:40	0:57	cloudy
	12:11	13:40	1:29	fine
	15:15	16:40	1:25	cloudy
	18:14	19:42	1:28	cloudy
	21:44	22:50	1:06	cloudy
29-Nov	0:16	1:45	1:29	fine
	3:13	4:45	1:32	
	6:14	7:45	1:31	cloudy
	9:09	10:46	1:37	fine
	12:10	12:55	0:45	fine
	15:13	16:48	1:35	fine
	18:13	19:30	1:17	cloudy
	21:26	22:50	1:24	fine
30-Nov	0:14	1:43	1:29	fine
	3:12	4:36	1:24	
	6:13	7:46	1:33	fine
	9:25	10:50	1:25	fine
	12:12	13:47	1:35	fine
	15:11	16:45	1:34	fine
	18:10	19:40	1:30	fine
	21:39	22:45	1:06	fine
1-Dec	0:16	1:40	1:24	fine
	3:16	4:40	1:24	
	6:14	7:40	1:26	fine
	9:25	10:30	1:05	fine
	12:12	13:40	1:28	fine
	15:10	16:45	1:35	fine
	18:10	19:37	1:27	fine
	21:28	22:50	1:22	fine
2-Dec	0:13	1:40	1:27	fine
	3:14	4:45	1:31	
	6:12	7:45	1:33	fine
	9:41	10:35	0:54	fine
	12:12	13:40	1:28	fine
	15:08	16:46	1:38	fine
	18:12	19:38	1:26	fine
	21:52	22:48	0:56	fine
3-Dec	0:12	1:40	1:28	fine
	3:12	4:45	1:33	fine
	6:10	7:45	1:35	fine
	9:10	10:40	1:30	fine
	12:10	13:30	1:20	fine
	15:11	16:43	1:32	fine
	18:10	19:38	1:28	fine
	21:35	22:47	1:12	fine

Table 6.4-1: (continued)

4-Dec	0:12	1:43	1:31	fine
	3:12	4:44	1:32	fine
	6:10	7:04	0:54	fine
	9:25	10:40	1:15	cloudy
	12:10	13:43	1:33	fine
	15:08	16:44	1:36	fine
	18:10	19:40	1:30	fine
	21:45	22:40	0:55	fine
5-Dec	0:14	1:44	1:30	fine
	3:11	4:38	1:27	
	6:10	7:37	1:27	cloudy
	9:25	10:40	1:15	fine
	12:10	13:43	1:33	fine
	15:10	16:40	1:30	fine
	18:13	19:38	1:25	fine
	21:37	22:50	1:13	fine
6-Dec	0:11	1:43	1:32	fine
	3:14	4:40	1:26	
	6:12	7:42	1:30	fine
	9:40	10:42	1:02	fine
	12:08	13:44	1:36	fine
	15:10	16:20	1:10	fine
	18:09	19:37	1:28	fine
	21:47	22:47	1:00	fine
7-Dec	0:11	1:46	1:35	fine
	3:10	4:38	1:28	
	6:10	7:35	1:25	fine
	9:09	10:23	1:14	fine
	12:09	13:41	1:32	fine
	15:09	16:58	1:49	fine
	18:11	19:45	1:34	fine
	21:31	22:47	1:16	fine
8-Dec	0:13	1:43	1:30	fine
	3:14	4:40	1:26	
	6:11	7:40	1:29	fine
	9:26	10:41	1:15	fine
	12:10	13:40	1:30	fine
	15:12	16:40	1:28	fine
	18:12	19:37	1:25	fine
	21:45	22:50	1:05	fine
9-Dec	0:17	1:40	1:23	fine
	3:13	4:38	1:25	
	6:11	7:45	1:34	fine
	9:22	10:47	1:25	fine
	12:10	13:43	1:33	fine
	15:10	16:40	1:30	fine
	18:10	19:30	1:20	fine
	21:32	22:45	1:13	fine
10-Dec	0:12	1:45	1:33	fine
	3:12	4:35	1:23	
	6:10	7:45	1:35	fine
	9:39	10:52	1:13	fine
	12:10	13:38	1:28	fine
	15:10	16:37	1:27	fine
	18:10	19:45	1:35	cloudy
	21:48	22:55	1:07	cloudy
11-Dec	0:15	1:45	1:30	fine
	3:15	4:40	1:25	
	6:11	7:43	1:32	fine
	9:51	10:32	0:41	fine
	12:10	13:45	1:35	fine
	15:11	16:40	1:29	fine
	18:10	19:45	1:35	fine
	21:32	22:46	1:14	fine
12-Dec	0:13	1:45	1:32	fine
	3:14	4:40	1:26	
	6:09	7:40	1:31	fine
	9:10	10:40	1:30	fine
	12:10	13:33	1:23	fine
	15:10	16:37	1:27	fine
	18:10	19:42	1:32	fine
	21:44	22:45	1:01	fine

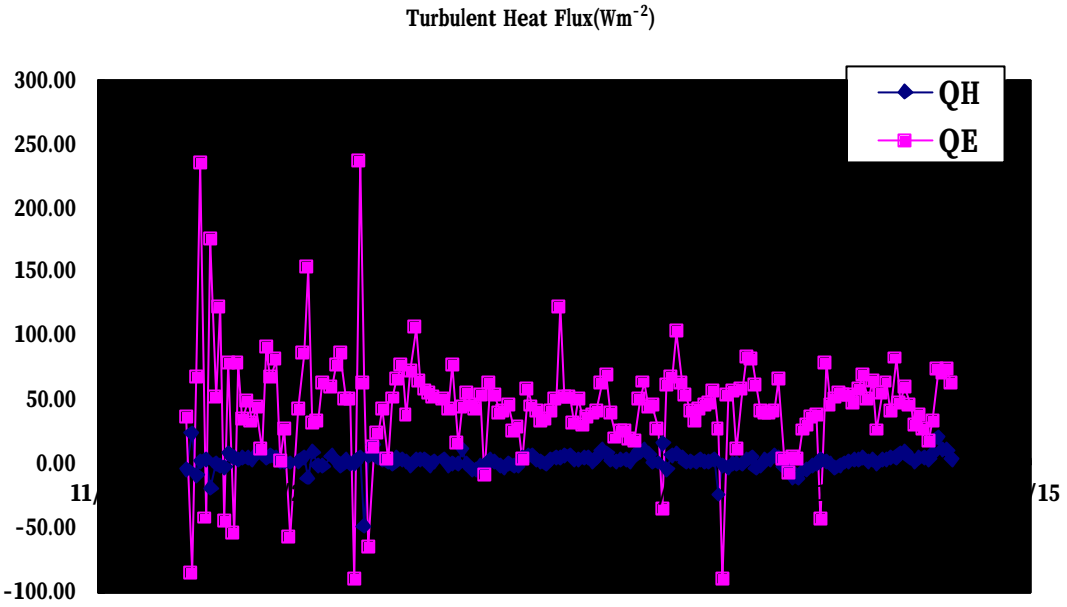

Fig.6.4-2: Time series of three-hourly turbulent fluxes of sensible heat (QH) and latent heat (QE) during the stationary observation period.

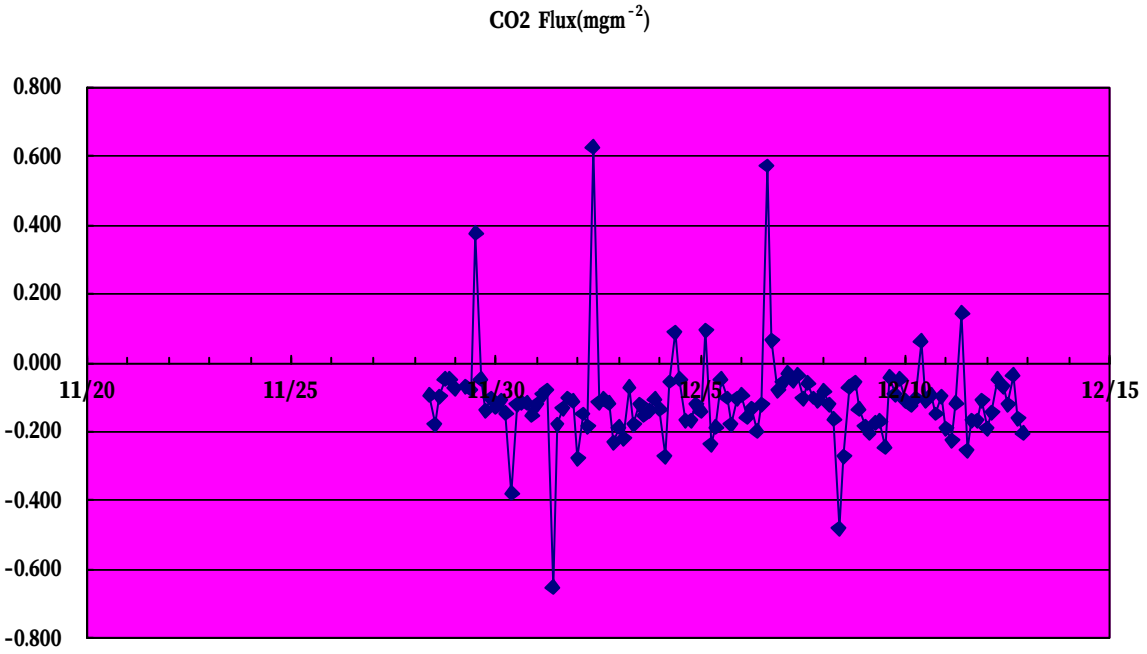

Fig.6.4-3: The same as Fig.6.4-2 except for CO2 fluxes. The data obtained before 27 November are omitted because they include many unreasonable values.

6.5 Surface Meteorological Parameters

(1) Personnel

Kunio Yoneyama	(JAMSTEC):	Principal Investigator
Masaki Katumata	(JAMSTEC)	
Masaki Hanyu	(GODI):	Operation Leader
Souichiro Sueyoshi	(GODI)	
Norio Nagahama	(GODI)	

(2) Objective

The surface meteorological parameters are observed as a basic dataset of the meteorology. These parameters bring us the information about temporal variation of the meteorological condition surrounding the ship.

(3) Methods

The surface meteorological parameters were observed throughout MR02-K06 leg1 cruise from the departure of Sekinehama on 13 November 2002 to the arrival of Guam on 16 December 2002, excluding EEZ of the Republics of Palau and Indonesia.

This cruise, we used 3 systems for the surface meteorological observation.

1. Mirai meteorological observation system
2. Shipboard Oceanographic and Atmospheric Radiation (SOAR) system
3. Total Sky Imager (TSI)

(3-1) Mirai meteorological observation system

Instruments of Mirai meteorological system are listed in Table 6.5-1 and measured parameters are listed in Table 6.5-2. Data was collected and processed by KOAC-7800 weather data processor made by Koshin Denki, Japan. The data set has 6-second averaged every 6-second record and 10-minute averaged every 10-minute record.

Table 6.5-1: Instruments and their installation locations of Mirai met system

sensors	type	manufacturer	location (altitude from surface)
anemometer	KE-500	Koshin Denki, Japan	foremast (24m)
thermometer	FT	Koshin Denki, Japan	compass deck (21m)
	RFN1-0	Koshin Denki, Japan	4th deck (-1m, inlet -5m) SST
dewpoint meter	DW-1	Koshin Denki, Japan	compass deck (21m)
barometer	F-451	Yokogawa, Japan	weather observation room
			captain deck (13m)
rain gauge	50202	R. M. Young, USA	compass deck (19m)
optical rain gauge	ORG-115DR	Osi, USA	compass deck (19m)
radiometer (short wave)	MS-801	Eiko Seiki, Japan	radar mast (28m)
radiometer (long wave)	MS-202	Eiko Seiki, Japan	radar mast (28m)
wave height meter	MW-2	Tsurumi-seiki, Japan	bow (10m)

Table 6.5-2: Parameters of Mirai meteorological observation system

	Parameters	Units	Remarks
1	latitude	degree	
2	longitude	degree	
3	ship's speed	knot	Mirai log, DS-30 Furuno
4	ship's heading	degree	Mirai gyro, TG-6000, Tokimec
5	relative wind speed	m/s	6 sec./10 min. averaged
6	relative wind direction	degree	6 sec./10 min. averaged
7	true wind speed	m/s	conducted by 3/4/5/6
			6 sec./10 min. averaged
8	true wind direction	degree	conducted by 3/4/5/6
			6 sec./10 min. averaged
9	barometric pressure	hPa	adjusted to the sea surface level
			6 sec./10 min. averaged
10	air temperature (starboard side)	degC	6 sec./10 min. averaged
11	air temperature (port side)	degC	6 sec./10 min. averaged
12	dewpoint temperature (starboard side)	degC	6 sec./10 min. averaged
13	dewpoint temperature (port side)	degC	6 sec./10 min. averaged
14	relative humidity (starboard side)	%	6 sec./10 min. averaged
			conducted by 9/10/12
15	relative humidity (port side)	%	6 sec./10 min. averaged
			conducted by 9/11/13
16	sea surface temperature	degC	6 sec./10 min. averaged
17	rain rate (optical rain gauge)	mm/hr	hourly accumulation
18	rain rate (capacitive rain gauge)	mm/hr	hourly accumulation
19	down welling shortwave radiometer	W/m2	6 sec./10 min. averaged
20	down welling infra-red radiometer	W/m2	6 sec./10 min. averaged
21	significant wave height (fore)	m	hourly
22	significant wave period (fore)	second	hourly

(3-2) Shipboard Oceanographic and Atmospheric Radiation (SOAR) system

SOAR system, designed by BNL (Brookhaven National Laboratory, USA), is consisted of 3 parts.

1. Portable Radiation Package (PRP) designed by BNL – short and long wave down welling radiation
2. Zeno meteorological system designed by BNL – wind, Tair/RH, pressure and rainfall measurement
3. Scientific Computer System (SCS) designed by NOAA (National Oceanographic and Atmospheric Administration, USA) – centralized data acquisition and logging of all data sets SCS recorded PRP data every 6.5 seconds, Zeno/met data every 10 seconds.

Instruments and their locations are listed in Table 6.5-3 and measured parameters are listed in Table 6.5-4

Table 6.5-3: Instrument installation locations of SOAR system

sensors	type	manufacturer	location (altitude from the baseline)
Zeno/Met			
anemometer	05106	R. M. Young, USA	foremast (25m)
T/RH	HMP45A	Vaisala, USA	foremast (24m)
	with 43408 Gill aspirated radiation shield (R. M. Young)		
barometer	61201	R. M. Young, USA	foremast (24m)
	with 61002 Gill pressure port (R. M. Young)		
rain gauge	50202	R. M. Young, USA	foremast (24m)
optical rain gauge	ORG-815DA	Osi, USA	foremast (24m)
SSST	SST-100	BNL, USA	bow, 5m extention (-1cm)
	TRFN1-0	Koshin Denki, Japan	bow, 5m extention (-1cm)
	FT	Koshin Denki, Japan	bow, 5m extention (-1cm)
PRP			
radiometer (short wave)	PSP	Eppley labs, USA	foremast (25m)
radiometer (long wave)	PIR	Eppley labs, USA	foremast (25m)
fast rotating shadowband radiometer		Yankee, USA	foremast (25m)
Upwelling radiation			
radiometer (short wave)	MS-801	Eiko Seiki, Japan	bow, 8m extention (10m)
radiometer (long wave)	MS-202	Eiko Seiki, Japan	bow, 8m extention (10m)

Table 6.5-4: Parameters of SOAR system

	Parameters	Units	Remarks
1	Latitude	degree	
2	Longitude	degree	
3	Sog	knot	
4	Cog	degree	
5	Relative wind speed	m/s	
6	Relative wind direction	degree	
7	Barometric pressure	hPa	
8	Air temperature	degC	
9	Relative humidity	%	
10	Rain rate (optical rain gauge)	mm/hr	
11	Precipitation (capacitive rain gauge)	mm	reset at 50mm
12	SSST	degC	- 1cm, Seasnake
13	Down welling shortwave radiation	W/m2	
14	Down welling infra-red radiation	W/m2	
15	Defuse irradiation	W/m2	
16	Upwelling short wave radiation	W/m2	
17	Upwelling long wave radiation	W/m2	

(3-2) Total Sky Imager (TSI)

The Total Sky Imager (TSI) was installed at the top deck midship, altitude of 17m from sea level. TSI was developed jointly by Penn Status University, BNL and Yankee Environmental Systems, Inc. and manufactured by YES Inc. TSI recorded every 5 minutes from dawn to sunset. Measured parameters are listed in Table 6.5-5.

Table 6.5-5: Parameters of TSI system

	Parameters	Unit
1	Opaque cloud cover	%
2	Thin cloud cover	%

(4) Preliminary results

The daytime cloud cover ratio obtained from TSI during the stationary observation period, from 22 November 2002 to 12 December 2002 is shown in Figure 6.5-1. Tair (SOAR), SST (from EPCS), RH, rainfall intensity, pressure, solar radiation (from SOAR) and Wind (converted to U, V component, from SOAR), observed during the stationary observation are shown in Figure 6.5-2. In the figures, 30 minutes accumulated precipitation data from SOAR capacitive rain gauge was converted to the rainfall intensity and obvious noises were eliminated but not calibrated. Other figures show the uncorrected data at every 5 minutes.

(5) Data archives

These raw data will be submitted to the Data Management Office (DMO) in JAMSTEC just after the cruise.

(6) Remarks

(a) SSST and upwelling radiation sensors of SOAR system were deployed on 2310UTC November 21

(b) SSST sensors and observation periods are as follows:

SST-100 (BNL, U.S): 2310UTC Nov.21 to 1352UTC Nov.22
TRFN1-0 (Koshin Denki, Japan): 0922UTC Nov.26 to 1056UTC Nov.26
FT (Koshin Denki, Japan): 0531UTC Nov.30 to 1047UTC Dec.09

(c) Upwelling radiation was observed untill 2304UTC December 12.

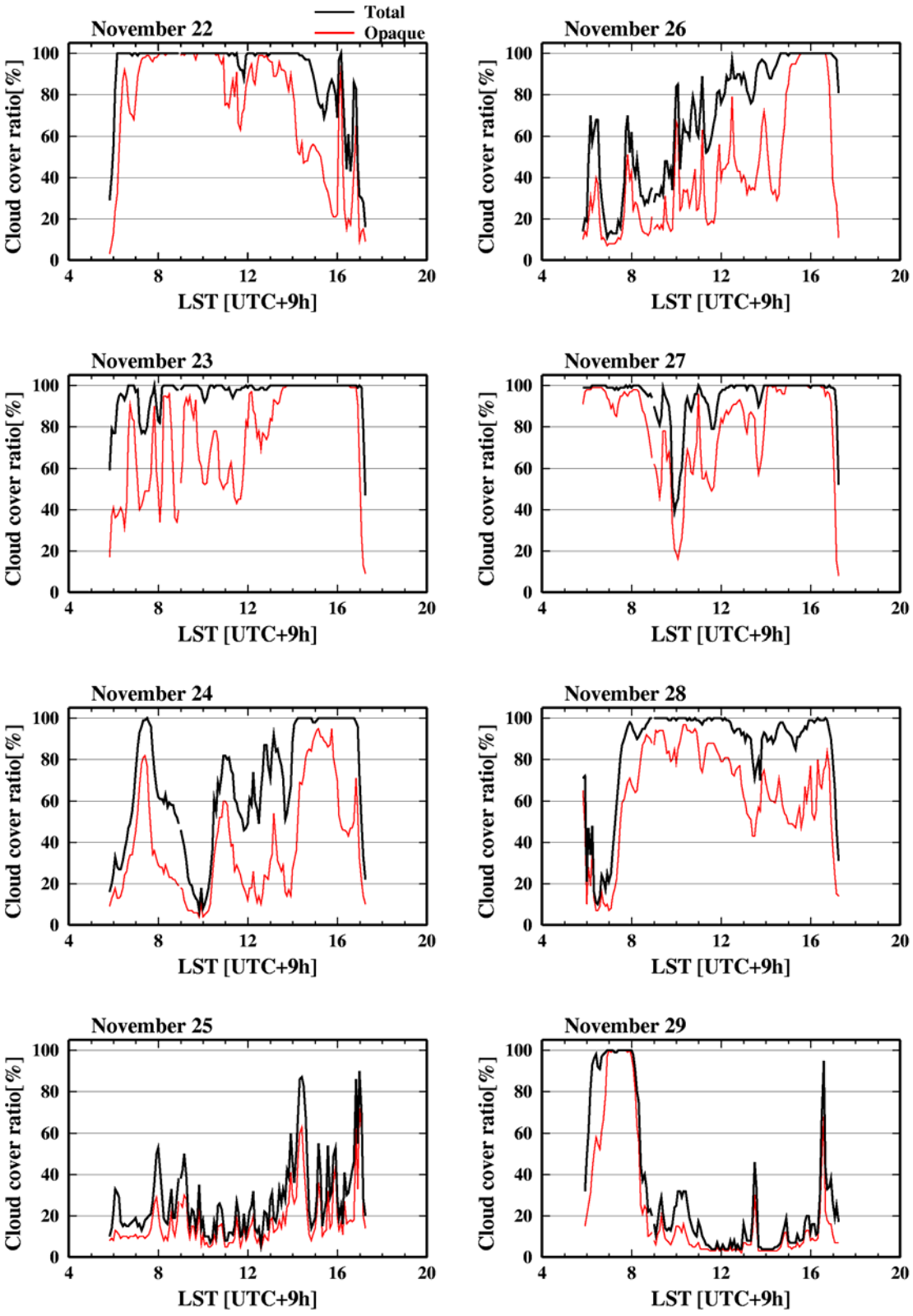

Figure 6.5-1: Daytime cloud cover ratio from TSI during the stationary observation.

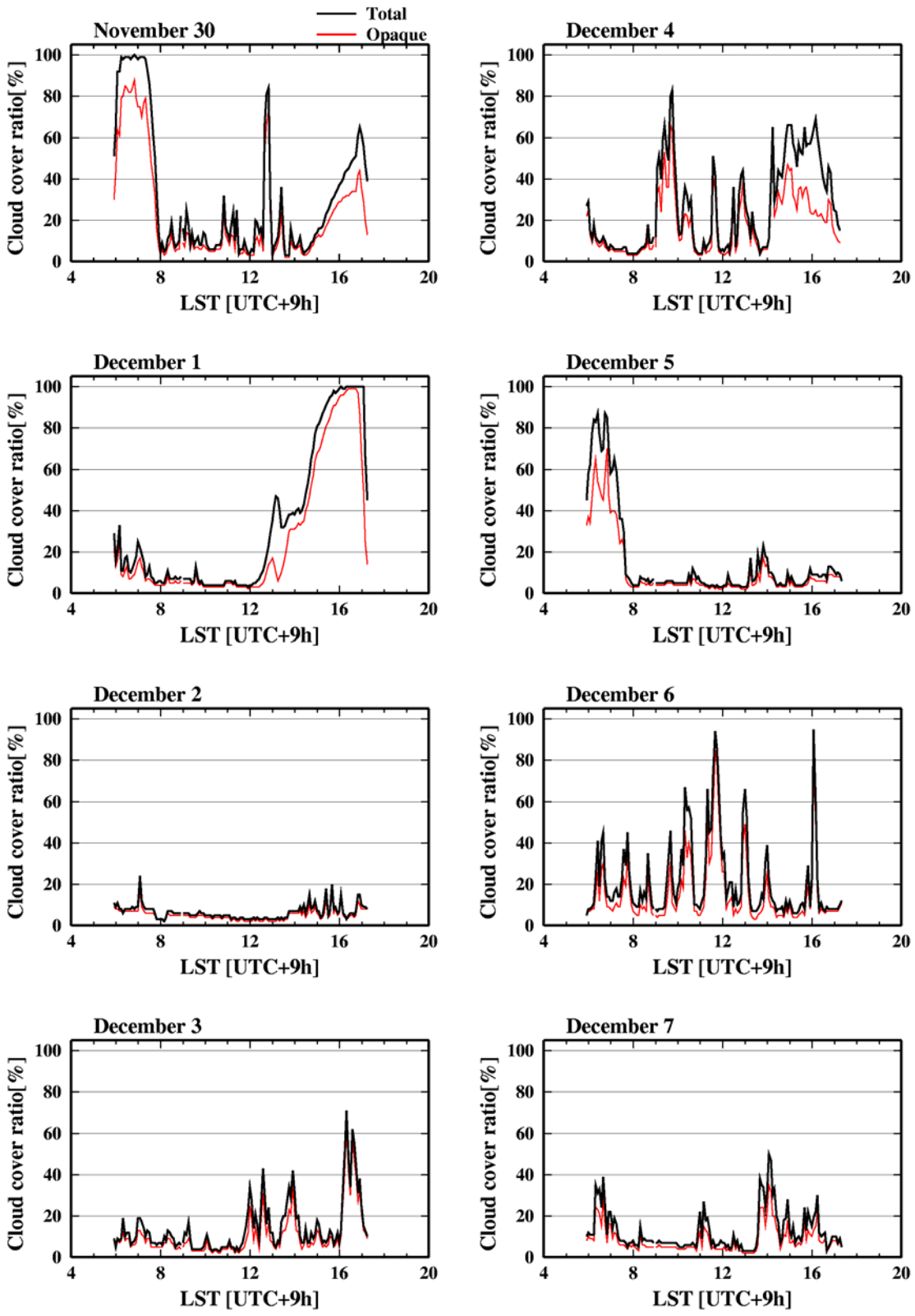

Figure 6.5-1: (continued)

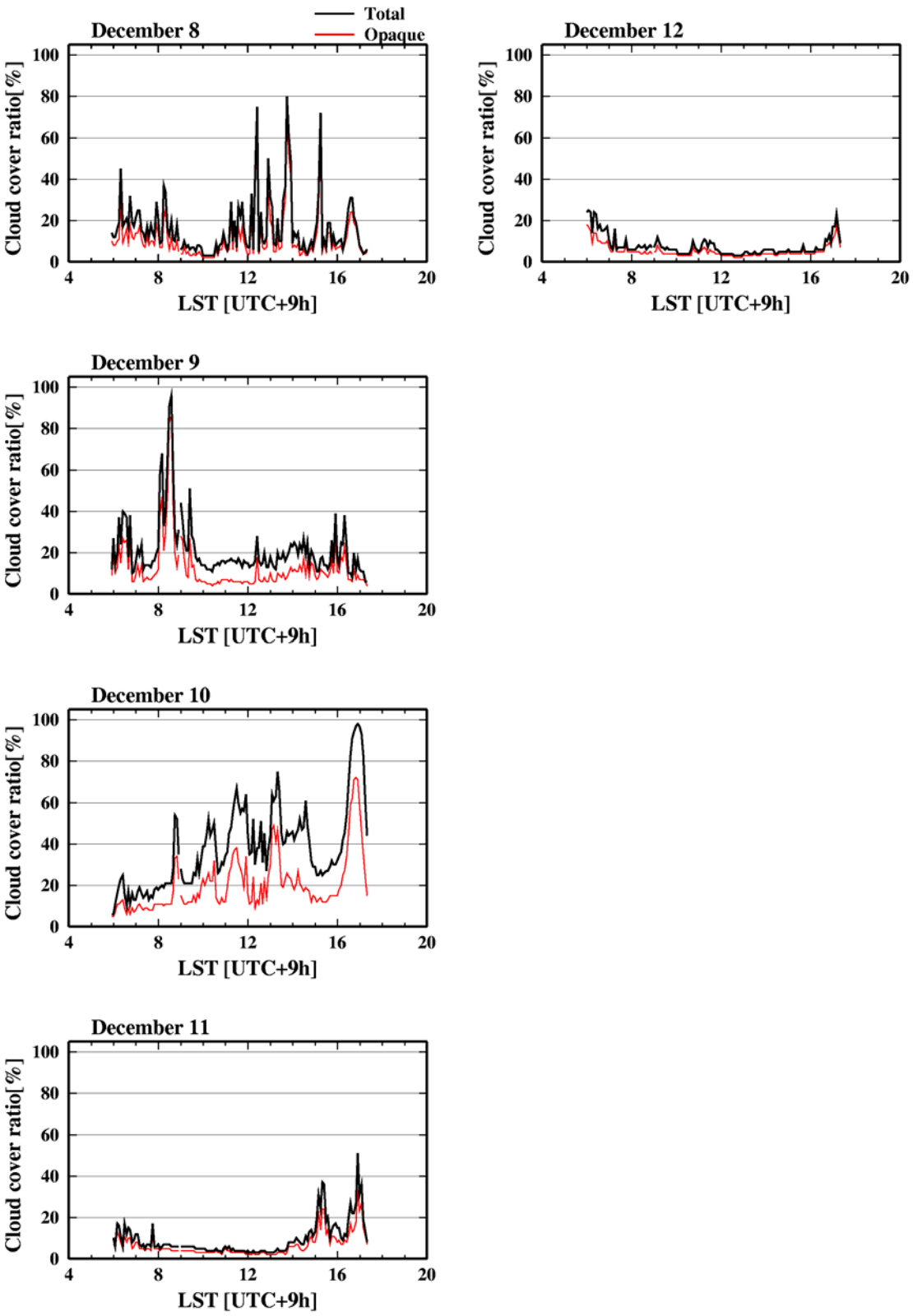

Figure 6.5-1: (continued)

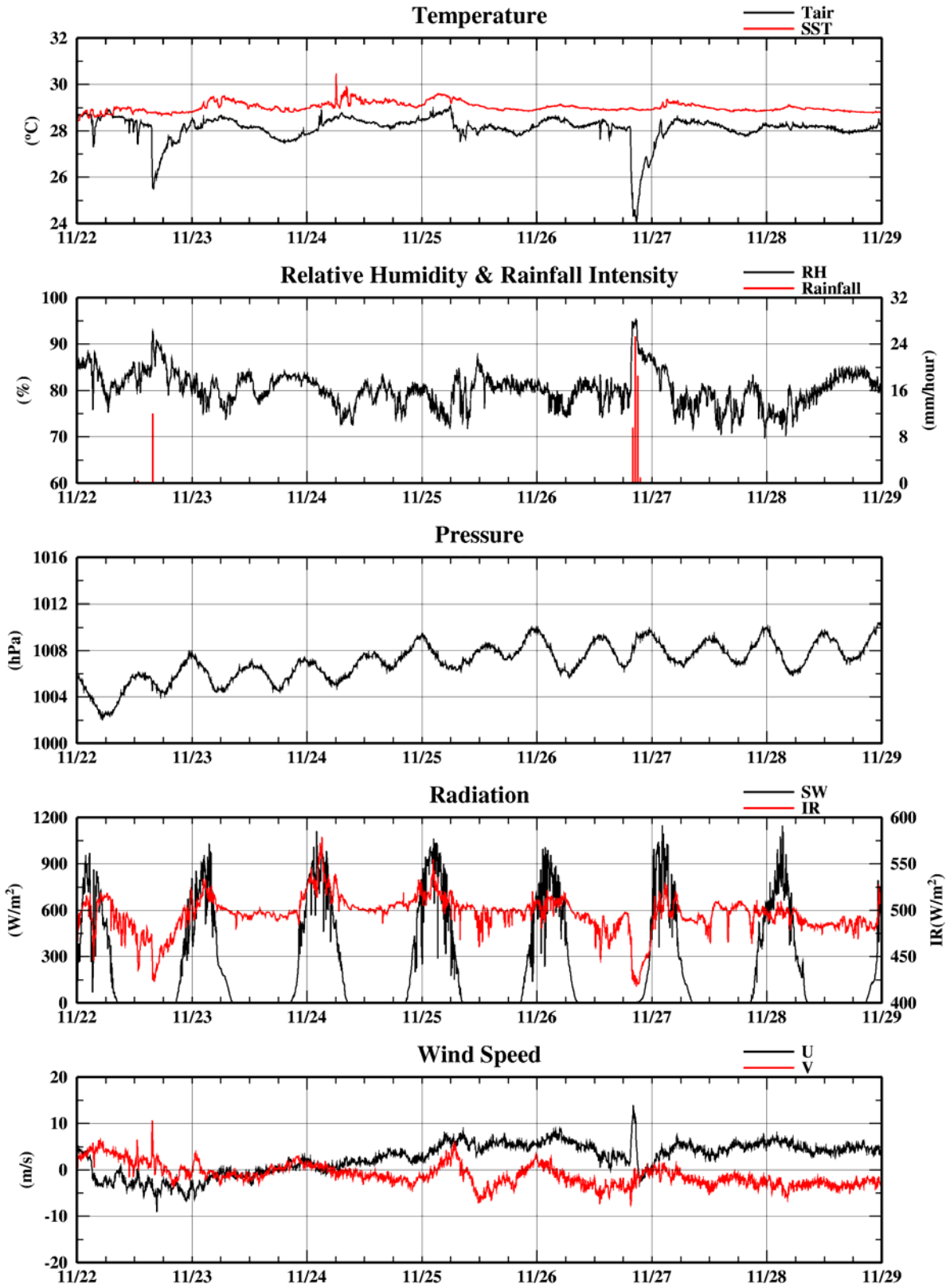

Figure 6.5-2: Time series of surface meteorological parameters during the stationary observation.

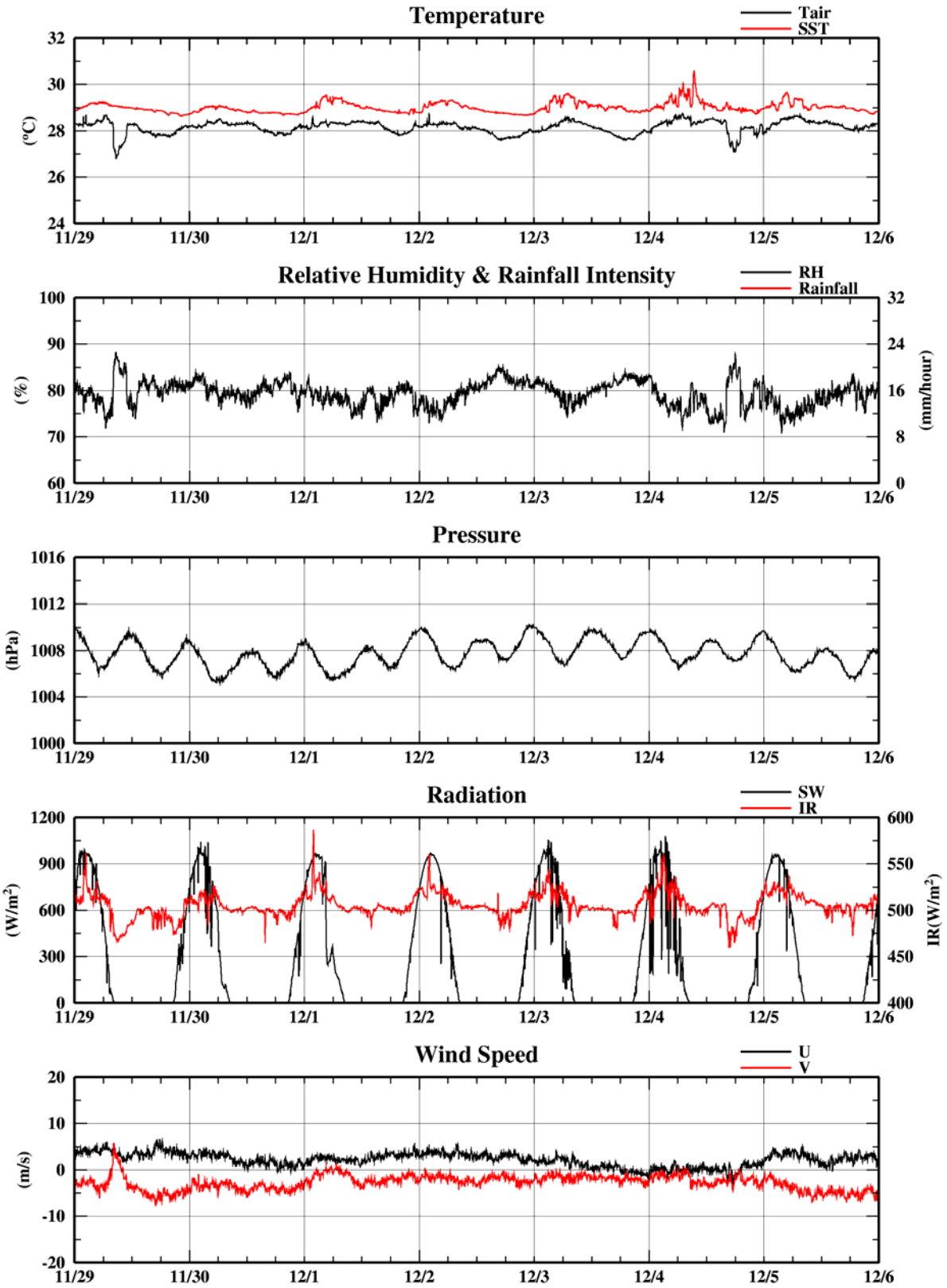

Figure 6.5-2: (continued)

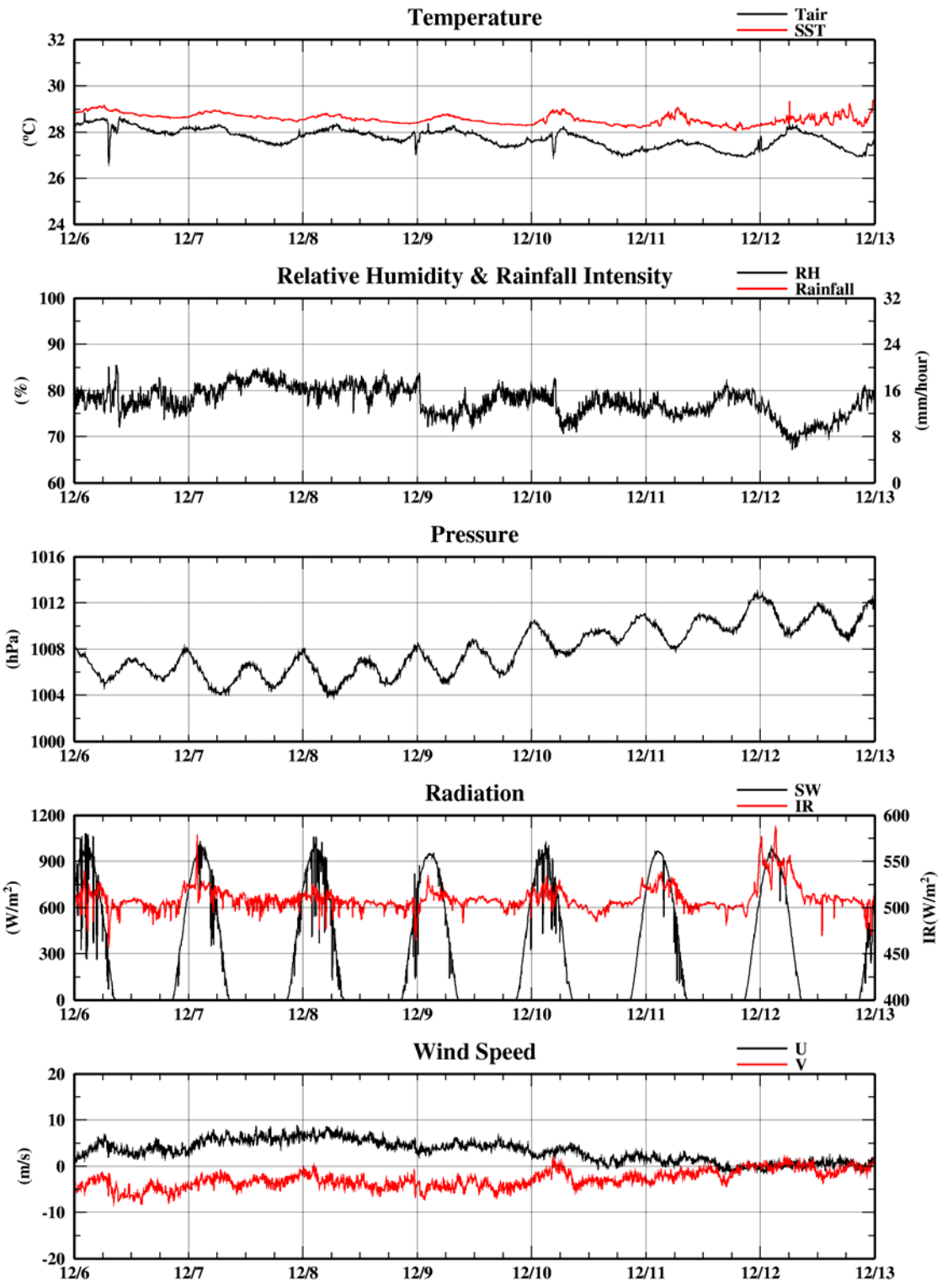

Figure 6.5-2: (continued)

6.6 Greenhouse Effect Gasses

6.6.1 CO_2, N_2O, NOx and SOx

(1) Personnel

Mitsuru HAYASHI (Maritime University of Kobe): Principal Investigator
Masakazu NAKAGAWA (Maritime University of Kobe)
Takehiro SHIBUYA (Osaka University)

(2) Objective

N_2O (Nitrous oxide) and CO_2 (Carbon dioxide) gasses play important roles and function of the global warming. It is required to get more accurate information of those gasses exchanges between the sea and atmosphere in order to understand the mechanism of the global warming process. So we carried out measurements of N_2O and CO_2 concentrations in the atmosphere and sea water. And NOx and SOx concentrations in the atmosphere were measured as background data.

(3) Methods

N_2O, CO_2, NOx and SOx concentrations in the atmosphere were measurement using flowing analyzer. N_2O and CO2 concentrations in sea water were obtained by the babbling method.

N_2O analyzer : MODEL:46C (Thermo Environmental Instruments Inc.)
Accuracy : 10 % of full scale < 50 ppm (using 1ppm scale)
CO_2 analyzer : MODEL:VIA-510 (HORIBA Ltd.)
Accuracy: 0.5 % of full scale
NOx analyzer : MODEL:42C-TL (Thermo Environmental Instruments Inc.)
Accuracy : 0.05 ppb (using 50 ppb range)
SOx analyzer : MODEL:43C (Thermo Environmental Instruments Inc.)
Accuracy : 1 % of measuring value or 1 ppb

N_2O and CO_2 concentration in the atmosphere and surface sea water were measured during southward cruise from 15 Nov. 15 LMT to 19 Nov. 18 LMT. The sample air was intaken at the foremast about 11m height above the sea level, and surface sea water was intaken at about 5m depth.

Water sampling depth and day to measure N_2O concentration in sea water at 2N, 138.5E are showed below. Sea water was sampled by the niskin sampler and bucket.

Depth (db)	Day
0, 25, 50, 75, 100, 125, 150, 175, 200, 250, 300, 400, 500	26, 27 and 30 Nov. and 1, 4, 5, 8 and 9 Dec.
0, 50, 100, 150, 200, 350, 450, 550, 600, 700, 800, 900, 1000	24 and 28 Nov. and 2, 6, 10 Dec.

NOx and SOx concentrations in the atmosphere were measured continuously from 16 Nov. to 12 Dec. except in the EEZ of The Republic of Palau and The Republic of Indonesia, and were collected to PC every 50 sec.

(4) Preliminary Results

Fig 6.6.1-1 shows N_2O and CO_2 concentrations in the atmosphere and surface sea water from 12N to 35N. CO_2 concentrations in the atmosphere are higher than those in the surface sea water and those variation is very small (371 ppm to 378 ppm). CO_2 concentrations in the surface sea water increased from 315 ppm to 354 ppm. N_2O concentrations in the atmosphere are almost higher than those in the surface sea water and varied from 235 ppb to 290 ppb. N_2O concentrations in surface sea water varied from 175 ppb to 283 ppb.

Fig.6.6.1-2 shows the vertical distributions of N_2O concentrations from surface to 1,000 db in depth from 24 Nov. to 10 Dec. at 2N, 138.5E. N_2O concentrations tend to increase from surface to 250 db in depth and are variable from 250 db to 1000db in depth.

All observational data will be analyzed in detail later.

(5) Data Archive

The data are archived in MO disks and will have a quality check in Maritime University of Kobe, and will be distributed to public later. The raw data is submitted to JAMSTEC DMO.

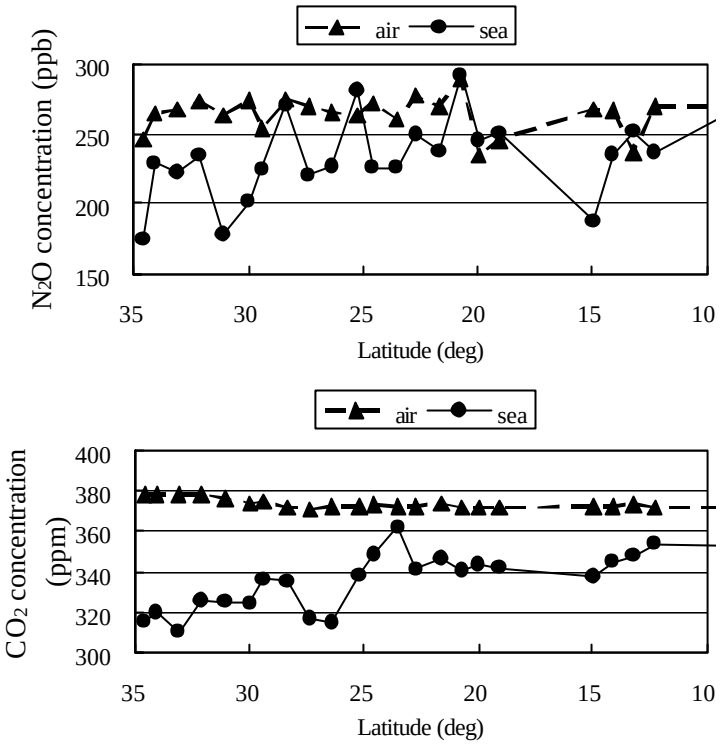

Fig 6.6.1-1 N_2O and CO_2 concentrations in the atmosphere and surface sea water.

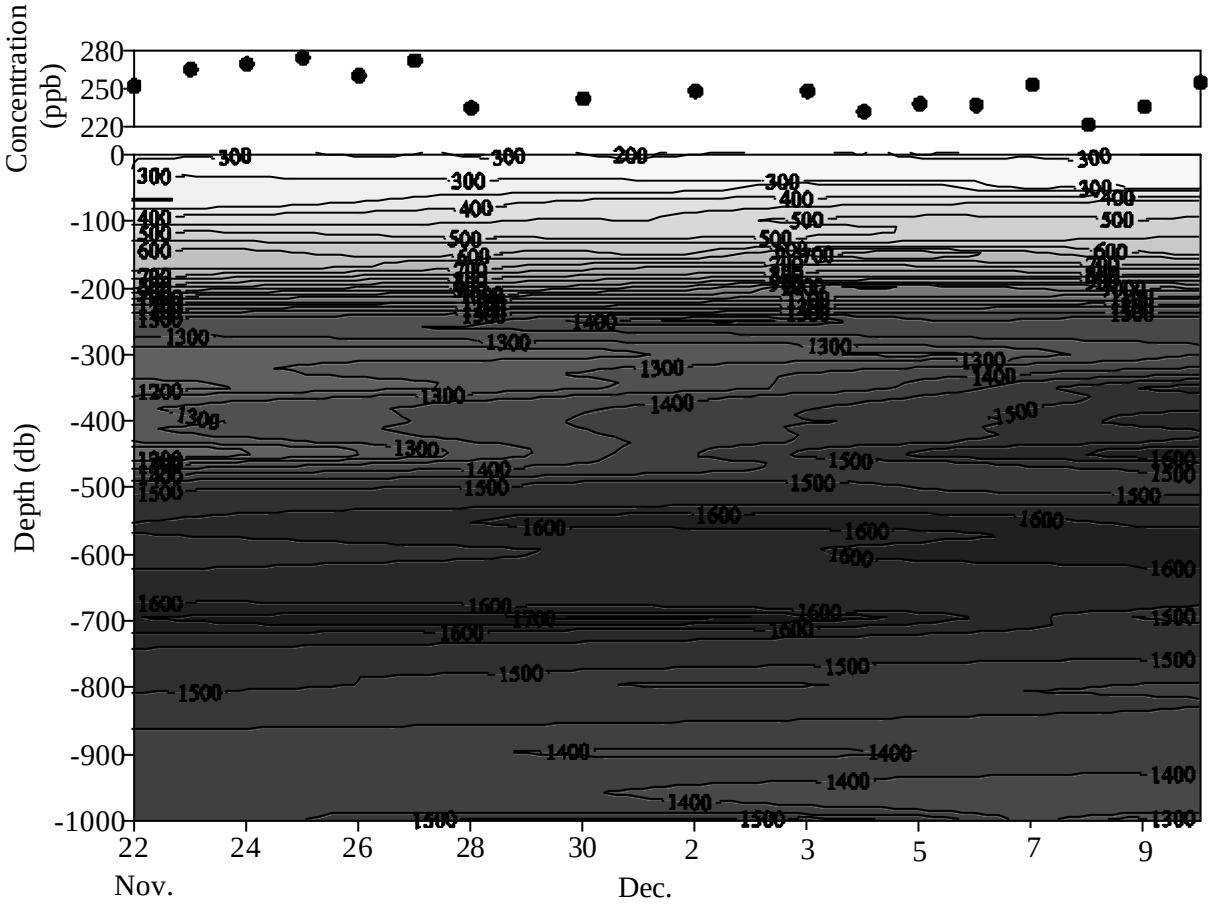

Fig.6.6.1-2 N_2O concentrations in air and the vertical distribution of N_2O in sea water from 24 Nov. to 2 Dec.

6.6.2 Surface Atmospheric / Oceanic CO_2

(1) Personnel

Masao Ishii (MRI): Principal Investigator
Hisayuki Y. Inoue (Hokkaido University)
Koichi Goto (KANSO): Operation Leader

(2) Objective

Carbon dioxide (CO_2), known as a major greenhouse gas, has been increasing in the atmosphere as a result of the anthropogenic emission. Its current concentration is approximately 30% higher than that in the pre-industrial era (280ppm). In order to predict the future atmospheric CO_2 variation due to anthropogenic emission and the potential alteration of the carbon cycle as a result of the climate change, it is necessary to understand the processes controlling CO_2 fluxes among the global carbon reservoirs, the atmosphere, the terrestrial biosphere and the ocean, as well as to estimate the present CO_2 inventory in these reservoirs.

The eastern and the central equatorial Pacific is now known to act as a significant source of the CO_2 to the atmosphere due primarily to the equatorial upwelling. The western equatorial Pacific, where warm water prevails in the surface layer, also occasionally exhibits a large CO_2 emission from the sea to the atmosphere. Flux of CO_2 from the equatorial Pacific has been reported to show a significant interannual variability that is associated with the ENSO event. However, the temporal and spatial variation in the whole CO_2 system in seawater enough to elucidate its controlling mechanism has not been well documented.

In this cruise, we made concurrent underway measurements of CO_2 concentration in the atmosphere and in surface seawater and total inorganic carbon (T CO_2) in surface seawater. The purpose of these observations is to describe the oceanic CO_2 system in the western equatorial Pacific and to clarify the controlling factors that are responsible for its variation in space and time as well as to investigate the air-sea CO_2 flux in this region.

(3) Methods

a) Underway measurements of CO_2 concentration in marine boundary air and in the air equilibrated with surface seawater :

We made measurements of the CO_2 concentration (mole fraction of CO_2 in air; χCO_2) in marine boundary air twice every 1.5 hour and that in air equilibrated with the great excess of surface seawater four times every 1.5 hour during the whole cruise except for EEZ of the Republic of Palau and the Republic of Indonesia using the automated CO_2 measuring system (Nippon ANS Co.). Marine boundary air was taken continuously from the foremast. Seawater was taken continuously from the bottom of ship located ca.5m below the sea level and introduced into the MRI-shower-type equilibrator.

Non-dispersive infrared (NDIR) gas analyzer (BINOS 4) was used as a detector. It was calibrated with four CO2 reference gases (299, 349, 399, 449 ppm in air, Nippon Sanso Co.) once every 1.5 hour. Concentration of CO_2 will be published on the scale that is traceable to the WMO X85 mole fraction scale. Corrections for the temperature-rise from the bottom of ship to the equilibrator and the drift of CO_2 concentration in reference gases are also to be made. Partial pressure of CO_2 will be calculated from χCO_2 by taking the water vapor pressure and the atmospheric pressure into account.

b) Underway measurements of total inorganic carbon (T CO_2) in surface seawater:

We made underway measurement of TCO2 in surface seawater using the automated T CO_2 analyzer (Nippon ANS Co.) equipped with carbon coulometer 5012 (UIC Co.). Seawater was taken continuously from the bottom of ship and a portion of the seawater (～22cm^3) was introduced into the water-jacketed pipette of the analyzer twice every 1.5 hours for analysis. We also analyzed T CO_2 in reference Seawaters prepared in MRI that is traceable to the CRM provided by Dr. A. Dickson in Scripps Institution of Oceanography. The analysis of the reference seawater was made at least once during the each run of the coulometric cathode- and anode-solution.

(4) Results

Data analysis will be made soon.

(5) Data Archive

The original data will be archived at Geochemical Research Department, Meteorological Research Institute. Data will be also submitted to Data Management Office at JAMSTEC within 3 years.

6.6.3 CO_2 Measurement

(1) Personnel name and affiliation

Eiji YAMASHITA (Okayama University of Science): Principle investigator
Takehiko KONO (Okayama University)
Tomohiko MACHIDA (Okayama University of Science)
Jun INOUE (Osaka University)

(2) Objective

The air-sea transport of CO_2 is driven by the difference between partial pressure of CO_2 in sea water (pCO_2) and that in the atmosphere (PCO_2).

Based on this cruise data, characteristics of the latitudinal distribution, time variation and vertical profile of pCO_2 are reported in the present paper.

(3) Instruments and Methods

pCO_2 and PCO_2 were measured using the CO_2 measurement system which is made by the S-ONE company. This system can continuously measure pCO_2 and PCO_2 every 30 minutes and can measure pCO_2 with only 500 ml of seawater sample. Sample sea water was pumped up continuously from the depth of 4.5 m. Sample air was taken from the foremast at 14 m height from the mean sea level through a teflon tube. We had measured from Nov. 13 to Dec. 12, 2002 except for Palau EEZ area. We checked the system everyday.

Sea water of vertical was sampled with the CTD-CMS casts and was stored in 500ml brown bottles and temperature was controlled at 27 - 29^{o}C before the analysis. Sampling depth was 0, 25, 50, 75, 100, 150, 200, 250, 300, 400, 500, 750 and 1000 m. We measured vertical distribution of pCO_2 in Nov.16, 17, 18, 24, 28, Dec.2, 6 , 10 and 13, 2002.

Specification of the carbon dioxide measurement system was listed below.

Unit 1: CO_2 analyzer Model: LI-6252 LI-COR, INC.
Serial number: IR-62-286, Measurement range: 0-5V.
Unit 2: Gas mixing unit. Model: SO96NL-T, S-ONE, INC.
Unit 3: CO_2 equilibrator. Model: SO96NL-T, S-ONE, INC.
Unit 4: Data processing equipment (personal computer)

(4) Results

Fig. 6.6.3-1 shows Latitudinal distribution of pCO_2 and PCO_2 along the 140^{o}E line. Blue and Red line are partial pressure of carbon dioxide in sea water and Atmosphere, respectively. Based on the pCO_2 latitudinal distribution measurements, it was found that CO_2 was absorbed from the atmosphere into the ocean in the study area except for 23^{o}N, 17^{o}N and in the south of 5^{o}N.

Fig.6.6.3-2 shows time variation of pCO_2 at the Station (2^{o}N, 138^{o}E) in November 22, 24, 26, 30, December 2, 4, 6 and 8, 2002. The pCO_2 concentrations were higher than concentrations of PCO_2 on this station. It is clearly observed that pCO_2 values show a time variation with high values in 12-24 hours and low values in 0-12 hours.

Fig.6.6.3-3 shows vertical profile of pCO_2 along the 140°E line. As a whole, pCO_2 increased with increasing the depth. The pCO_2 values of 1000m depth were about 2000 μ atm. This suggests that the main factor controling the vertical pCO_2 distribution is considered as biological pump.

(6) Data archive

The raw data were stored on a magnetic optical disk which will be kept on Ocean Research Department, JAMSTEC. The raw data will be corrected and published.

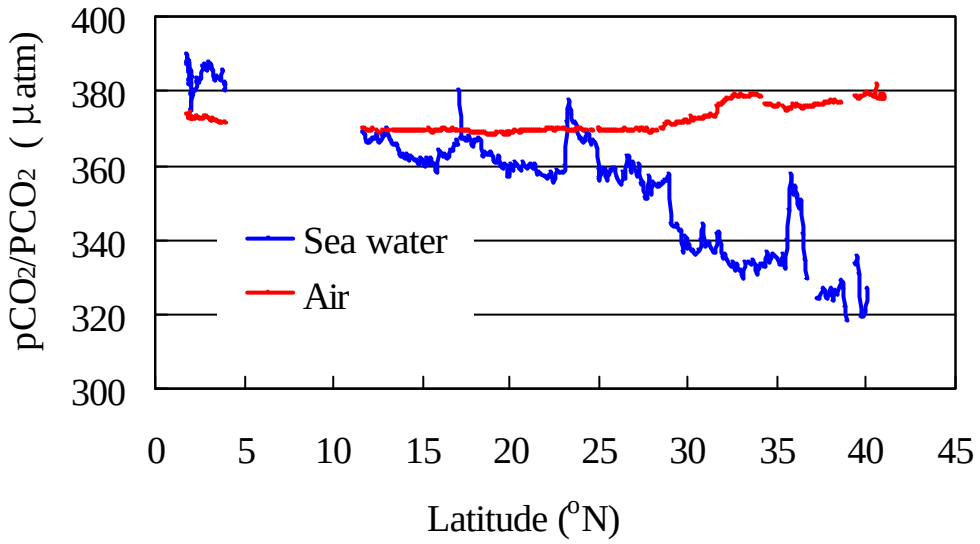

Fig. 6.6.3-1: Latitudinal distribution of pCO_2 and PCO_2 along the 140°E line.

Blue and Red line are partial pressure of carbon dioxide in sea water and Atmosphere, respectively.

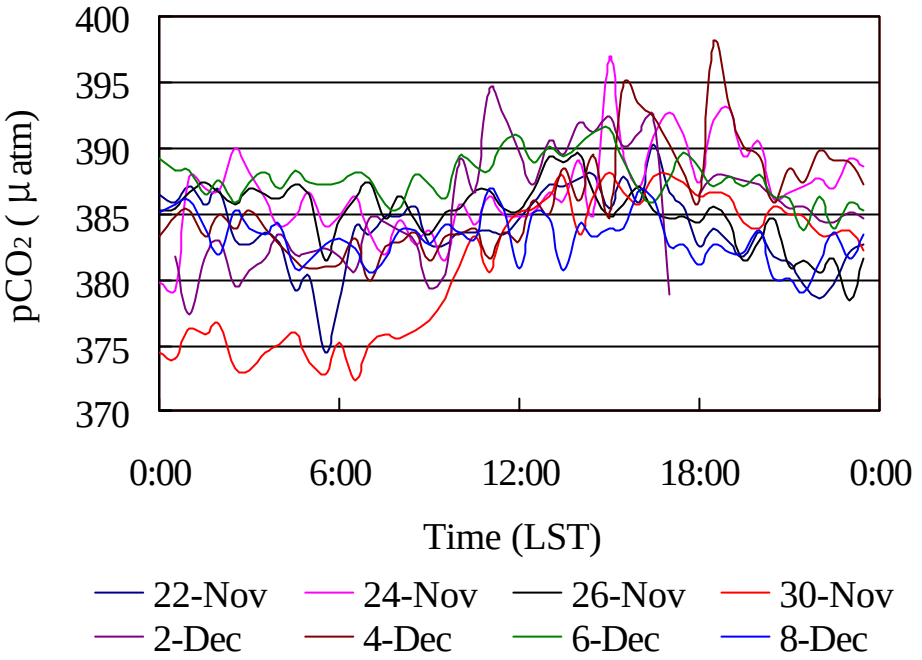

Fig.6.6.3-2: Time variation of pCO_2 at the Station (2^{o}N,138^{o}E) in November 22, 24, 26, 30, December 2, 4, 6 and 8, 2002.

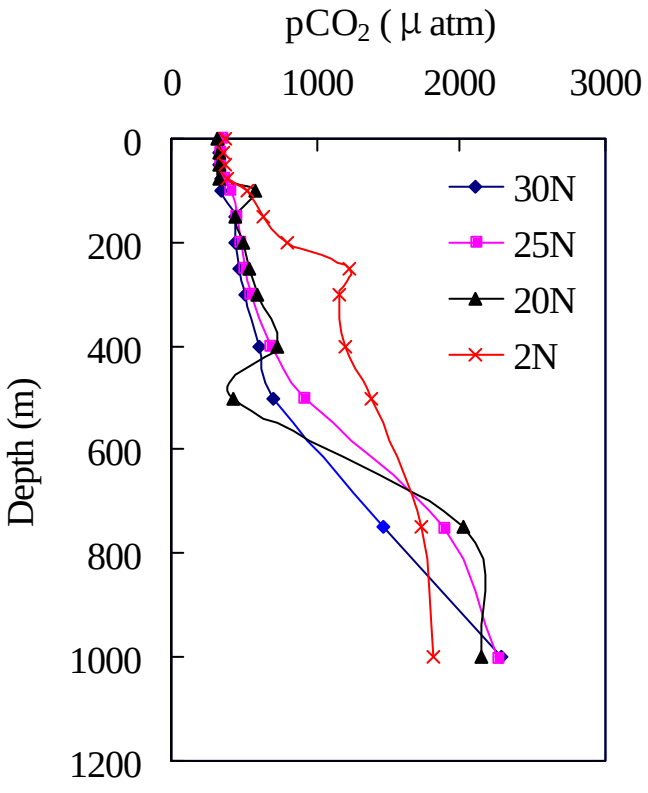

Fig.6.6.3-3: Vertical profile of pCO_2 along the 140^{o}E line.

6.6.4 Total Dissolved Inorganic Carbon

(1) Personnel

Eiji YAMASHITA (Okayama University of Science)
Takehiko KONO (Okayama University of Science)
Tomohiko MACHIDA (Okayama University of Science)
Jun INOUE (Okayama University of Science)
Katsunori SAGISHIMA (MWJ)
Masaki MORO (MWJ)

(2) Introduction

Since the global warming is becoming an issue world-widely, studies on the green house gas such as CO_2 are drawing high attention. Because the ocean plays an important roll in buffering the increase of atmospheric CO_2, studies on the exchange of CO_2 between the atmosphere and the sea becomes highly important. When CO_2 dissolves in water, chemical reaction takes place and CO_2 alters its appearance into several species. Unfortunately, the concentrations of the individual species of CO_2 system in solution cannot be measured directly. There are, however, four parameters that could be measured; alkalinity, total dissolved inorganic carbon, pH and pCO_2. If two of these four are measured, the concentration of CO_2 system in the water could be estimated (DOE, 1994).

(3) Objective

The current investigation was carried out in order to verify carbon dioxide parameters in the Pacific Ocean by measuring TDIC with analytical instruments installed on the research vessel MIRAI during this cruise.

(4) Sampling elements

Total Dissolved Inorganic Carbon (TDIC)

(5) Inventory information

Table 1. is showing the site name, date and the position where the water column samples were collected.

Table 1. Inventory information of the collected water column samples.

Station No.	Date	Latitude	Longtitude
001	2002/11/16	30-00.00N	140-41.22E
002	2002/11/16	25-00.01N	139-19.00E
003	2002/11/17	20-00.05N	138-00.00E
024	2002/11/24	01-59.37N	138-30.45E
056	2002/11/28	02-00.08N	138-29.84E
088	2002/12/2	02-00.01N	138-29.68E
120	2002/12/6	02-00.56N	138-30.60E
152	2002/12/10	02-00.27N	138-30.37E

(6) Materials and Methods

(6)-1. Seawater sampling

Seawater from various depths was collected by 12L Niskin bottles from 9 stations (last station not included in Table 1.). To collect the surface seawater, a plastic bucket was used. Seawater from different depths was sampled in a 250ml glass bottle, which was previously soaked in 5% non-phosphoric acid detergent (pH13) solution for at least 2 hours and was cleansed by fresh water and Milli-Q deionized water for 3 times each. A sampling tube was connected to the Niskin bottle when the sampling was carried out. The glass bottles were filled from the bottom, without rinsing, and were overflowed for 10 seconds with care not to leave any bubbles in the bottle. After collecting the samples on the deck, the glass bottles were removed to the lab to be analyzed. Prior to the analysis, 3ml of the sample (1% of the bottle volume) was removed from the glass bottle in order to make a headspace. The samples were then poisoned with 100 μl of 100% saturated solution of mercury chloride within one hour from the sampling point. After poisoning, the samples were sealed using grease (Apiezon M grease) and a stopper-clip. The samples were stored in a refrigerator in darkness at approximately 5℃ until analyzed. The samples were kept in the refrigerator no longer than 24 hours. The samples collected at station 003 were measured without poisoning since they were measured immediately after the collection.

Apart from the sample collection from various depths, surface seawater was also collected 12 times, once in two hours, to investigate the variation over time on the same day.

(6)-2. Seawater analysis

Using a coulometer (Carbon Dioxide Coulometer Model 5012, UIC Inc.) and an automated sampling system controlled by a computer, the concentration of TDIC was measured as the followings.

The sampling cycle set in the system was composed of 3 measuring factors; 70ml of standard CO_2 gas, 2ml of 10% saturated phosphoric acid solution and 6 seawater samples. The standard CO_2 gas was measured to confirm the constancy of the calibration factor during a run and phosphoric acid was measured for acid blank correction.

The seawater samples were measured as the followings. From the glass bottle, approximately 20ml of seawater was measured in a receptacle and was mixed with 2ml of 10% (v/v) phosphoric acid. The carbon dioxide gas evolving from the chemical reaction was purged by nitrogen gas (carbon dioxide free) for 12 minutes at the flow rate of 130ml/min and was absorbed into an electrolyte solution. In the electrolyte solution, acids forming from the reaction between the solution and the absorbed carbon dioxide were titrated with hydrogen ions in the coulometer and the counts of the titration were stored in the computer.

Before any of the samples were measured, the calibration factor (slope) was calculated by measuring series of sodium carbonate solutions (0~2.5mM) and this calibration factor was applied to all of the data acquired throughout the cruise. By measuring Certified Reference Material (CRM) (Scripps Institution of Oceanography) every time the cell was filled with fresh anode and cathode solutions, the slope was calibrated with the counts of this outcome. A set of cell solutions was not used for more than 60 seawater samples.

(7) Preliminary results

During the cruise, 8 bottles of CRM, twice for each bottle, was analyzed. The standard deviation of the absolute differences of duplicate measurements from these CRM, excluding one value obtained from a measurement which was carried out with insufficient sterilizing of the CRM bottle, was 1.05 μmol/kg (n=7). This result indicates that the analysis was accurate enough according to DOE (1994).

A duplicate analysis was made on samples of interest at each station and the differences between each pair of analyses were plotted on a range control chart (see Figure 1.). The average of the differences was 2.16 μmol/kg. The standard deviation of the absolute differences was 1.89 μmol/kg (n=26). The point that has fallen out of the control limit was obtained at station 003 from the depth of 50m.

Figure 2. is showing the variation of the TDIC over depth collected from 8 stations (not including the last station).

(8) Data Archive

All data was submitted to JAMSTEC Data Management Office (DMO) and Professor Eiji YAMASHITA and is currently under their control.

(9) Reference

DOE (1994), *Handbook of methods for the analysis of the various parameters of the carbon dioxide system in sea water*; version 2, A. G. Dickson & C. Goyet, Eds., ORNS/CDIAC-74.

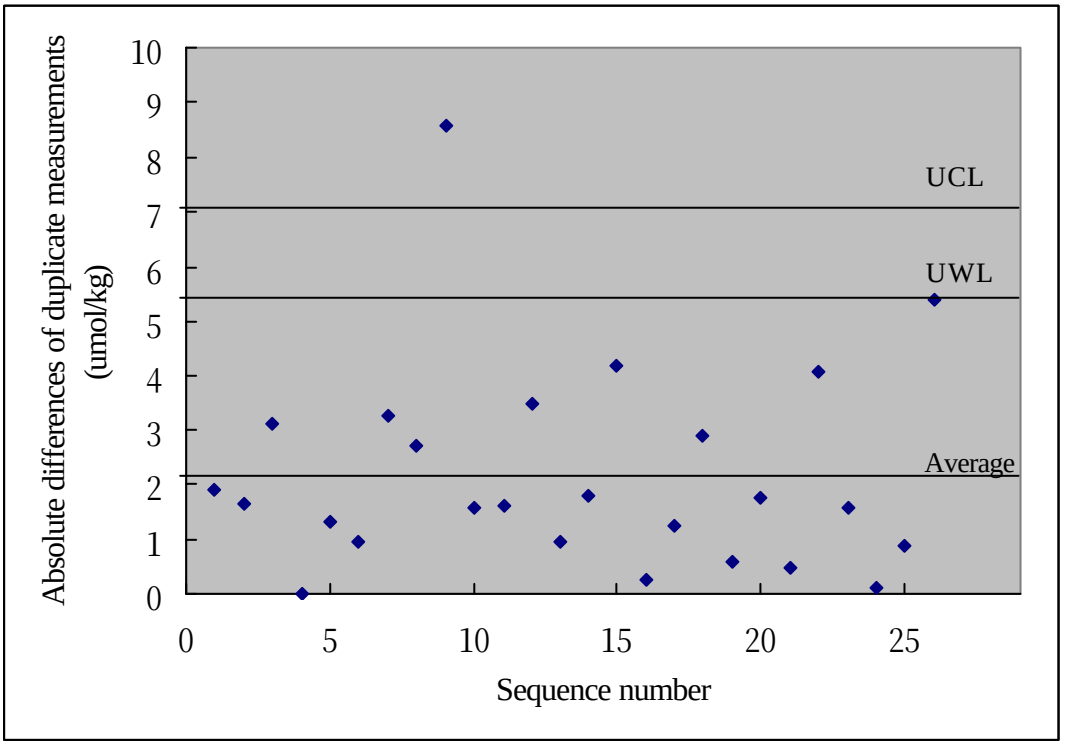

Fig.6.6.4-1: Range control chart of the absolute differences of the value obtained from duplicate samples.

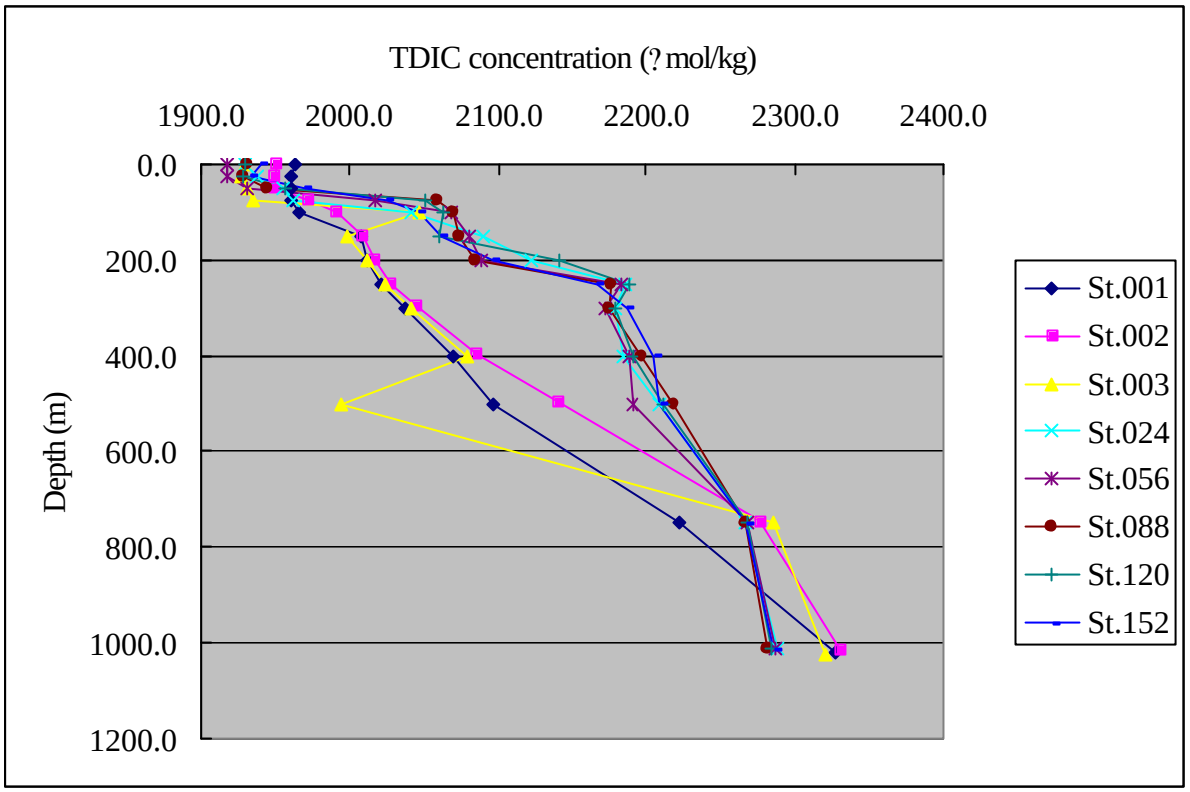

Fig.6.6.4-2: Variation of the TDIC over depth collected from 8 stations.

6.6.5 Total Alkalinity

(1) Personnel name and affiliation

Eiji YAMASHITA (Okayama University of Science): Principle investigator
Takehiko KONO (Okayama University): Observation leader
Katsunori SAGISHIMA (Marine Works Japan Ltd.)
Masaki MORO (Marine Works Japan Ltd.)

(2) Objectives

Global warming caused by green house gas such as carbon dioxide has become much to be paid attention all over the world. In the flux study of the equator area, it is important to understand its volume of transportation. In order to verify carbon cycle at the equator area, we measured total alkalinity (TA), which is one of carbon dioxide parameters, with analytical instruments installed on R/V MIRAI during this cruise. In this study, we measured its time variation (surface seawater) and vertical distribution along the 140°E line and also fixed point (2°N, 138°E) at the same day.

(3) Instruments and Methods

<Time variation>

Surface seawater samples were drawn from the jacket of pCO_2 measurement system into 250ml Nalgene polyethylene bottles with sampling tubes every 2 hours. Bottles were rinsed twice and filled from the bottom while taking care not to entrain any bubbles. The bottles were then sealed by a screw cap with an inner cap and stored in refrigerator for maximum of 36 hours prior to analysis.

<Vertical distribution>

Seawater samples were drawn from 12L Niskin™ bottles into 250ml Nalgene polyethylene bottles with sampling tubes at 21:00LST. Bottles were rinsed twice and filled from the bottom while taking care not to entrain any bubbles. The bottles were then sealed by screw cap with an inner cap and stored in refrigerator for maximum of 12 hours prior to analysis.

The method of total alkalinity measurement was titration of 0.05M hydrochlolic acid made from 0.65M sodium chloride. The titration system consists of a titration manager (Radiometer, TIM900), an auto-burette (Radiometer, ABU901), a pH glass electrode (Radiometer, pHG201-7), an installed reference operating software (Lab Soft, Tim Talk9) and another software for calculation.

Before titration, the temperature of the bottles was brought to 25 degree C in the water bath, and water sample was taken by a Knudsen pipette (50ml) into a tall beaker (100ml). The titration carried out adding HCl (0.1N) to seawater past the carbonic acid point with a set of electrodes used to measure electromotive force at 25 degree C. After titration, data of titrated HCl volume and electromotive force and temperature then were used to calculate to total alkalinity. All the reported values were corrected with the Dickson's CRM, sea temperature, and salinity.

(4) Results

We measured time variation and vertical distribution of total alkalinity (TA) in Nov.16, 17, 18, 24, 28, Dec.2, 6 and 10, 2002. Vertical distribution total alkalinity along the 140°E line is represented in Figure 6.6.5-1. It is found that TA increased with depth and TA vertical distribution has systematically changed. . TA increased with increasing the depth with a hump at 150 m depth.

(5) Data archive

The raw data were stored on a magnetic optical disk which will be kept on Ocean Research Department, JAMSTEC. The raw data will be corrected and published.

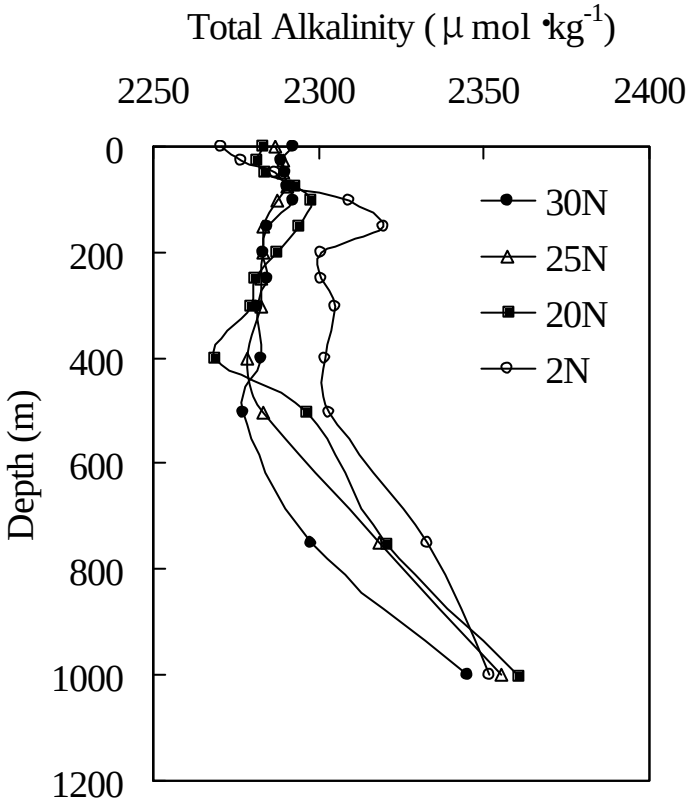

Fig. 6.6.5-1: Vertical distribution total alkalinity along the 140°E line.

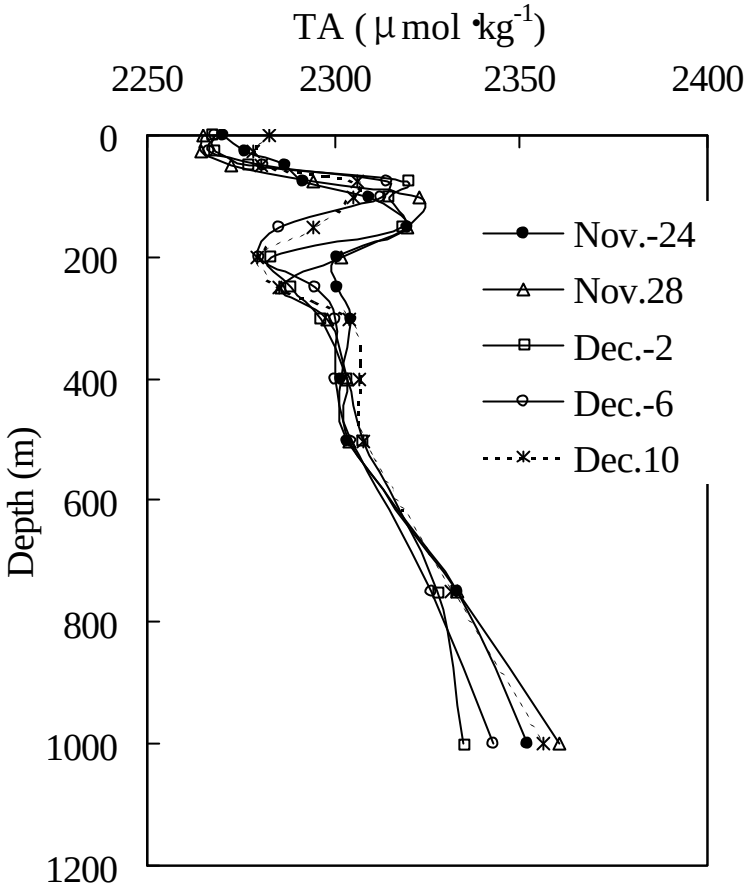

Fig. 6.6.5-2: Vertical distribution of total alkalinity at the fixed point (2°N, 138°E).

6.7 Ocean Color

(1) Personnel

Tetsuya Takemi (Osaka University): On-board leader
Takuhei Shiozaki (Osaka Prefecture University)
Jun Miyake (Kobe University of Mercantile Marine)
Jinsuke Takami (Okayama University)
Ryutaro Sanjiki (Kinki University)

On-shore scientist:
Katsutoshi Kozai (Kobe University of Mercantile Marine): Principal Investigator
Osamu Tsukamoto (Okayama University)

(2) Objective

Radiative energy budget at the surface plays an important role in controlling the global weather and climate. The purpose of the present observation is to estimate the reflectance of solar radiation at the ocean surface and the skin sea surface temperature and to collect ground-truth data for the validation of satellite-derived parameters.

(3) Methods

Spectroradiometer (Geophysical and Environmental Research Corp., GER1500) was used to measure the spectral reflectance of solar radiation at the sea surface. GER1500 resolves 512 spectral bands in the ultraviolet, visible, and near-infrared wavelengths (350-1050 nm), having 4 degrees of field-of-view. In order to derive the spectral reflectance, the calibrated whiteboard spectral radiance and the upward spectral radiance from the ocean surface are measured. This observation was conducted in clear conditions four times a day (10, 11, 13, and 14 LT) when the satellites SeaStar and NOAA pass over Mirai.

Thermal infrared radiometer (CIMEL Electronique, CE312) was used to measure sea surface spectral radiation temperature (spectral skin temperature). The specification of this instrument is as follows:

Temperature range	-80 to 50 degrees C,
Resolution	broad band 8 mK at 20 degrees C,
	Other band 50 mK at 20 degrees C,
Response time	1 second,
Field-of-view	10 degrees,
Spectral bandpass	four bands (8-13, 11.5-12.5, 10.5-11.5, 8.2-9.2 ?m),
Detector	Thermopile.

This observation was conducted in no-rain conditions during the daytime and also through the night if the condition permits.

In addition to conducting the above measurements, LAC (Local Area Coverage) data obtained from SeaWiFS (Sea-viewing Wide Field-of-view Sensor) installed on SeaStar were received at the station onboard Mirai once or twice a day (at around a noon time) under the authorization of the NASA SeaWiFS project as a temporary real-time agreement. The sensor has eight bands in the visible and near-infrared wavelengths (402-422, 433-453, 480-500, 500-520, 545-565, 660-680, 745-785, 845-885 nm) and tile mechanism to avoid sun glitter (scan plane tilt: +20, 0, and −20 degrees). The satellite crosses the equator at a local noon (within 20 min difference) in a

descending mode. The orbit is a sun-synchronous type at a 705 km altitude. The spatial resolution is 1.13 km for LAC and 4.5 km for GAL. The swath width is 2801 km for LAC and 1502 km for GAC.

Table 6.7-1 summarizes the observation activity for each measurement during the cruise. On 20 and 21 November no observations were carried out because Mirai was in the EEZs of Palau and Indonesia.

Table 6.7-1: Summary of observation activity.

day	GER1500 direct	CIMEL	SeaWIFS	Remarks
13-Nov			○	
14-Nov			○	
15-Nov			○	
16-Nov			○	
17-Nov	○		○	GER obs at (20N, 140E)
18-Nov			○	
19-Nov				No SeaWiFS data obtained
20-Nov				No observation in the Palau and Indonesia EEZs
21-Nov				
22-Nov	○	○	○	GER obs at 11LT
23-Nov	○	○	○	
24-Nov	○		○	
25-Nov	○	○	○	
26-Nov	○	○	○	CIMEL obs from 6:30 to 22:00
27-Nov	○	○	○	
28-Nov	○	○		GER obs at 11LT / No SeaWiFS data obtained
29-Nov	○	○	○	CIMEL obs for 24 hours (6:45-6:45)
30-Nov	○	○	○	CIMEL obs continuously from 14:00
1-Dec	○	○	○	CIMEL obs continuously / GER obs except 14:00
2-Dec	○	○	○	CIMEL obs continuously
3-Dec	○	○	○	CIMEL obs continuously
4-Dec	○	○	○	CIMEL obs continuously to 18:00
5-Dec	○	○	○	CIMEL obs continuously from 10:00
6-Dec	○	○	○	CIMEL obs continuously except 16:00 to 17:30
7-Dec	○	○	○	CIMEL obs continuously
8-Dec	○	○	○	CIMEL obs continuously
9-Dec	○	○	○	CIMEL obs continuously
10-Dec	○	○	○	CIMEL obs continuously except 11:00 to 17:30
11-Dec	○	○	○	CIMEL obs continuously
12-Dec	○	○	○	CIMEL obs continuoysly till 21:00
13-Dec	○		○	GER obs at (5N, 140E)
14-Dec			○	
15-Dec			○	

(4) Preliminary Results

Sea surface spectral reflectances observed on some selected days are shown in Fig.6.7-1. The cases of good conditions are chosen as a preliminary result. The maximum reflectances are seen at about 370 nm, which corresponds to a blue wavelength, and the values ranges from 3.1 to 4.5 %. At the wavelengths longer than 600 nm, the reflectances go under 0.5 %. Theoretically, the reflectance should be zero in the near-infrared wavelengths longer than 550 nm (i.e., solar radiation is completely absorbed); however, non-zero reflectances are found in these wavelengths, which may be cause by unfavorable sea surface conditions such as glittering, form, and breaking wave.

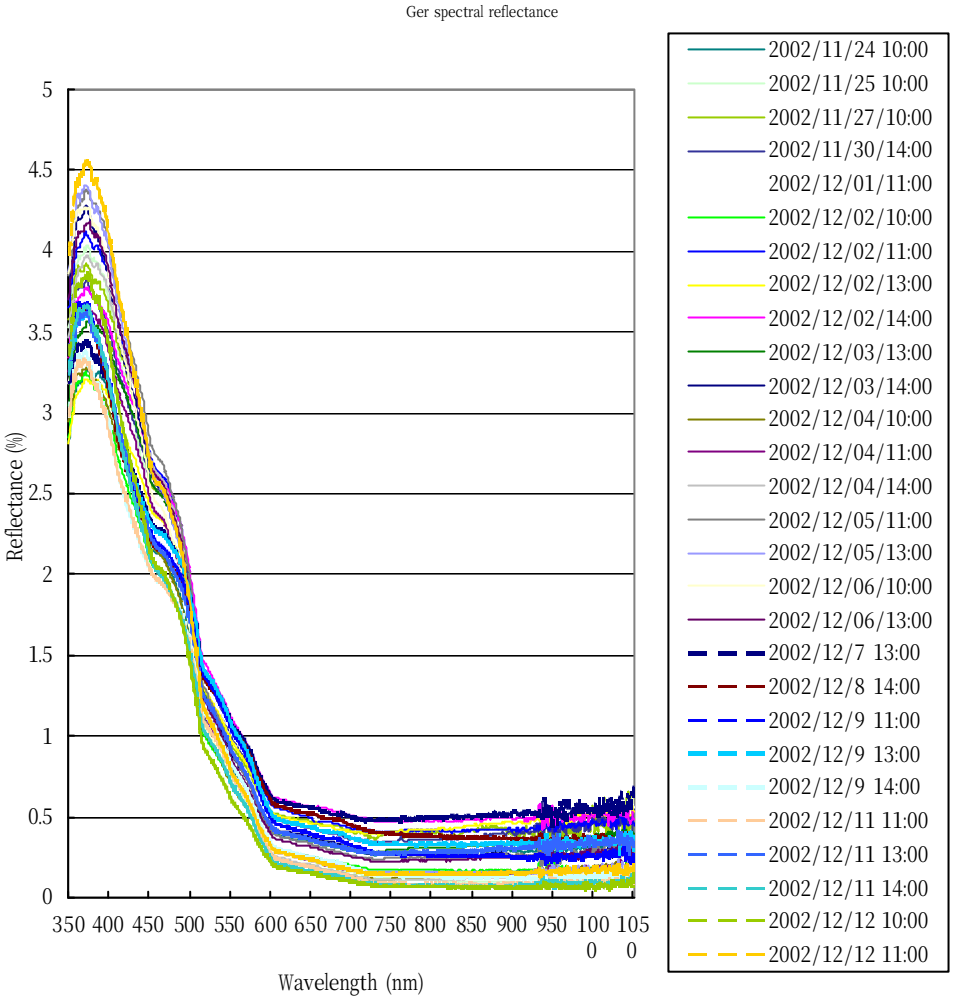

Fig.6.7-1: Sea surface reflectance on some selected days.

All the SeaWiFS original data (Level 1) were converted to higher-level products by using the SeaDAS software provided by NASA. Fig.6.7-2 shows the spatial distribution of chlorophyll-a concentration (a Level-2 product) on 7 December as an example. At the stationary observation point (2N, 138.5E) the concentration is low, while around the coastal areas the values are much larger.

The skin sea surface temperatures (SSSTs) obtained by CIMEL are shown in Fig.6.7-3. The sea surface temperatures (SSTs) at the 5-m depth are also plotted in the figure for comparison. Generally, SSSTs were lower than SSTs, which may be resulted from surface evaporation by winds; however, in weak-wind conditions (e.g., Dec. 4th), SSSTs became larger and eventually reached above 31 degrees C.

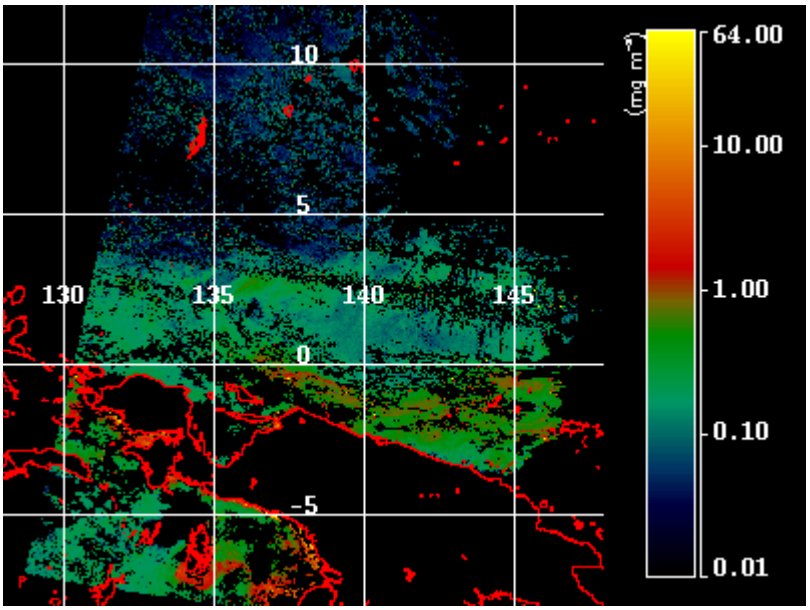

Fig.6.7-2: Chlorophyll-a concentration around the Mirai location on 7 December.

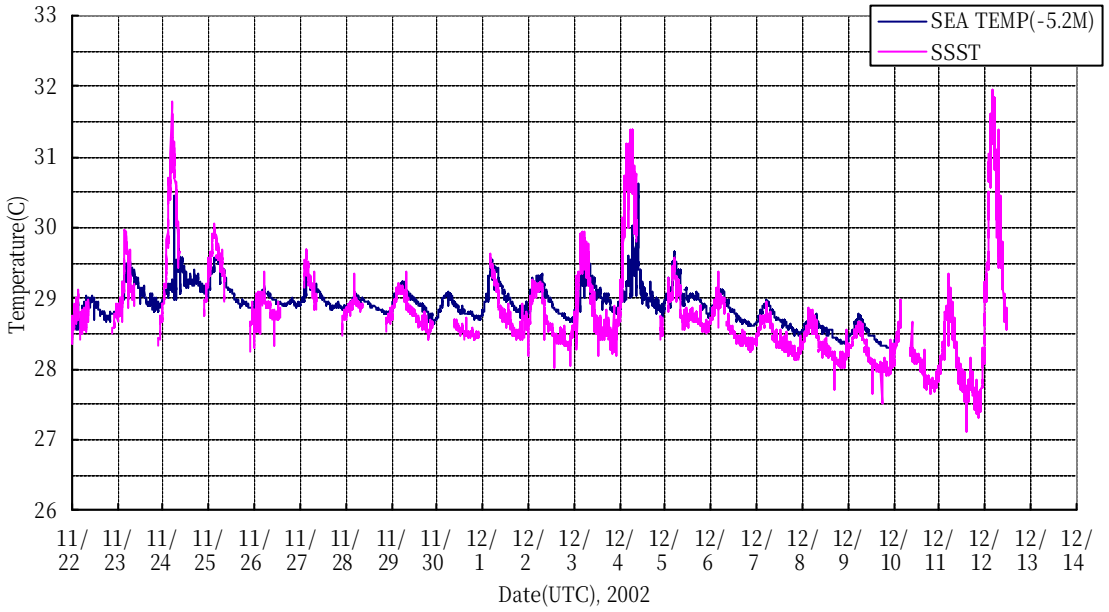

Fig.6.7-3: Time series of skin temperature (SSST) obtained by CIMEL and SST at the 5m depth.

(5) Data Archive

All the data obtained during this cruise are archived at Kobe University of Mercantile Marine, and will be open to public after quality checks and corrections. The CIMEL data are also archived at Okayama University. Interested scientists should contact Prof. Katsutoshi Kozai at Kobe University of Mercantile Marine. The corrected data and inventory information will be submitted to JAMSTEC Data Management Office. The SeaWiFS data will be submitted to NASA according to the license agreement.

6.8 Sea Surface Water Monitoring

(1) Personnel name and affiliation

Katsunori Sagishima (Marine Works Japan Ltd)
Masaki Moro (Marine Works Japan Ltd)

(2) Objective

To monitor continuously the physical, chemical and biological characteristics of near-sea surface water.

(3) Methods

The *Continuous Sea Surface Water Monitoring System* (Nippon Kaiyo co., Ltd.) is located in the "*sea surface monitoring laboratory*" on R/V Mirai. It can automatically measure temperature, salinity, dissolved oxygen, fluorescence and particle size of plankton in the near-surface water every 1-minute. Measured data are saved every one-minute together with time and the position of ship, and displayed in the data management PC machine. This system is connected to shipboard LAN-system and provides the acquired data for p-CO_2 measurement system, etc.

The uncontaminated seawater intake is 4.5m below the sea surface. Near-surface water was continuously pumped up about 200L/min from the intake to the laboratory and then flowed into *the Continuous Sea Surface Water Monitoring System* and p-CO_2 measurement system etc. through a steel pipe. The flow rate of surface water for this system was 12L/min, which controlled by some valves and passed through some sensors except with fluorometer (about 0.3L/min) through vinyl-chloride pipes.

The Continuous Sea Surface Water Monitoring System has six kinds of sensors, which TSG comprises of two SBE sensor modules. Sea surface temperature is measured by a ship bottom oceanographic thermometer situated on the suction side of the uncontaminated seawater supply in the forward hold. Specification and calibration date of the each sensor in this system of listed below.

a-1) Temperature and salinity sensors

SEACAT THERMOSALINOGRAPH

Model:	SBE-21, SEA-BIRD ELECTRONICS, INC.
Serial number:	2113117-3126
Measurement range:	Temperature -5 to +35 deg-C, Salinity 0 to 6.5 S/m
Accuracy:	Temperature 0.01 deg-C/6month, Salinity 0.001 S/m/month
Resolution:	Temperature 0.001 deg-C, Salinity 0.0001 S/m
Calibration date:	02-Sep.-'02 (mounted on 13-Nov.-'02 in this system)

a-2) Ship bottom oceanographic thermometer (mounted at the back of the pump for surface water)

Model:	SBE 3S-A, SEA-BIRD ELECTRONICS, INC.
Serial number:	032607
Measurement range:	-5 to +35 deg-C
Initial Accuracy:	0.001 deg-C per year typical
Stability:	0.002 deg-C per year typical
Calibration date:	02-Sep.-'02 (mounted on 13 - Nov.-'02 in this system)

b) Dissolved oxygen sensor

Model:	2127, Oubisufair Laboratories Japan INC.
Serial number:	31757
Measurement range:	0 to 14 ppm
Accuracy:	±1% at 5 deg-C of correction range
Stability:	1% per month
Calibration date:	13-Jun-00

c) Fluorometer

Model:	10-AU-005, TURNER DESIGNS
Serial number:	5562 FRXX
Detection limit:	5 ppt or less for chlorophyll a
Stability:	0.5% per month of full scale

d) Particle size sensor

Model:	P-05, Nippon Kaiyo LTD.
Serial number:	P5024
Accuracy:	±10% of range
Measurement range:	0.02681mm to 6.666mm
Reproducibility:	±5%
Stability:	5% per week

e) Flowmeter

Model:	EMARG2W, Aichi Watch Electronics LTD.
Serial number:	8672
Measurement range:	0 to 30 L/min
Accuracy:	±1%
Stability:	±1% per day

The monitoring periods (UTC) during this cruise are listed below.
14 Nov. 2002, 05:50, to 19 Nov. 2002, 11:59 (UTC)
21 Nov. 2002, 08:05, to 15 Dec. 2002, 01:25 (UTC)

We stopped the measurement in EEZ areas at The Republic of palau and The Republic of Indnesia.
19 Nov. 2002, 11:59, to 21 Nov. 2002, 08:05 (UTC)

(5) Preliminary Result.

Every 10 minutes data are plotted along the ship's track in the period of Nov.14 to Dec. 13 (fig. 6.8-1).

This figure showed the respective trend of temperature, fluorescence dissolved oxygen and salinity distributions.

(6) Data archive

The format of raw data files is ASCII, The calibrated values of each sensors are in files with Microsoft Excel format and ASCII format. All the data will be submitted to the DMO at JAMSTEC.

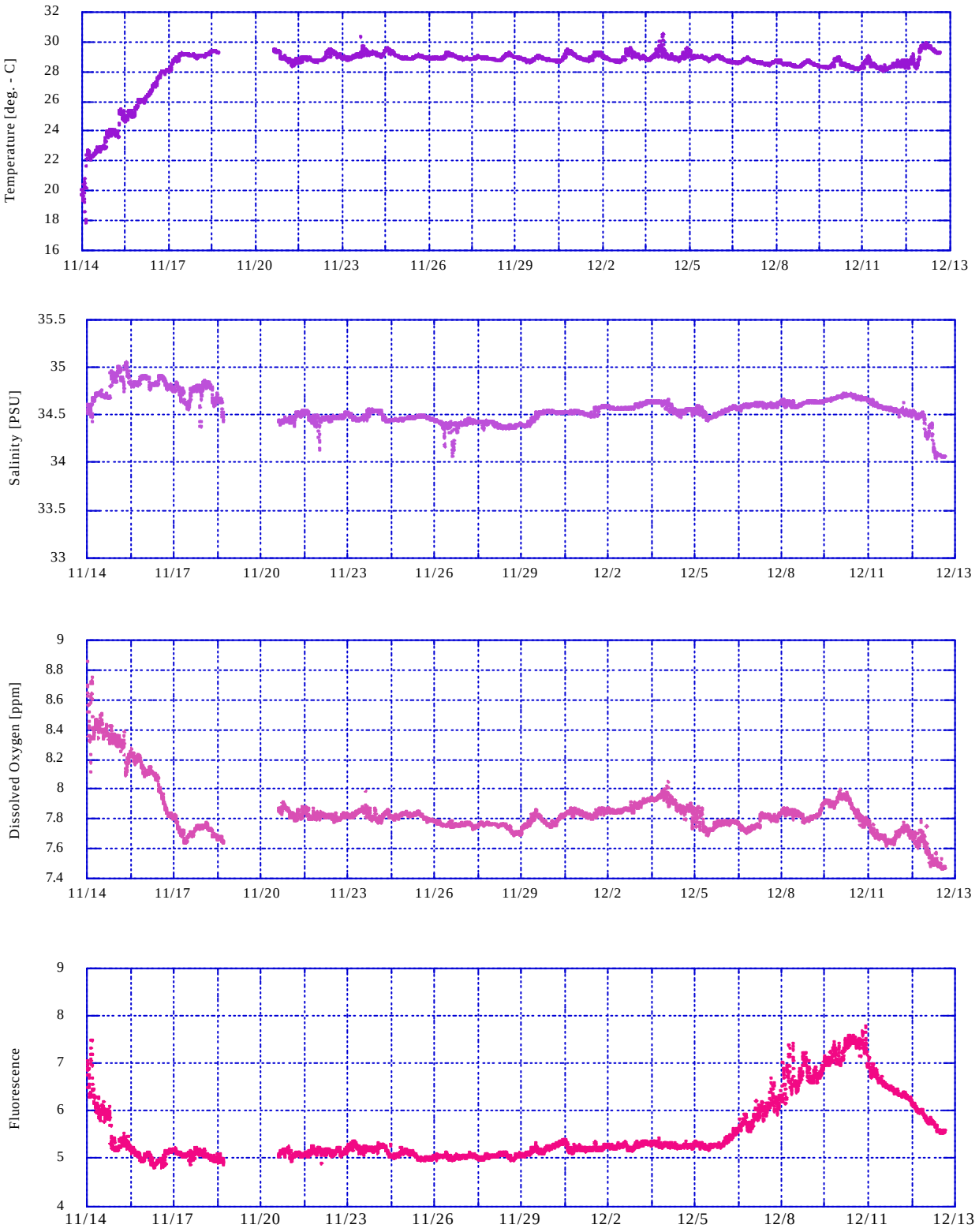

Fig. 6.8-1: Trend of temperature, salinity, D.O. and fluorescence in surface sea water..

6.9 Oceanic Profiles

6.9.1 CTD Observations

(1) Personnel

Kunio Yoneyama	(JAMSTEC):	Principal Investigator
Satoshi Ozawa	(MWJ):	Operation leader
Asako Inoue	(MWJ)	
Naoko Takahashi	(MWJ)	
Tomohiko Sugiyama	(MWJ)	
Nozomi Umezu	(MWJ)	
Yoshiyuki Hisatsune	(MWJ)	

(2) Objectives

Investigation of the oceanic structure and its time variation by measuring vertical profiles of temperature and salinity.

(3) Methods

We observed vertical profile of temperature and salinity by CTD / Carousel (Conductivity Temperature Depth profiler / Carousel Multi Water Sampler). The sensors attached on CTD were for temperature, conductivity, pressure, and dissolved oxygen. Salinity was calculated by measurement values of pressure, conductivity and temperature. The CTD / Carousel was deployed from starboard on working deck. Descending rate and ascending were kept about 1.2 m/s respectively. Sea surface temperature (SST) measurement was done in each time, too.

The CTD raw data was acquired in real time by using the SEASAVE utility from SEASOFT software (ver.5.25b for Windows) provided by SBE and stored on the hard disk of an IBM personal computer. Water samplings were made during up-cast by sending a fire command from the computer. Every day we sampled water on 11:30 (UTC) at 1000 m to calibrate salinity data. In several casts sea water at 12 layer were sampled for Oceanic Carbon analysis.

We were carried out CTD measurements at stationary station (2N, 138E) and 6 stations along 138E. In stationary station, CTD casting was conducted every 3 hours (02:30, 05:30, 08:30, 11:30, 14:30, 17:30, 20:30, 23:30, UTC). Measurement depth was 1,000m at 11:30'cast, other cast measurement depth was 500m. In total, 172 casting were carried out (see Table 6.9.1-1).

The CTD raw data was processed using SEASOFT (ver.5.27a for Windows). Data processing procedures and used utilities of SEASOFT were as follows:

DATCNV: Converts the binary raw data to output on physical unit.
This utility selects the CTD data when bottles closed to output on another file.

SECTION: Remove the unnecessary data.

ALIGNCTD: ALIGNCTD aligns oxygen measurements in time relative to pressure.
Secondary conductivity sensor relative to pressure=0.073 seconds
Primary dissolved oxygen sensor relative to pressure = 6.0 seconds

WILDEDIT: Obtain an accurate estimate of the true standard deviation of the data.
Std deviations for Pass 1:10
Std deviations for Pass 2:20
Points per block: 1000

CELLTM: Remove to conductivity cell thermal mass effects from the measured conductivity.
Primary alpha = 0.03, 1/beta = 7.0
Secondary alpha=0.03,1/beta=7.0

FILTER: Run a low-pass filter on one or more columns of data.
Filter A = 0.15sec
Variable to Filter: Pressure: Low Pass Filter A
LOOPEDIT: Marks scans bad by setting the flag value associated with the scan to badflag in input Cnv files that have pressure slowdowns or reversals.
Minimum Velocity Selection = Fixed Minimum Velocity
Minimum CTD Velocity [m/sec] = 0.0
Exclude Scan Marked Bad in LOOPEDIT = Yes
BINAVG: Calculation the averaged data in every 1db.
DERIVE: Calculates oceanographic parameters from the input.cnv file.
SPLIT: Splits the data made in CNVfiles into upcast and downcast files.
ROSSUM: Edits the data of water sampled to output a summary file.

Specifications of sensors are listed below.
Under water unit: CTD 9plus (S/N 79511 Sea-bird Electronics, Inc.)
Calibrated Date: 07-Feb-2002
Primary Temperature Sensor: SBE3-04/F (S/N 031524 Sea-bird Electronics, Inc.)
Calibrated Date: 06-Sep-2002
Secondary Temperature Sensor: SBE3-04/F (S/N 031464 Sea-bird Electronics, Inc.)
Calibrated Date: 07-Sep-2002
Primary Conductivity Sensor: SBE4-04/0 (S/N 041206 Sea-bird Electronics, Inc.)
Calibrated Date: 06-Sep-2002
Secondary Conductivity Sensor: SBE4-04/0 (S/N 041203 Sea-bird Electronics, Inc.)
Calibrated Date: 06-Sep-2002
Dissolved Oxygen sensor: SBE43 (S/N 430205 Sea-bird Electronics, Inc.)
Calibrated Date: 06-Sep-2002
Deck unit: SBE11 (S/N 11P7030-0272, Sea-bird Electronics, Inc.)
Carousel water sampler: SBE32 (S/N3222295-0389 Sea-bird Electronics, Inc.)

(5) Preliminary Results

Time-depth cross sections of temperature, salinity, dissolved oxygen and sigma-theta are shown in Fig. 6.9.1-1. The temporal variation of SST is shown in Fig. 6.9.1-2. Vertical profiles at each CTD cast are attached in the following APPENDIX-E. Note that, in these figures, the correction of salinity and oxygen data by sampled water is not applied.

(6) Troubles

It was found that noisy data from dissolved oxygen sensor have found from surface to 60 m in 112nd and 156nd casts. Both casts were just after repairing disconnection trouble, though the cause was uncertain.

(7) Data archive

All raw and processed CTD data files are submitted to JAMSTEC Data Management Office (DMO) and will be under their control.

Table 6.9.1-1: CTD cast table

Station	File name	Date (UTC)	Start time	End time	Latitude (N)	Longitude (E)	Max.Press (db)	NOTE
001	K6S001	2002/11/16	1:18	2:20	30-00.02	140-41.10	1020.97	
002	K6S002	2002/11/16	22:22	23:19	24-59.93	139-19.95	1020.63	
003	K6S003	2002/11/17	20:01	20:56	20-00.07	137-59.91	1023.58	
004	K6S004	2002/11/21	23:29	0:52	01-59.57	138-30.52	2000.09	
005	K6S005	2002/11/22	2:26	2:53	01-55.74	138-29.99	505.57	
006	K6S006	2002/11/22	5:25	5:54	01-52.75	138-34.75	500.07	
007	K6S007	2002/11/22	8:25	8:55	01-59.67	138-30.13	503.4	
008	K6S008	2002/11/22	11:27	12:29	01-55.29	138-26.35	1516.29	
009	K6S009	2002/11/22	14:27	15:01	01-58.93	138-30.61	510.83	
010	K6S010	2002/11/22	17:27	17:57	01-59.46	138-29.34	511.75	
011	K6S011	2002/11/22	20:27	20:55	01-59.76	138-30.30	511.95	
012	K6S012	2002/11/22	23:26	23:54	02-00.46	138-29.99	515.1	
013	K6S013	2002/11/23	2:24	2:52	01-59.73	138-29.26	504.12	
014	K6S014	2002/11/23	5:24	5:52	02-00.09	138-30.29	504.78	
015	K6S015	2002/11/23	8:21	8:49	01-59.89	138-30.20	505	
016	K6S016	2002/11/23	11:26	12:28	01-59.93	138-31.50	1016.8	
017	K6S017	2002/11/23	14:26	14:58	01-59.33	138-30.62	510.07	
018	K6S018	2002/11/23	17:26	17:55	01-59.61	138-30.55	509.98	
019	K6S019	2002/11/23	20:26	20:55	01-59.62	138-30.31	510.58	
020	K6S020	2002/11/23	23:27	0:32	01-59.69	138-30.24	1019.28	
021	K6S021	2002/11/24	2:20	2:50	01-59.83	138-30.41	504.25	
022	K6S022	2002/11/24	5:25	5:53	02-00.12	138-30.17	504.75	
023	K6S023	2002/11/24	8:22	8:52	01-59.80	138-30.61	505	
024	K6S024	2002/11/24	11:28	12:26	01-59.37	138-30.51	1013.46	
025	K6S025	2002/11/24	14:25	14:56	01-59.48	138-30.79	509.24	
026	K6S026	2002/11/24	17:27	17:57	01-59.56	138-30.28	511.5	
027	K6S027	2002/11/24	20:27	20:56	01-59.74	138-30.58	511	
028	K6S028	2002/11/24	23:25	23:54	01-59.69	138-30.19	511.35	
029	K6S029	2002/11/25	2:25	2:53	01-59.60	138-30.54	509.65	
030	K6S030	2002/11/25	5:25	5:54	01-59.36	138-30.07	501.6	
031	K6S031	2002/11/25	8:25	8:52	01-59.89	138-30.21	509	
032	K6S032	2002/11/25	11:27	12:14	01-59.70	138-30.52	1011.21	
033	K6S033	2002/11/25	14:22	14:58	01-59.77	138-30.11	507.32	
034	K6S034	2002/11/25	17:27	18:01	01-59.64	138-29.80	508.81	
035	K6S035	2002/11/25	20:27	20:57	01-59.94	138-30.23	511.13	
036	K6S036	2002/11/25	23:25	0:09	01-59.93	138-30.17	510.49	
037	K6S037	2002/11/26	2:25	2:53	01-59.92	138-30.42	511.86	
038	K6S038	2002/11/26	5:25	5:54	01-59.98	138-30.33	503.72	
039	K6S039	2002/11/26	8:26	8:52	02-00.61	138-30.01	508.27	
040	K6S040	2002/11/26	11:27	12:27	01-59.88	138-30.30	1012.62	
041	K6S041	2002/11/26	14:27	14:57	02-00.14	138-30.73	508.57	
042	K6S042	2002/11/26	17:27	17:54	01-59.49	138-30.31	511.42	
043	K6S043	2002/11/26	20:27	20:59	02-00.16	138-30.47	512.29	
044	K6S044	2002/11/26	23:25	0:11	01-59.96	138-30.09	511.34	
045	K6S045	2002/11/27	2:25	2:52	01-59.91	138-30.52	504.48	
046	K6S046	2002/11/27	5:26	5:53	02-00.03	138-30.24	503.69	

Station	File name	Date (UTC)	Start time	End time	Latitude (N)	Longitude (E)	Max.Press (db)	NOTE
047	K6S047	2002/11/27	8:25	8:52	01-59.84	138-30.10	504.4	
048	K6S048	2002/11/27	11:27	12:09	01-59.87	138-30.09	1013.25	
049	K6S049	2002/11/27	14:26	14:56	02-00.21	138-30.29	503.84	
050	K6S050	2002/11/27	17:26	17:56	02-00.01	138-29.95	510.61	
051	K6S051	2002/11/27	20:27	20:57	01-59.87	138-30.68	510.48	
052	K6S052	2002/11/27	23:25	0:26	02-00.25	138-30.09	1021.5	
053	K6S053	2002/11/28	2:26	2:53	02-00.07	138-30.17	507.8	
054	K6S054	2002/11/28	5:29	5:56	01-59.29	138-29.68	503.92	
055	K6S055	2002/11/28	8:27	8:53	01-59.96	138-30.73	503.67	
056	K6S056	2002/11/28	11:30	12:26	02-00.01	138-29.95	1014.66	
057	K6S057	2002/11/28	14:25	14:58	02-00.15	138-30.63	510.7	
058	K6S058	2002/11/28	17:27	17:55	01-59.82	138-30.62	510.99	
059	K6S059	2002/11/28	20:27	20:56	01-59.91	138-30.03	511.23	
060	K6S060	2002/11/28	23:25	23:53	01-59.36	138-30.19	509.93	
061	K6S061	2002/11/29	2:27	2:52	01-59.92	138-30.35	504.97	
062	K6S062	2002/11/29	5:26	5:54	01-59.84	138-30.45	507.64	
063	K6S063	2002/11/29	8:26	8:53	01-59.72	138-29.83	507.16	
064	K6S064	2002/11/29	11:27	12:10	01-59.92	138-30.30	1013.54	
065	K6S065	2002/11/29	14:26	14:56	01-59.95	138-30.58	507.76	
066	K6S066	2002/11/29	17:27	17:55	01-59.98	138-30.52	511.31	
067	K6S067	2002/11/29	20:27	20:55	01-59.86	138-30.17	511.58	
068	K6S068	2002/11/29	23:25	0:06	01-59.80	138-29.79	510.39	
069	K6S069	2002/11/30	2:26	2:53	02-00.03	138-30.17	510.7	
070	K6S070	2002/11/30	5:26	5:53	01-59.59	138-30.42	506.2	
071	K6S071	2002/11/30	8:26	8:52	01-59.75	138-30.33	506.58	
072	K6S072	2002/11/30	11:27	12:21	01-59.93	138-30.84	1013.85	
073	K6S073	2002/11/30	14:26	14:58	02-00.13	138-29.86	510.09	
074	K6S074	2002/11/30	17:27	17:57	01-59.82	138-30.52	510.2	
075	K6S075	2002/11/30	20:27	20:56	01-59.78	138-30.46	511.23	
076	K6S076	2002/11/30	23:25	0:08	01-59.92	138-30.24	510.36	
077	K6S077	2002/12/1	2:24	2:52	02-00.10	138-30.31	508.35	
078	K6S078	2002/12/1	5:27	5:52	02-00.06	138-30.09	508.82	
079	K6S079	2002/12/1	8:24	8:53	01-59.80	138-30.20	509.39	
080	K6S080	2002/12/1	11:26	12:12	01-59.85	138-30.48	1014.97	
081	K6S081	2002/12/1	14:26	14:55	01-59.87	138-30.28	508.38	
082	K6S082	2002/12/1	17:23	17:56	02-00.08	138-30.14	512.01	
083	K6S083	2002/12/1	20:23	20:55	02-00.13	138-30.12	511.39	
084	K6S084	2002/12/1	23:23	0:24	01-59.93	138-30.20	1020.11	
085	K6S085	2002/12/2	2:26	2:53	01-59.77	138-30.27	506.35	
086	K6S086	2002/12/2	5:25	5:51	01-59.63	138-30.29	510.73	
087	K6S087	2002/12/2	8:24	8:53	01-59.78	138-30.03	510.26	
088	K6S088	2002/12/2	11:25	12:33	01-59.90	138-29.91	1012.51	
089	K6S089	2002/12/2	14:26	14:55	02-00.04	138-30.21	509.19	
090	K6S090	2002/12/2	17:26	17:55	01-59394	138-30.21	510.15	
091	K6S091	2002/12/2	20:23	20:52	02-00.01	138-30.09	511.16	
092	K6S092	2002/12/2	23:23	23:52	01-59.82	138-29.90	511.45	
093	K6S093	2002/12/3	2:24	2:51	02-00.11	138-30.18	508.73	

Station	File name	Date (UTC)	Start time	End time	Latitude (N)	Longitude (E)	Max.Press (db)	NOTE
094	K6S094	2002/12/3	5:24	5:54	01-59.94	138-30.19	510.65	
095	K6S095	2002/12/3	8:24	8:51	01-59.51	138-30.05	512.24	
096	K6S096	2002/12/3	11:26	12:17	01-59.63	138-30.38	1013.85	
097	K6S097	2002/12/3	14:27	14:55	01-59.79	138-30.44	509.5	
098	K6S098	2002/12/3	17:27	17:55	02-00.13	138-30.41	510.4	
099	K6S099	2002/12/3	20:23	20:53	02-00.18	138-39.50	510.95	
100	K6S100	2002/12/3	23:23	0:06	01-59.97	138-30.73	510.49	
101	K6S101	2002/12/4	2:24	2:53	02-00.25	138-30.07	510.22	
102	K6S102	2002/12/4	5:25	5:53	01-59.89	138-30.06	509.93	
103	K6S103	2002/12/4	8:24	8:52	01-59.53	138-30.38	510	
104	K6S104	2002/12/4	11:31	12:27	01-59.54	138-30.22	1014.18	
105	K6S105	2002/12/4	14:27	14:56	02-00.41	138-31.27	508.22	
106	K6S106	2002/12/4	17:26	17:55	02-00.15	138-30.48	509.79	
107	K6S107	2002/12/4	20:23	20:53	02-00.14	138-30.13	513.21	
108	K6S108	2002/12/4	23:23	0:07	02-00.02	138-30.06	511.93	
109	K6S109	2002/12/5	2:24	2:52	01-59.89	138-29.72	508.78	
110	K6S110	2002/12/5	5:24	5:51	01-59.95	138-29.99	506.59	
111	K6S111	2002/12/5	8:24	8:56	02-00.01	138-30.28	507.57	
112	K6S112	2002/12/5	12:07	12:38	01-59.71	138-30.69	507.3	Noise in D.O.
113	K6S113	2002/12/5	14:22	14:54	01-59.96	138-30.66	508.78	
114	K6S114	2002/12/5	17:26	17:57	02-00.37	138-30.49	510.64	
115	K6S115	2002/12/5	20:25	20:53	02-00.10	138-30.11	511.83	
116	K6S116	2002/12/5	23:23	0:23	02-00.03	138-30.23	1021.4	
117	K6S117	2002/12/6	2:25	2:51	01-59.84	138-30.51	512.38	
118	K6S118	2002/12/6	5:24	5:54	01-59.82	138-30.28	511.91	
119	K6S119	2002/12/6	8:26	8:52	02-00.06	138-29.79	514.48	
120	K6S120	2002/12/6	11:28	12:30	02-00.22	138-30.80	1012.97	
121	K6S121	2002/12/6	14:28	14:54	02-00.14	138-30.61	508	
122	K6S122	2002/12/6	17:26	17:54	02-00.04	138-30.25	510.75	
123	K6S123	2002/12/6	20:23	20:53	02-00.41	138-30.98	509.99	
124	K6S124	2002/12/6	23:23	23:52	02-00.22	138-30.25	510.86	
125	K6S125	2002/12/7	2:24	2:52	02-00.68	138-30.23	510.48	
126	K6S126	2002/12/7	5:24	5:53	01-59.72	138-30.54	509.84	
127	K6S127	2002/12/7	8:29	8:53	01-59.40	138-29.47	511.15	
128	K6S128	2002/12/7	11:25	12:14	01-59.84	138-30.25	1012.16	
129	K6S129	2002/12/7	14:25	14:55	02-00.13	138-30.19	507.95	
130	K6S130	2002/12/7	17:26	17:57	01-59.59	138-30.37	510.44	
131	K6S131	2002/12/7	20:23	20:55	02-00.13	138-30.23	510.89	
132	K6S132	2002/12/7	23:23	0:08	02-00.26	138-29.96	511.03	
133	K6S133	2002/12/8	2:25	2:53	02-00.19	138-30.27	510.45	
134	K6S134	2002/12/8	5:24	5:55	01-59.97	138-30.38	510.27	
135	K6S135	2002/12/8	8:25	8:53	02-00.26	138-30.54	509.34	
136	K6S136	2002/12/8	11:29	12:28	02-00.04	138-30.45	1012.17	
137	K6S137	2002/12/8	14:26	15:00	01-59.91	138-30.60	507.99	
138	K6S138	2002/12/8	17:27	17:57	01-59.99	138-30.35	507.21	
139	K6S139	2002/12/8	20:25	20:54	02-00.07	138-30.33	510.02	
140	K6S140	2002/12/8	23:23	0:05	02-00.07	138-30.24	514.22	

Station	File name	Date (UTC)	Start time	End time	Latitude (N)	Longitude (E)	Max.Press (db)	NOTE
141	K6S141	2002/12/9	2:24	2:52	02-00.14	138-30.42	510.46	
142	K6S142	2002/12/9	5:24	5:53	01-59.88	138-30.26	518.46	
143	K6S143	2002/12/9	8:24	8:52	02-00.25	138-30.65	509.81	
144	K6S144	2002/12/9	11:25	12:15	01-59.76	138-30.43	1012.43	
145	K6S145	2002/12/9	14:26	14:55	02-00.37	138-30.23	506.89	
146	K6S146	2002/12/9	17:26	17:55	02-00.01	138-30.34	511.15	
147	K6S147	2002/12/9	20:23	20:54	02-00.00	138-30.36	512.68	
148	K6S148	2002/12/9	23:23	0:23	02-00.00	138-30.40	1019.19	
149	K6S149	2002/12/10	2:25	2:51	02-00.17	138-30.10	509.71	
150	K6S150	2002/12/10	5:24	5:52	01-59.89	138-30.23	508.78	
151	K6S151	2002/12/10	8:24	8:52	02-00.10	138-30.47	511.94	
152	K6S152	2002/12/10	11:27	12:30	02-00.21	138-30.55	1014.47	
153	K6S153	2002/12/10	14:25	14:57	02-00.31	138-30.66	506.66	
154	K6S154	2002/12/10	17:26	17:59	02-00.25	138-30.22	510.65	
155	K6S155	2002/12/10	20:24	20:55	02-00.23	138-30.35	509.59	
156	K6S156	2002/12/11	0:04	0:36	01-59.74	138-31.05	511.86	Noise in D.O.
157	K6S157	2002/12/11	2:24	2:52	02-00.33	138-30.19	511.07	
158	K6S158	2002/12/11	5:24	5:55	02-00.26	138-30.34	510	
159	K6S159	2002/12/11	8:24	8:52	01-59.73	138-30.94	509.63	
160	K6S160	2002/12/11	11:26	12:15	02-00.09	138-30.20	1013.28	
161	K6S161	2002/12/11	14:26	14:57	02-00.05	138-29.99	506.74	
162	K6S162	2002/12/11	17:26	17:55	01-59.59	138-3012	509.9	
163	K6S163	2002/12/11	20:24	20:53	01-59.98	138-29.86	512.79	
164	K6S164	2002/12/11	23:24	23:55	01-59.95	138-29.93	510.53	
165	K6S165	2002/12/12	2:24	2:52	01-59.97	138-29.73	511.73	
166	K6S166	2002/12/12	5:24	5:52	01-59.98	138-29.94	510.31	
167	K6S167	2002/12/12	8:24	8:52	01-59.71	138-30.50	511.36	
168	K6S168	2002/12/12	11:26	12:27	02-00.01	138-30.03	1012.79	
169	K6S169	2002/12/12	14:26	14:56	01-59.96	138-30.06	509.98	
170	K6S170	2002/12/13	3:24	4:45	05-00.32	139-25.03	2001.26	
171	K6S171	2002/12/13	13:04	14:03	07-00.01	140-00.04	999.59	
172	K6S172	2002/12/13	14:56	16:22	07-00.68	139-59.73	2000.64	

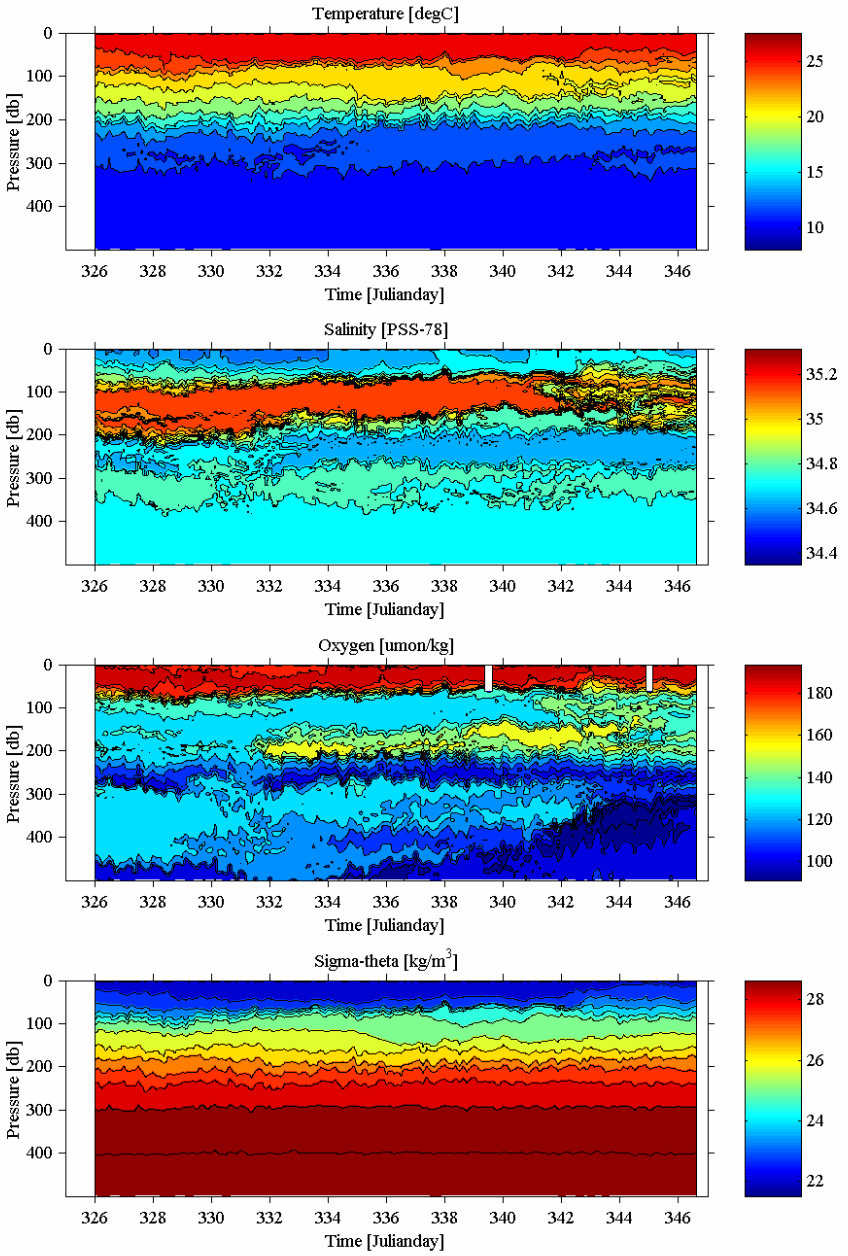

Fig. 6.9.1-1: Time-depth cross sections of temperature, salinity, oxygen, and sigma-theta.

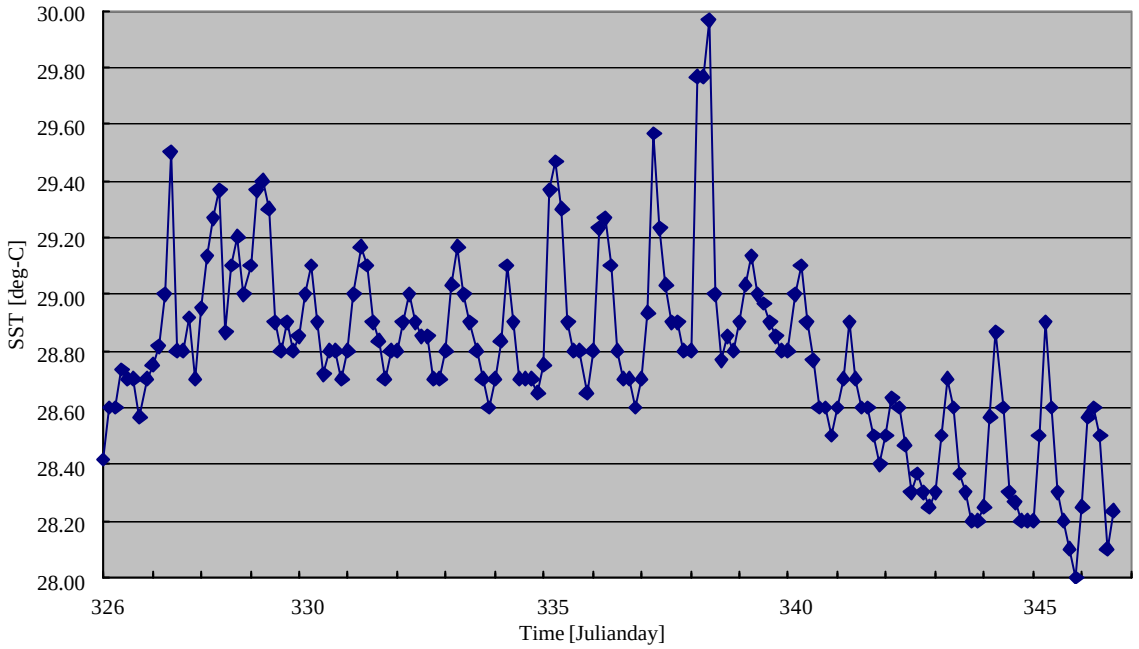

Fig. 6.9.1-2: The temporal variation of SST.

6.9.2 Salinity Measurements of Sampled Water

(1) Personnel

Naoko Takahashi	(MWJ):	Operation Leader
Satoshi Ozawa	(MWJ)	
Asako Inoue	(MWJ)	
Tomohiko Sugiyama	(MWJ)	

(2) Objective

Calibration of salinity measured by CTD sensors

(3) Instruments and Method

The salinity analysis was carried out on R/V MIRAI during the cruise of MR02-K06 leg1 using the Guildline Autosal salinometer model 8400B (S/N 62556), with additional peristaltic-type intake pump, manufactured by Ocean Scientific International.

The salinometer was operated in the constant temperature laboratory 'AUTOSAL ROOM' in the ship. The room was air-conditioned: a bath temperature was 24 degree C, while the ambient temperature varied from approximately 21 to 23 degree C.

(3-1) Standardization

Autosal model 8400B was standardized at the beginning of the sequence of measurements using IAPSO standard seawater (batch P142, Conductivity ratio; 0.99991, salinity; 34.997). Because of the good stability of the Autosal, calibration of the Autosal was performed only once: The value of the Standardize Dial was adjusted at the time. Instead of the calibration in middle and after the measurement, standard seawater were measured after the measurement of approximately 30 samples for the drift check. 28 ampoules of standard seawater were measured in total, and their standard deviation to the catalogue value was 0.0116 psu. (One ampoule was discarded because its measured value is too high to be used). The value is used for the calibration of the measured salinity.

We also used sub-standard seawater which obtained from 2000-m depth and filtered by Millipore filter (pore size of 0.45 μm), which was stored in a 20 liter polyethylene container. It was measured every 30 samples in order to check the drift of the Autosal.

The measurement was repeated (5 times in maximum), until the latest output value differ less than ±0.00002 to the output at immediately before. The value is determined from the average of the last two output values.

The CTD data of primary salinity and secondary salinity were used to compare the CTD salinity and the measurement data

(3-2) Samples

Seawater samples were collected with 12 liter Niskin-X (Non-coating for Teflon) bottle. The salinity sample bottle of the 250 ml brown grass bottle with screw cap was used to collect the sample water. Each bottle was rinsed three times with the sample water, and was filled with sample water to the bottle shoulder. Its cap was also thoroughly rinsed. The bottle was stored more than 24 hours in 'Autosal Room' before the salinity measurement.

A double conductivity ratio was defined as median of 31 times reading of the salinometer. Data collection started 5 seconds and it took about 10 seconds to collect 31 times reading by a personal computer.

Table 6.9.2.1: Kind and number of samples

Kind of Samples	#
Samples for CTD	99
Samples for EPCS	23
Total	122

(5) Result

The preliminary results are shown in Table 6.9.2-3.

The average of difference between Measurement data and CTD data were 0.0017 (PSU) and the Standard deviation was 0.0197. The average of difference between measurement data and CTD data with each deeper 1,000m were -0.0023 (PSU) and the Standard deviation was 0.0019.

Table 6.9.2-2:Result of measurement for CTD Samples

		Primary sensor	Secondary sensor
Total Sample for CTD	Average	0.0017	0.0043
	Std.dev.	0.0197	0.0192
>1000db (except Bad sample)	Average	-0.0023	0.0006
	Std.dev.	0.0019	0.0015

The replicate was also measured in order to check correlation of CTD-measured profile and the sampled seawater. The replicates were made by filling two glass bottles by sampled water from same Niskin-X bottle (#1). The differences between CTD-measured salinity and Autosal-measured salinity from replicate were calculated for each replicates. The difference from each replicate was compared, by substituting difference on Replicate-2 from difference on Replicate-1. The results are shown in Table 6.9.2-3, by the form of standard deviation and average, for all replicates and replicates made from the water sampled 1000 db depth or deeper.

Table 6.9.2-3: Result of difference of replicate of measurement for CTD samples

Total(28Pairs)	Avarage	-0.00003
	Std.dev	0.00073
>1000db (26pairs, except bad sample)	Avarage	-0.00003
	Std.dev	0.00074

(6) Data archive

The data of sample measured and worksheets of calculation of salinity concentration were stored in files. The data of sample will be submitted to JAMSTEC Data Management Office (DMO).

6.9.3 Dissolved Oxygen measurement of Sampled Water

(1) Personel

Katsunori Sagishima (Marine Works Japan Ltd.)
Masaki Moro (Marine Works Japan Ltd.)

(2) Introduction

Dissolved oxygen is major parameter for deciding the seawater characteristic on oceanography. In this cruise, the method of dissolved oxygen determination is based on WHP Operations and Methods manual (Culberson, 1991, Dickson, 1996).

(3) Methods

(a) Instruments and Apparatus

Glass bottle: Glass bottle for D.O. measurements consist of the ordinary BOD flask(ca.180 ml) and glass stopper with long nipple, modified from the nipple presented in Green and Carritt (1966).

Dispenser: Eppendorf Comforpette 4800 / 1000µl
OPTIFIX / 2 ml (for $MnCl_2$ & NaOH / NaI aq.)
Kyoto Electronics APB-510 / 20B (for KIO_3)

Titrator: Metrohm Model 716 DMS Titrino / 10 ml of titration vessel
Metrohm Pt Electrode / 6.0403.100 (NC)

Software: Data acquisition and endpoint evaluation / "The Brinkmann Titrino Workcell"

(b) Methods

Sampling and analytical methods were based on to the WHP Operations and Methods (Culberson, 1991, Dickson, 1996).

(b-1) Sampling

Seawater samples for dissolved oxygen measurement were collected from 12 litter Niskin bottles to calibrated dry glass bottles. During each sampling, 3 bottle volumes of seawater sample were overflowed to minimize contamination with atmospheric oxygen. The seawater temperature at the time of collection was measured for correction of the sample volume. After the sampling, $MnCl_2$ (aq.) 1ml and NaOH / NaI (aq.) 1ml were added into the glass bottle, and then shook the bottle well. After the precipitation has settled, we shook the bottle vigorously to disperse the precipitate.

(b-2) D.O. analysis

The samples were analyzed by Metrohm titrator with 10 ml piston burette and Pt Electrode using whole bottle titration. Titration was determined by the potentiometric methods and the endpoint for titration was evaluated by software of Metrohm, "The Brinkmann Titrino Workcell".

Concentration of D.O. was calculated by equation (10) and (13) of WHP Operations and Methods (Dickson, 1996). Salinity value of the equation (14) was used from the value of salinity of CTD. We prepared and used one batch of 5 liter of 0.03N thiosulfate solutions and 5 liter of 0.0100N standard KIO_3 solutions (JM020912).

(4) Preliminary Result

(4-1) Comparison of our KIO_3 standards to CSK standard solution.

On this cruise, we compared our standards with CSK standard solution (Lot. TCK8678) which is the commercially available standard solution prepared by Wako Pure Chemical Industries, Ltd. The results are shown in table 6.9.3.-1.

Table 6.9.3-1. Comparison of each standards

Titrator	KIO_3 Lot No.	Nominal Normality	Average Standard Titer (ml)	Deviation	n
	TCK8678	0.0100	3.279^0	0.0004	5
	JM020912	0.010012	3.288^0	0.0005	5

(4-2) Reproducibility

In this cruise, 153 samples for D.O. samples were collected. 29 pairs (23.3%) of total samples were analyzed as “duplicates” which were collected from same Niskin bottle. Average and precision (1 std. dev.) of difference of oxygen concentration obtained for duplicate samples analyses were 0.12 (μmol/kg) and 0.10 (?). Results of each casts show Fig.6.9.3-1 (1) – (3)

(5) Data Archive

The obtained data will be submitted to and will be archived at JAMSTEC Data Management Office.

(6) References

Culberson, C.H.(1991) Dissolved Oxygen, in WHP Operations and Methods, Woods Hole., ppl-15

Culberson, C.H., G.Knapp, R.T.Williams and F.Zemlyak(1991) A comparison of methods for the determination of dissolved oxygen in seawater. (WHPO 91-2)

Dickson, A.G. (1996) Determination of dissolved oxygen in sea water by Winkler titration, in WHP Operations and Methods, Woods Hole., ppl-14.

Green, E.J. and D.E.Carritt (1996) An Improved Iodine Determination Flask for Whole-bottle Titrations, Analyst, 91, 207-208.

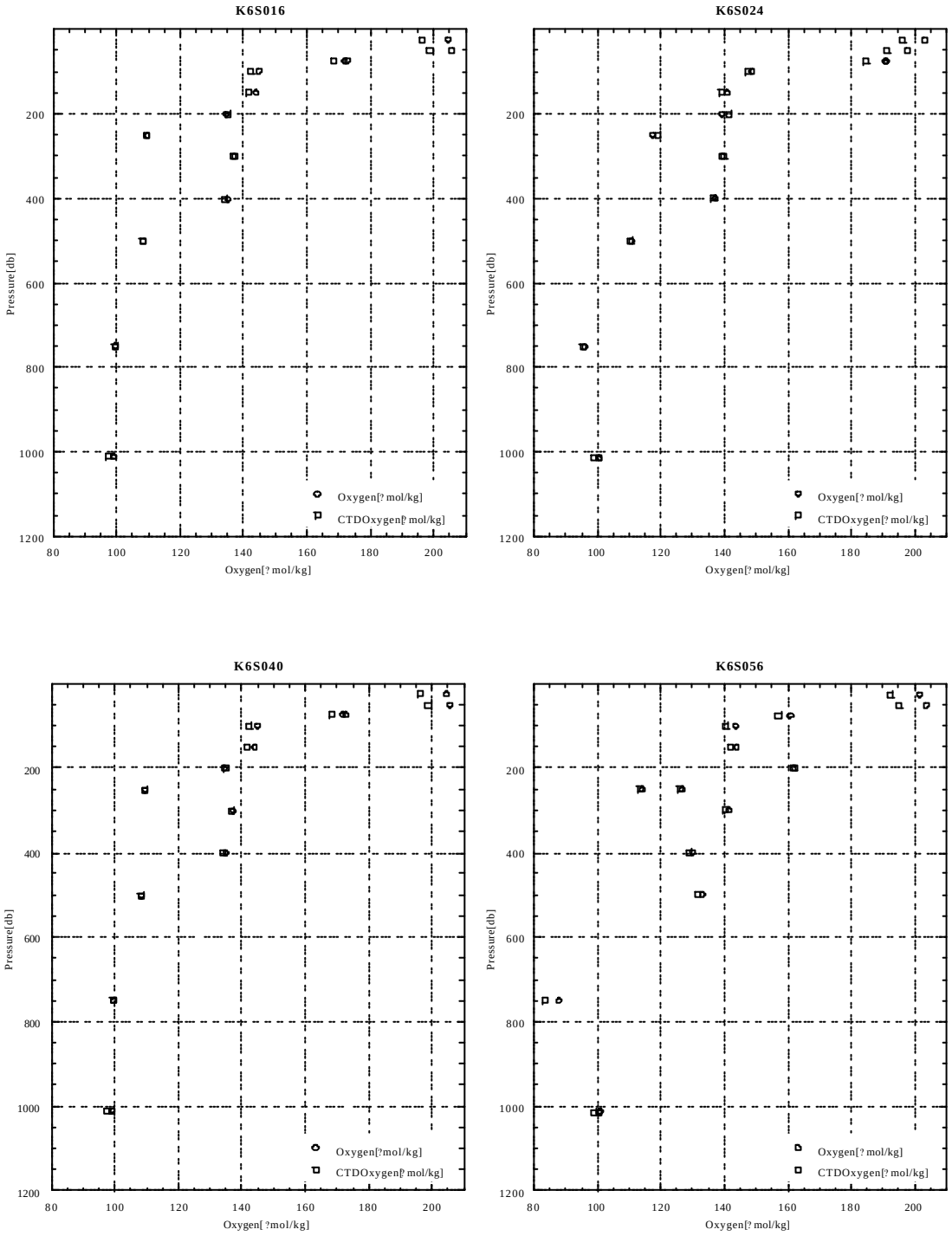

Fig.6.9.3-2(1) : Vertical profiles at each cast.

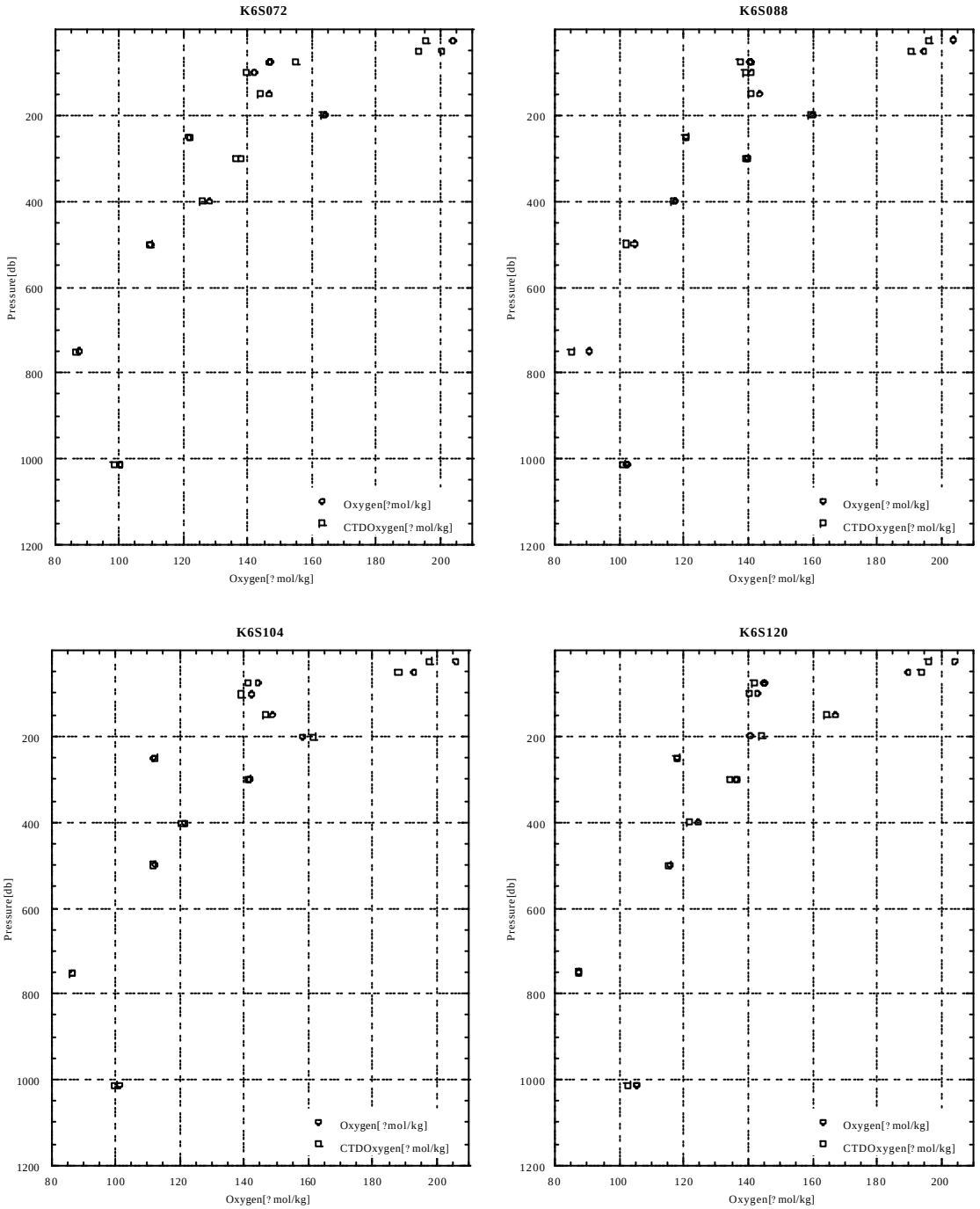

Fig.6.9.3-2(2) : Vertical profiles at each cast.

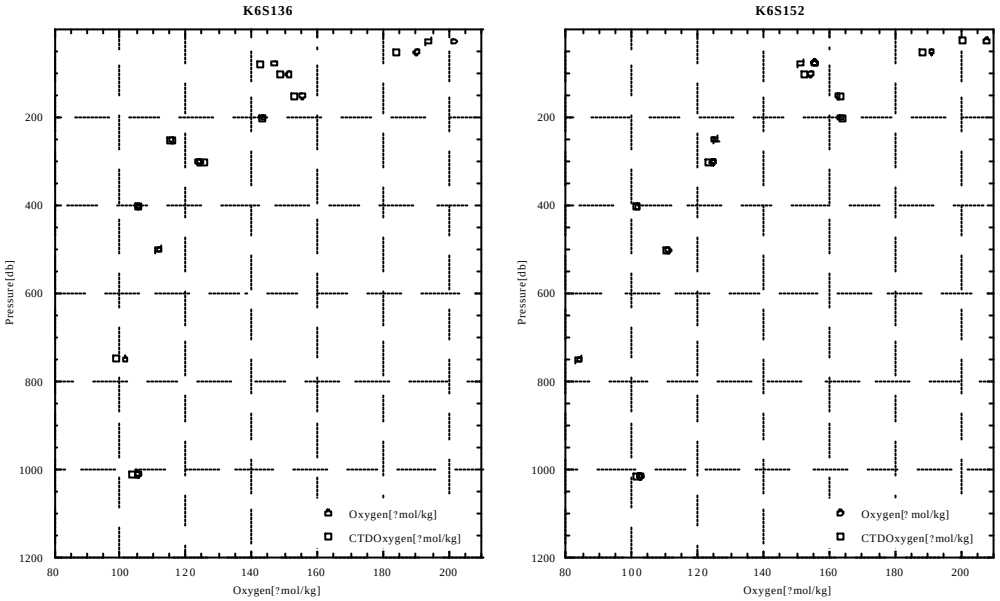

Fig. 6.9.3-2(3): Vertical profiles at each cast.

6.9.4 Shallow Water CTD and Chlorophyll

(1) Personnel

Mitsuru HAYASHI (Maritime University of Kobe): Principal Investigator
Masatsugu Tanaka (Osaka University)
Daisuke TANIGUCHI (Okayama University)
Kyoko HARADA (Okayama University)
Takuhei SHIOZAKI (Osaka Prefecture University)
Masakazu NAKAGAWA (Maritime University of Kobe)

(2) Objective

We curried out the shallow water observation to understand the biological structure in the euphotic layer.

(3) Methods

The vertical profiles of temperature, conductivity, fluorescence, light intensity, dissolved oxygen and turbidity were observed from 22 Nov. 09 LMT to 13 Dec. 00 LMT every 3 hours after the CTD observation by the shallow water measurement unit (Chlorothec ACL-220-RS, Alec Electronics Co. Ltd.) from surface to 200 m in depth every 0.2 sec. Accuracy of the sensors is as follows;

Depth : ±0.2 m	Temperature :±0.05 ℃
Conductivity : ±0.05 mS/cm	Fluorescence : ±0.1%FS
Light intensity : ±0.4%	Dissolved oxygen : ±0.2mg/l
Turbidity : ±0.2%.	

Fluorescence data are recorded as the raw data (N value: 0 to 65520), and we will calibrate the fluorescence data using the pigment analysis data by MWJ.

(4) Preliminary Results

Fig. 6.9.4-1 shows the depth-time cross sections of (a) temperature, (b) salinity, (c) fluorescence, (d) light intensity and (e) density at 2N, 138.5E. The depth of the mixing layer is 60 m to 80 m in depth, and the fluorescence maximum layer exists above thermocline.

The vertical profiles of all casts are shown in appendix. All observational data will be analyzed in detail later.

(5) Data Archive

The data are will have a quality check in Maritime University of Kobe and Osaka Prefecture University, and will be distributed to public later. The raw data is submitted to JAMSTEC DMO.

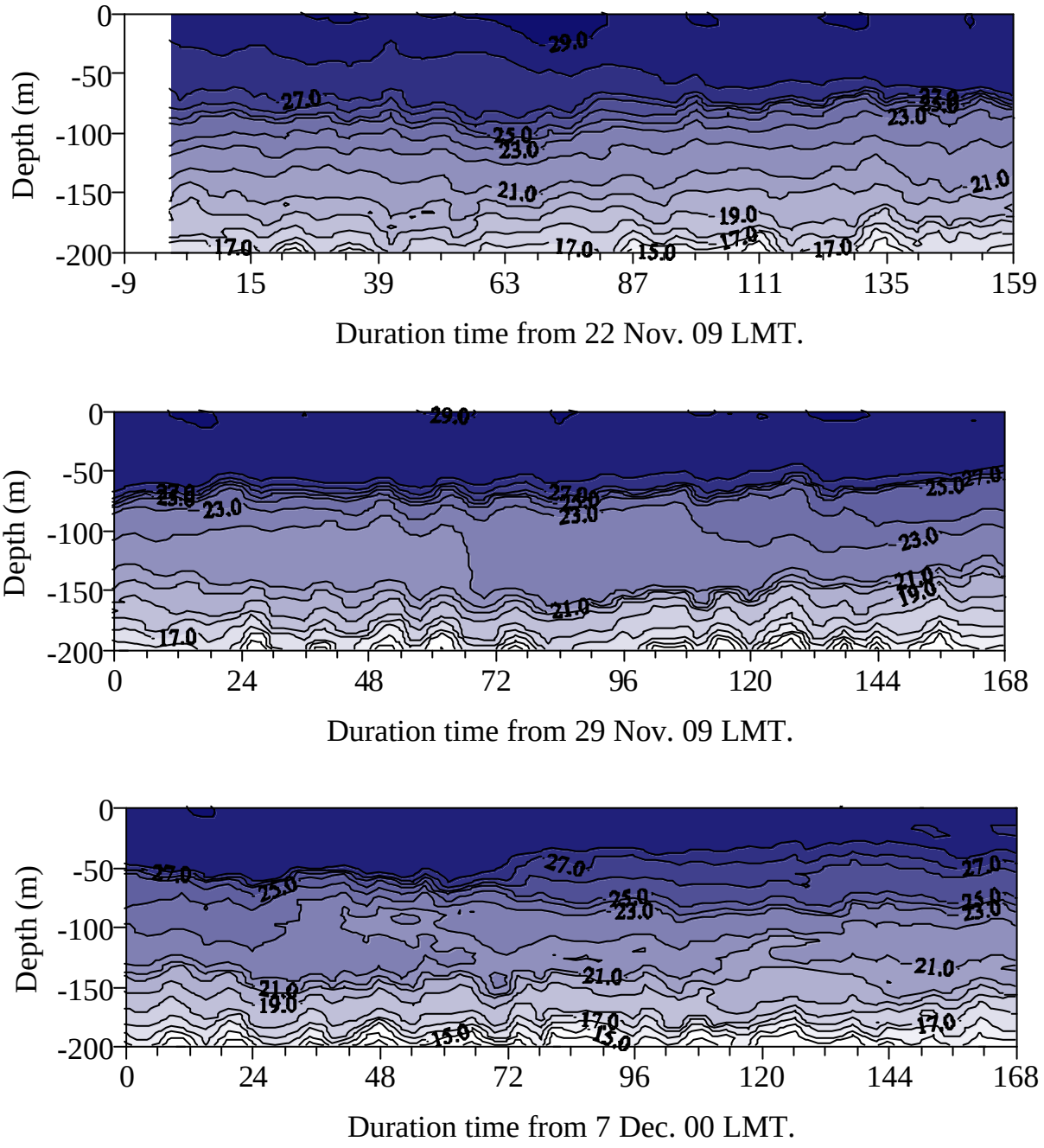

Fig.6.9.4-1(a): Vertical distribution of temperature (deg-C) from 22 Nov. 09 LMT to 13 Dec. 00 LMT.

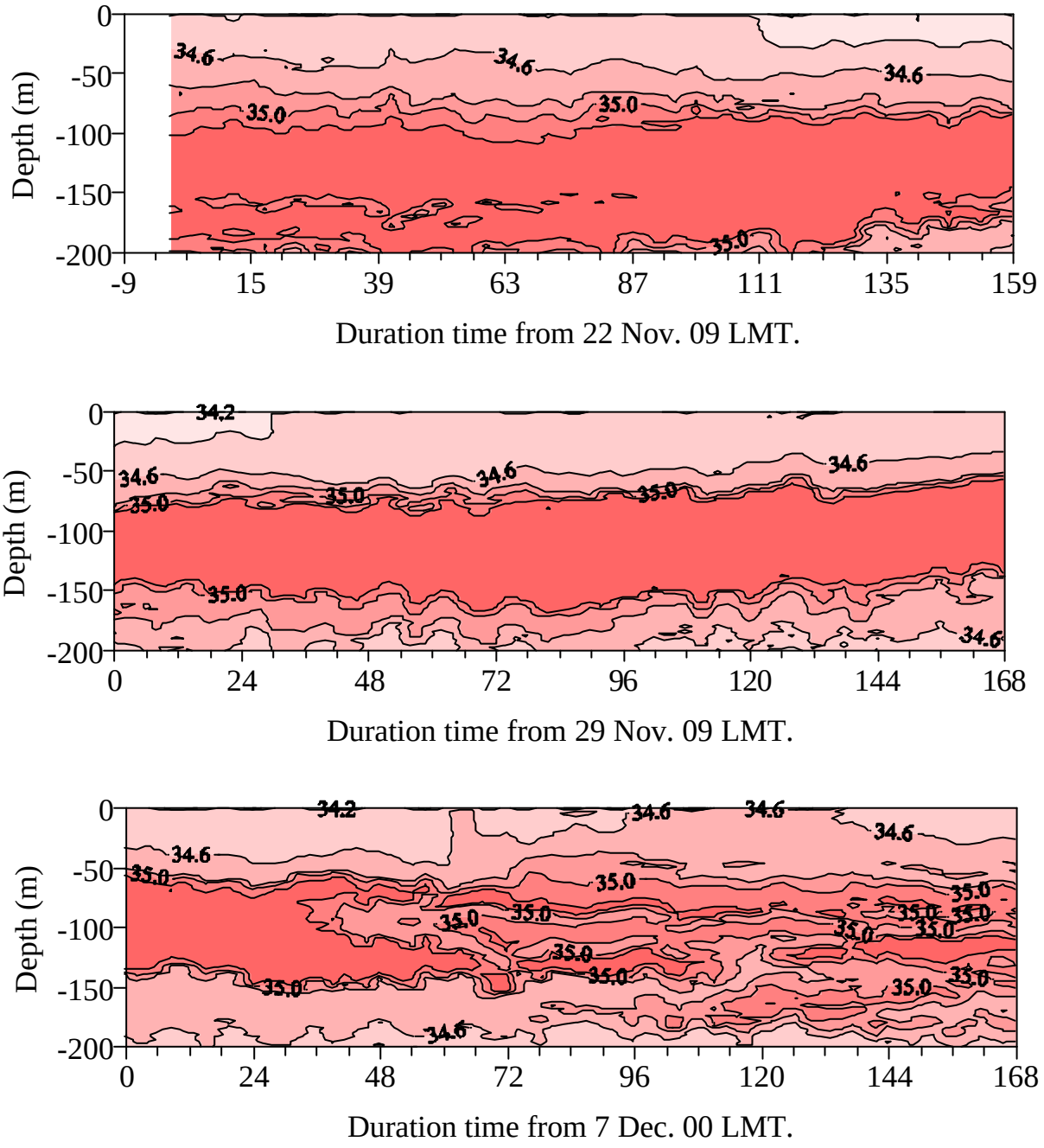

Fig.6.9.4-1(b): Vertical distribution of salinity (psu) from 22 Nov. 09 LMT to 13 Dec. 00 LMT.

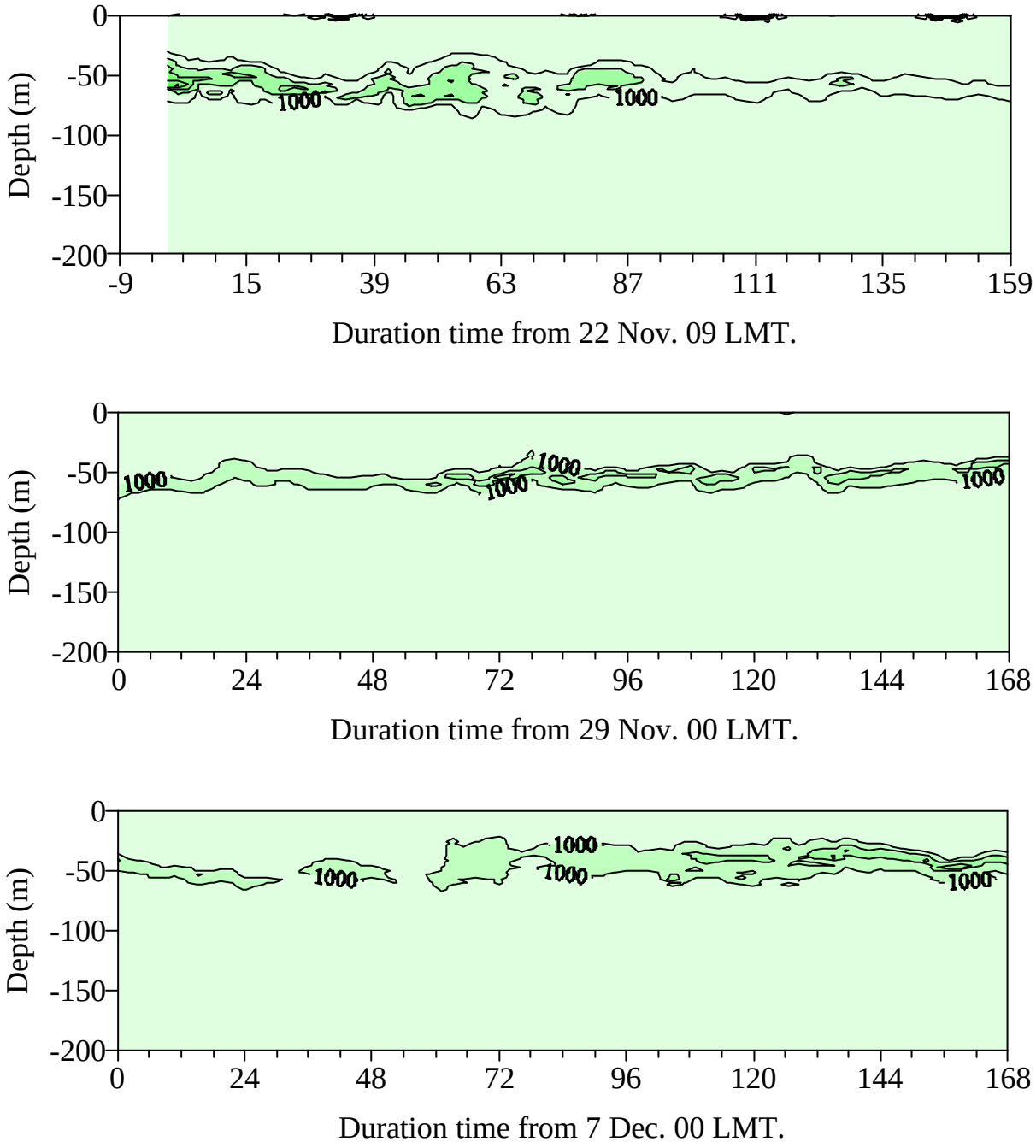

Fig.6.9.4-1(c): Vertical distribution of fluorescence(N value) from 22 Nov. 09 LMT to 13 Dec. 00 LMT.

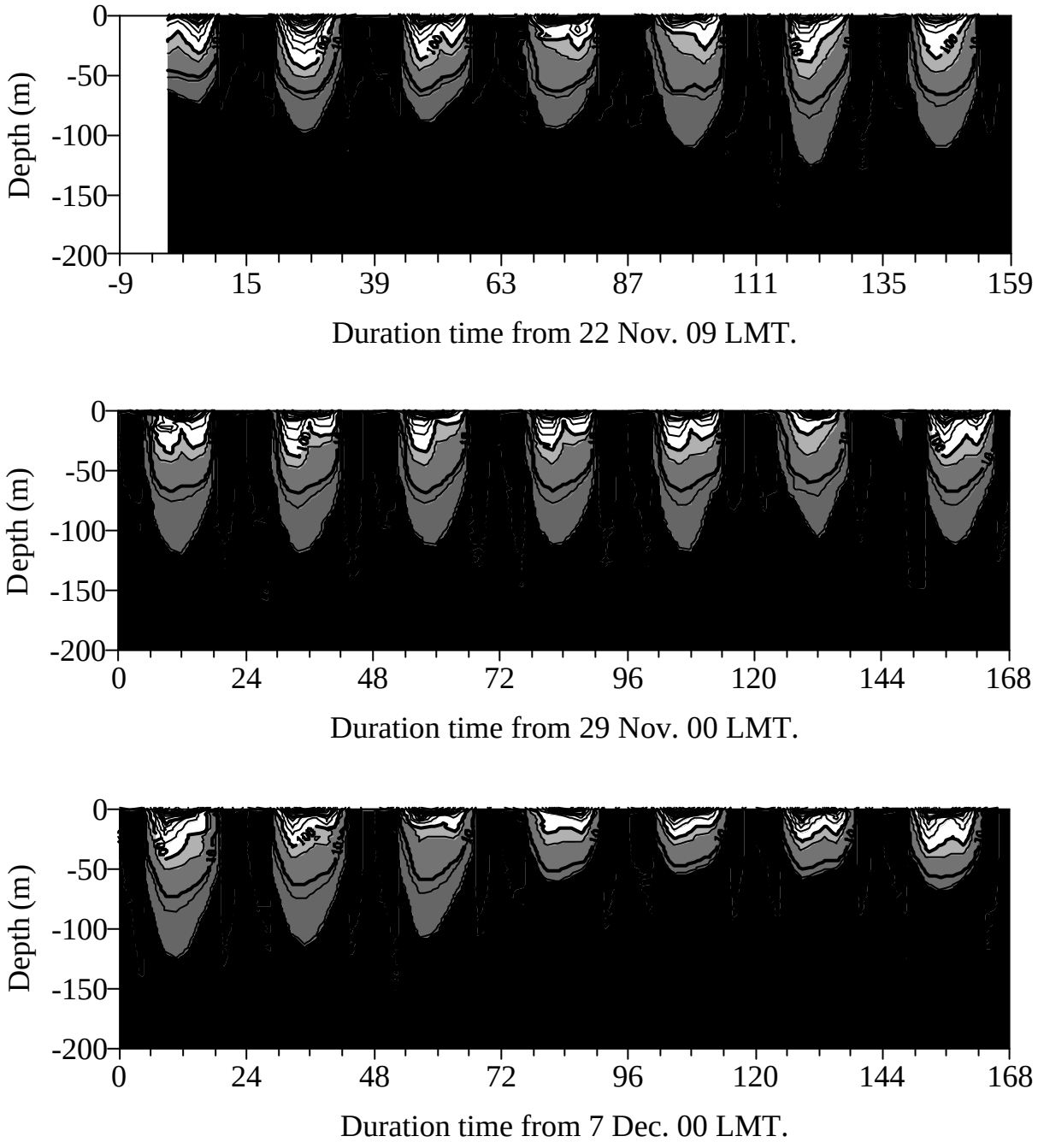

Fig.6.9.4-1(d): Vertical distribution of light intensity from 22 Nov. 09 LMT to 13 Dec. 00 LMT.

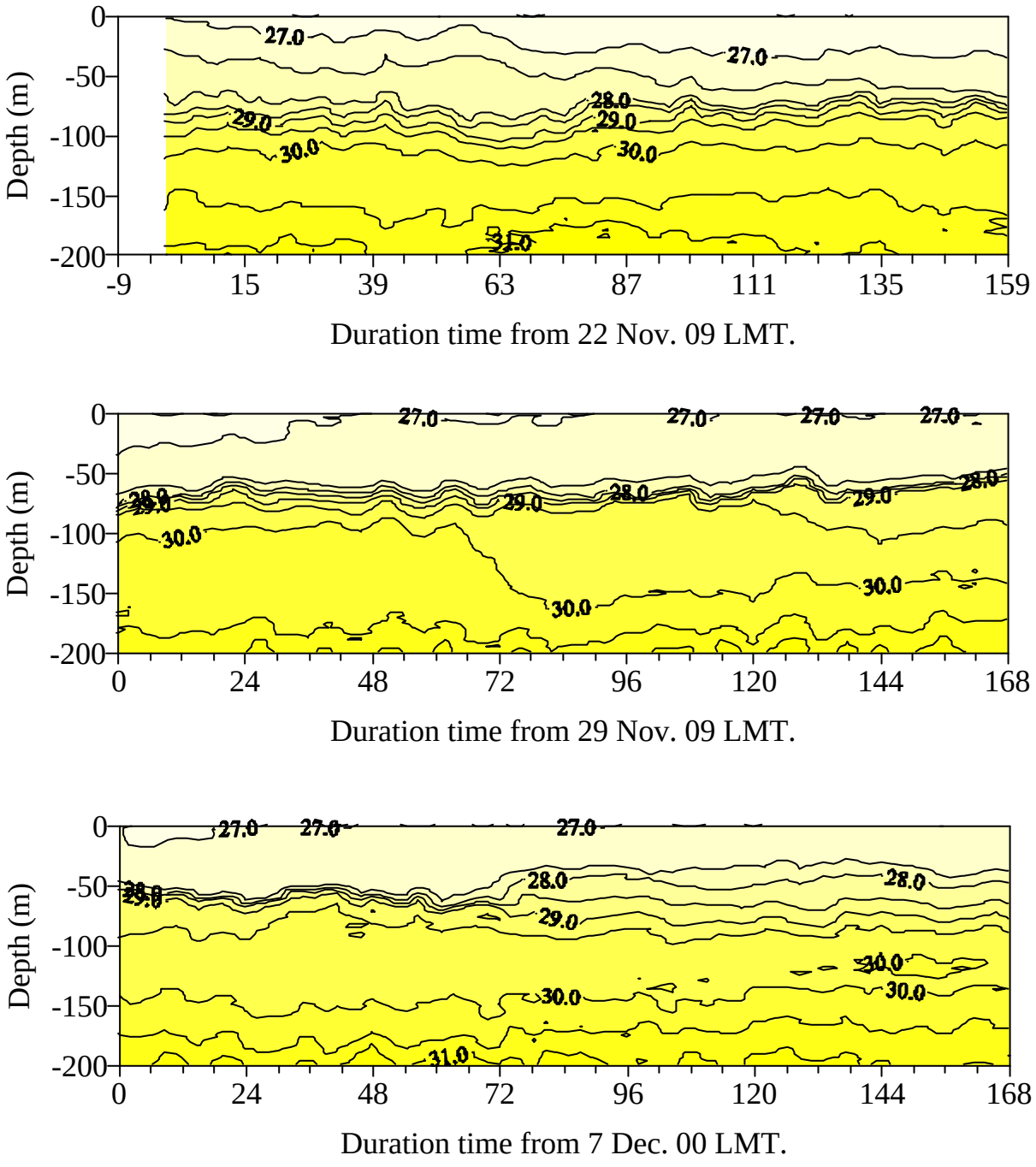

Fig.6.9.4-1(d): Vertical distribution of sigma-t from 22 Nov. 09 LMT to 13 Dec. 00 LMT.

6.9.5 Shipboard ADCP

(1) Personnel

Kunio Yoneyama	(JAMSTEC)
Masaki Hanyu	(GODI): Operation Leader
Souichiro Sueyoshi	(GODI)
Norio Nagahama	(GODI)

(2) Parameters

Current velocity of each depth cell [mm/s]

(3) Methods

Upper ocean current measurements were made throughout MR02-K06 Leg1 cruise (Departure from Sekinehama on 13 November 2002 to the arrival at Guam on 16 December) except for EEZ of the Republic of Palau and the Republic of Indonesia, using the hull-mounted Acoustic Doppler Current Profiler (ADCP) system that is permanently installed on the R/V Mirai. The system consists of following components;

1) a 75 kHz Broadband (coded-pulse) profiler with 4-beam Doppler sonar operating at 75 KHz (RD Instruments, USA), mounted with beams pointing 30 degrees from the vertical and 45 degrees azimuth from the keel;
2) the Ship's main gyro compass (Tokimec , Japan), continuously providing ship's heading measurements to the ADCP;
3) a GPS navigation receiver (Leica MX9400) providing position fixes;
4) an IBM-compatible personal computer running data acquisition software (VmDas version 1.3 ; RD Instruments, USA). The clock of the logging PC are adjusted to GPS time every 5 minutes.

The ADCP was configured for 16-m pulse length, 16-m processing bin, and a 8-m blanking interval. The sound speed is calculated from temperature (thermistor near the transducer faces), salinity (constant value; 35.0 psu) and depth (6.5 m; transducer depth) by equation in Medwin (1975). The transducer depth was 6.5 m; 40 velocity measurements were made at 16-m intervals starting 31m below the surface. Each 1 ping was recorded as raw ensemble data. Also, 60 seconds and 300 seconds average data were recorded as short term average (STA) and long term average (LTA) data.

(4) Preliminary result

Fig.6.9.5-1 shows time series of water current profile during the stationary observation.

(5) Data archive

These data obtained in this cruise will be submitted to the JAMSTEC DMD (Data Management Division), and will be opened to the public via "R/V Mirai Data Web Page" in JAMSTEC home page.

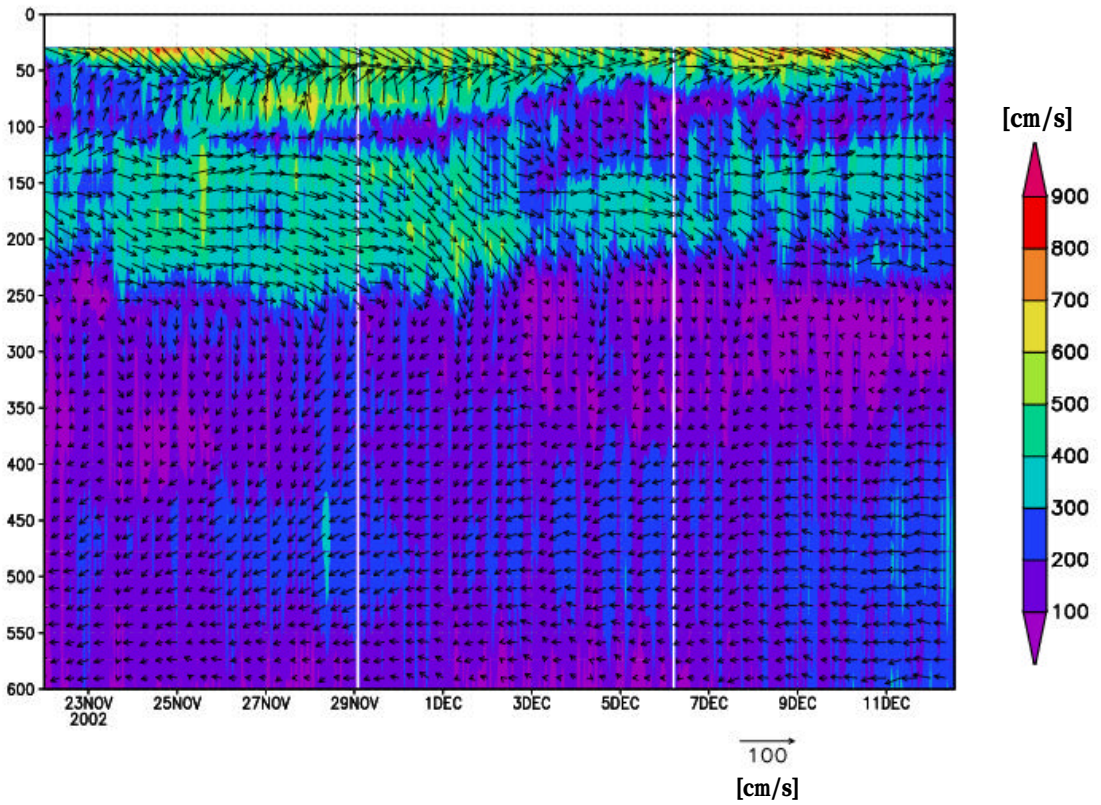

Fig.6.9.5-1: Time-depth cross section of the horizontal current. The vector represents the horizontal current (northbound for up). The shading represents absolute current speed.

6.9.6 Deployment of ARGO Float

(1) Personnel

Kensuke Takeuchi	(FORSGC): Principal Investigator (not on board)	
Nobuo Shikama	(FORSGC)	not on board
Eitarou Oka	(FORSGC)	not on board
Asako Inoue	(MWJ)	
Katsunori Sagishima	(MWJ)	
Naoko Takahashi	(MWJ)	

(2) Objectives

The objective of deployment is to clarify variations of temperature and salinity in association with interannual variations such as ENSO events to intraseasonal variations.

The profiling floats launched in this cruise measure vertical profiles of temperature and salinity automatically every ten days. The data from the floats will enable us to understand the variations mentioned above with time scales much smaller than those in the previous studies.

(3) Methods

1) Profiling float deployment

We launched 3 APEX floats manufactured by Webb Research Ltd. Each float equips SBE41 CTD sensor manufactured by Sea-Bird Electronics Inc.

These floats usually drift at a depth of 1500 dbar (called the parking depth), and rise up to the sea surface every ten days by increasing their volume and changing the buoyancy. During the ascent, they measure temperature, salinity, and pressure. They stay at the sea surface for approximately nine hours, transmitting their positions and the CTD data to the land via the ARGOS system, and then return to the parking depth by decreasing volume. The status of floats and their launches are shown in Table 6.9.6-1.

2) CTD observation

A CTD cast to a depth of 2000 m was made just before the launch of each float for calibration of the float sensor (see Section 6.9.1).

(6) Data archive

All data acquired through the ARGOS system is stored at FORSGC. The real-time data are provided to meteorological organizations via Global Telecommunication System (GTS) and utilized for analysis and forecasts of sea conditions.

Table 6.9.6-1 Status of floats and their launches

Float

Float Type	APEX floats manufactured by Webb Research Ltd.
CTD sensor	SBE41 manufactured by Sea-Bird Electronics Inc.
Cycle	10 days (approximately 9 hours at the sea surface)
ARGOS transmit interval	30 sec
Target Parking Pressure	1500 dbar
Sampling layers	66 (1500, 1400, 1300, 1250, 1200, 1150, 1100, 1050, 1000, 975, 950, 925, 900, 875, 850, 825, 800, 780, 760, 740, 720, 700, 680, 660, 640, 620, 600, 580, 560, 540, 520, 500, 480, 460, 440, 420, 400, 380, 360, 340, 320, 300, 280, 260, 240, 220, 200, 190, 180, 170, 160, 150, 140, 130, 120, 110, 100, 90, 80, 70, 60, 50, 40, 30, 20, 10 [dbar])

Launches

Float S/N	ARGOS PTT ID	Date and Time of Reset (UTC)	Date and Time of Launch (UTC)	Location of Launch
723	16353	00:15, Nov 22	01:14, Nov 22	1-58.55 N, 138-31.26 E
724	16354	01:20, Dec 13	04:42, Dec 13	5-00.41 N, 139-24.87 E
725	16355	14:18, Dec 13	16:26, Dec 13	7-00.85 N, 139-59.54 E

6.10 Underway Geophysics

(1) Personnel

Toshiya Fujiwara	(JAMSTEC) (not on board)
Masaki Hanyu	(GODI): Operation Leader
Souichiro Sueyoshi	(GODI)
Norio Nagahama	(GODI)

(2) Objective

The spatial and temporal variation of parameters at / below the sea bottom are basic data for the many fields of geophysics. During this cruise, we observed gravity, magnetic force and sea bottom depth.

(3) Methods

We measured relative gravity value by S116 onboard gravity meter (LaCoste-Romberg, USA), magnetic force by SFG-1214 three axes fluxgate magnetometer (Tierra technica, Japan) on the top of foremast at 8 Hz sampling ratio and sea bottom depth by SeaBeam2112.004 (SeaBeam, Inc., USA) 12kHz multi-narrow beam echo sounding system.

To obtain absolute gravity value, we usually measure relative value by portable gravity meter (Scintrex gravity meter CG-3M) at comparable points. Three component magnetic force was sampled at 1 sec controlled by the 1 pps standard clock of GPS signal. Navigation information, 8 Hz three component magnetic force and vertical reference unit data were recorded at every 1 sec. At SeaBeam system, to get accurate sounding velocity of water column for ray-path correction of acoustic multibeam, we used temperature and salinity profiles from CTD data calculated sound velocity by equation in Mackenzei (1981).

All of these observations were carried out from the departure of Sekinehama 13 November 2002 to the arrival of Guam 16 December 2002, excluding EEZ of the Republic of Palau and Indonesia.

(4) Preliminary results

The results will be public after the analyses in future.

(5) Data archives

The dataset obtained during this cruise will be submitted to the DMO (Data Management Office), JAMSTEC and will be archived there.

6.11 Ship Maneuvering

(1) Personnel

Captain Masaharu Akamine, Master of R/V"MIRAI"
And Ship's Crew

(2) Objectives

To investigate the principle factors for maneuvering the ship

(3) Methods

The following parameter is monitored and recorded:

- Ship's position, course, speed,
- Direction of wind/current, Velocity of wind/current,
- Vector of wind and current, resultant force,
- Use of side thrusters.

(3.1) Measurement of the actual ship-movement

Measurement of the ship-movement is executed with a radio navigation device assembled by Sena Co. Ltd., Japan.

(3.2) Measurement of the wind and the current

The wind direction and speed is measured by KOAC-7800 weather data processor and sensors assembled by Koshin Denki.

The current direction and speed are continuously measured by a Doppler sonar "DS-30" installed at the bottom of the ship.

The vector resultant force is calculated by the wind and the current data in real-time according to the following vector diagram. The wind is transformed into the vector of the drift using an approximate formula given by some hydrodynamic tests.

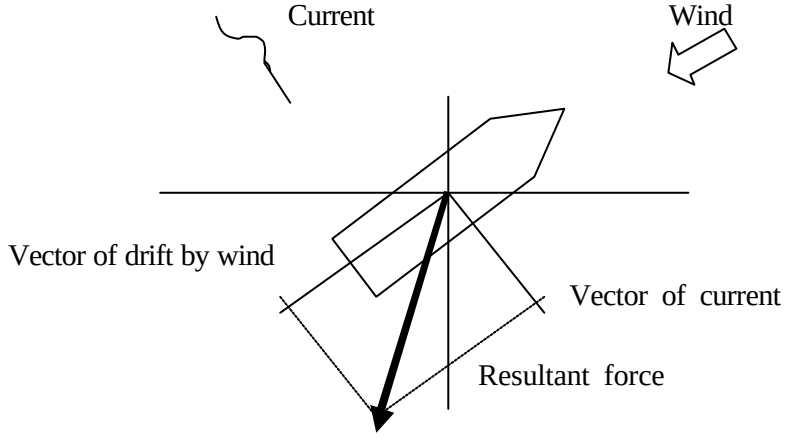

(3.3) Measurement of the side thruster-use

The measurement was executed with the record device of the joystick control system assembled by the Mitsubishi heavy industries Ltd.

(3.4) Conditions

From the standpoint of the ship's maneuvering, the necessary condition for each observation is as follows.

1) A fixed point observation

To keep the ship's position from a TRITON buoy (2-00N, 138-00E) at 30 miles or more except the flux measurement operation.

2) Conditions of each observation are as follows.

A) Radiosonde Operation

(1)To keep the ship's head so as to get the wind from the port bow (more than 15 degrees).

(2)To adjust the ship's speed with the wind velocity of under 10 m/s by relative scale.

B) CTD/Sampling Seawater Operation and chlorophyll operation

(1) To stop the ship at a fixed point.

(2) To manage the ship's movement so as to lead the CTD cable right below.

(3) Not to churn sea surface at CTD observation area with discharged currents from a right propeller and stern thruster.

(4) Not to make shade while observing chlorophyll and not to shine the sea surface with the search light at nighttime.

C) Flux measurement Operation

(1) To set the ship's course so as to face the wind.

(2) To maintain the ship's speed of 5-8 knots at the ship's through-the-water.

(3) To set up the ship's speed on the high side of ? in case of breeze condition.

(4) To receive the wind to the prow while the ship turns back to the starting point after the flux measurement ends.

(5) To keep an initial speed/course of the ship even if there is any change in the weather/ wind.

D) Skin Sea Surface Temperature Float (Snake sensor) Operation

(1) To keep the ship's speed of 3 knots and under. However in this time, the ship's speed is not limited especially since it gives priority to the flux measurement observation

(2) To avoid jumping up of the skin SST Float away from sea surface due to violent wave.

3)Typical pattern of ship's handling

A) Radiosonde Operation (The time required: about 10 minutes)

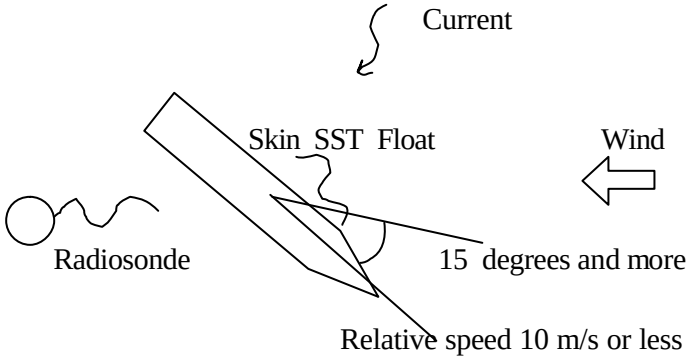

B) CTD/Sampling Seawater Operation (The time required: 30 – 60 minutes)

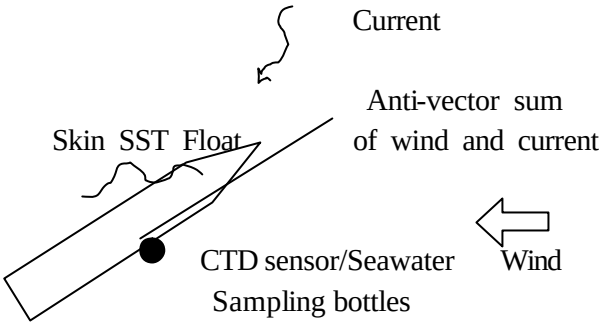

C) Chlorophyll Operation (The time required: about 15 minutes)

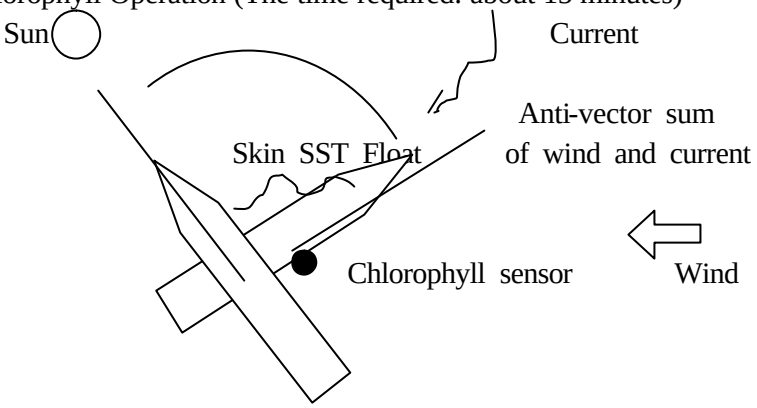

D) Flux Measurement Operation (The time required: 60- 85 minutes)

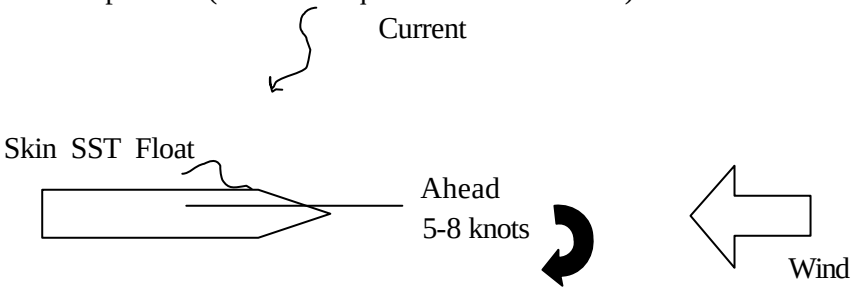

Return to the origin point after the flux measurement operation finished.
(It is necessary to receive the wind to the prow)
(The time required: 35 to 40 minutes)

3) A model time schedule every three hours
08:20 Arrive at the origin point
08:29 Launch the radiosonde
08:00 Commence the CTD/sampling seawater operation
09:00 Finish the CTD/sampling seawater operation and resume the chlorophyll operation
09:15 Finish the chlorophyll operation and start the flux measurement operation
10:45 End the flux measurement operation and return to the origin point
11:20 Arrive at the origin point

(4) Results

(4.1) Ship's tracking chart

The result is shown in Fig.8-1. All tracks of the ship in the observation of 20 days are plotted on the chart. It is understood that a lot of course are taken North-Westerly by seeing this chart. It makes a special mention that this is corresponding in an anti-direction of the following external force influences.

(4.2) Ship's through-the-water course and speed

The ship's speed between 5 knots and 8 knots and the fixed course are required while the flux measurement operation is being done. The condition of the speed/course is understood from this data.

The data of December 1st is shown in Fig.8-2 as one example of this data.

The results show that the average speed was 5 knots the unchanged course was kept during the flux measurement operation. This condition is the same through all observation period.

(4.3) Relative wind direction and speed

The direction and the velocity of the wind received to the prow were investigated through all observations. The wind received to the right of the prow is +(plus), the wind received to the left of the prow is - (Minus), and the unit is degrees. The velocity of the wind is shown at the knot.

The result on December 1st is illustrated in Fig.8-3.

According to the result, the wind was almost received from the prow to range of plus or minus 30 degrees in case of the flux measurement operation. In case of others, the wind was received from the prow to range of plus or minus 90 degrees except the turn of the ship.

This is to be able to say through the observation all periods.

(4.4) Vector of wind and current, resultant force,

The wind, the current, and the wave and the swell are thought as the external force, and the wind and the current which can be quantitatively understood are investigated here.

The data is indispensable to control the ship safely and efficiently while the CTD/sampling seawater/chlorophyll operation are being done.

The data is also useful for catching the tendency to the drift of the ship when the course for the flux measurement operation is decided.

The investigation result of December 1st is shown in Fig.6.11-4 for an example.

The result shows that the external force works constantly in the direction of ESE and this tendency is seen through all the observation periods.

As described in the above-mentioned, the external force influence by the wind includes the forecasting factors. It has been understood that there is no big difference in the forecast and the realities depending on this data.

The ship proceeds while being drifted in the direction of the vector resultant force of the wind and the current after setting the ship's course for the flux measurement operation.

The ship's course (Gyro course) and speed (log speed) that were set are compared about the direction (OG course) where the ship drifted and the drifting amount (OG speed), both indicate the numerical value of approximation.

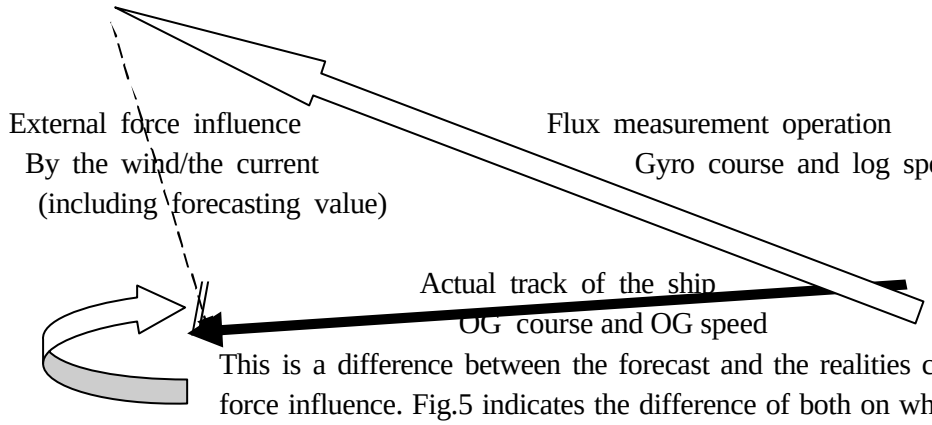

This is a difference between the forecast and the realities concerning the external force influence. Fig.5 indicates the difference of both on which the data December 1st is based.

(4.5) Use state of side thrusters

To move the influence which the side thrusters gave to the flux measurement, the use state of the side thrusters was investigated. The ship is equipped with 2 units of the bow thruster (power: 11.5 tons) and 1 unit of the stern thruster (power: 11.5 tons).

The power output (tons), use time, and on-off condition of the switch of each thruster were investigated in real time.

Fig.6 shows the investigation result on December 1st.

It is understood that the side thrusters were not used while all flux measurement operation was being done. This can be said through all the observation periods.

(5) Data archive

All data will be archived on board. Following raw data is recorded as a constant format and will be submitted to the DMO of JAMSTEC.

Date	JST	Thru the water		Over the ground		Relative wind		External Force	
		Course	Speed	Course	Speed	Direction	Velocity	Direction	speed
		degree	knot	degree	knot	degree	knot	degree	knot
2002/11/22	8:00:00	236	2.5	198	2.7	3	10.7	105	1.5
2002/11/22	8:01:00	238	2.2	193	2.3	0	10.7	103	1.5
2002/11/22	8:02:00	259	1.4	180	1.7	-17	9.9	102	1.5

JST	Power outlet (ton) of Thrusters			ON-OFF of switch of Thrusters		
	Minus: Port Plus: Starboard			1:ON 0:OFF		
	Bow 1	Bow 2	Stern	Bow 1	Bow 2	Stern
8:06:00	0	0	0	1	1	1
8:07:00	0.028386	-0.03863	0.008251	1	1	1
8:08:00	0.028386	0	0.008251	1	1	1

(6) Remarks

This time, there were a lot of ships which encountered it unlike the ordinary year. Therefore when the ship's course for the flux measurement operation was decided, it was necessary to include it in the matter that should be considered.

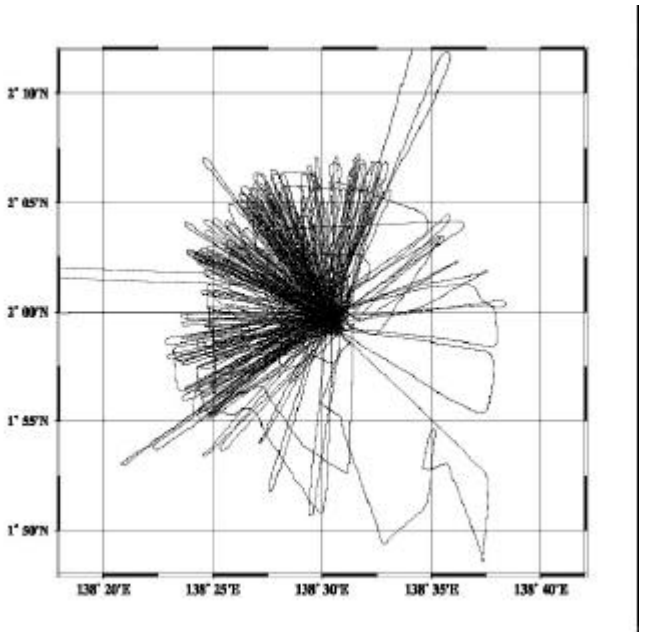

Fig.6.11-1: Ship's tracking chart.

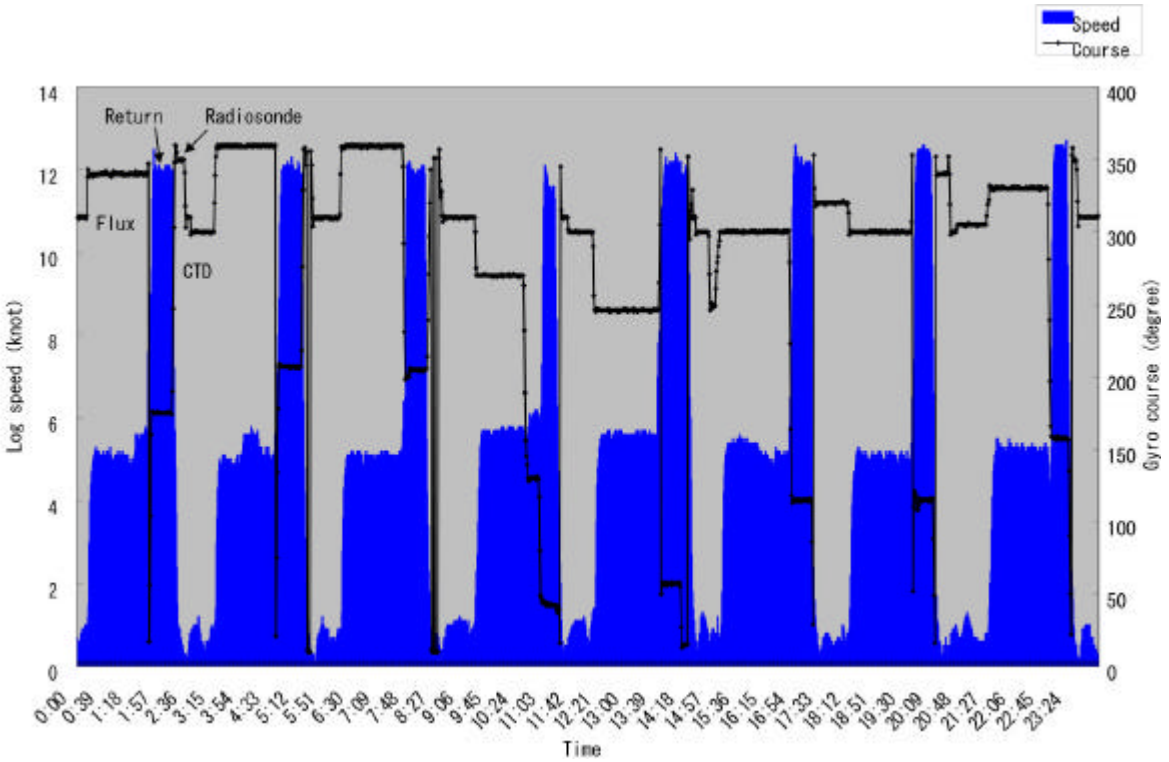

Fig.6.11-2: An example of the temporal variation of the ship's course and speed through the water in Dec.1, 2002.

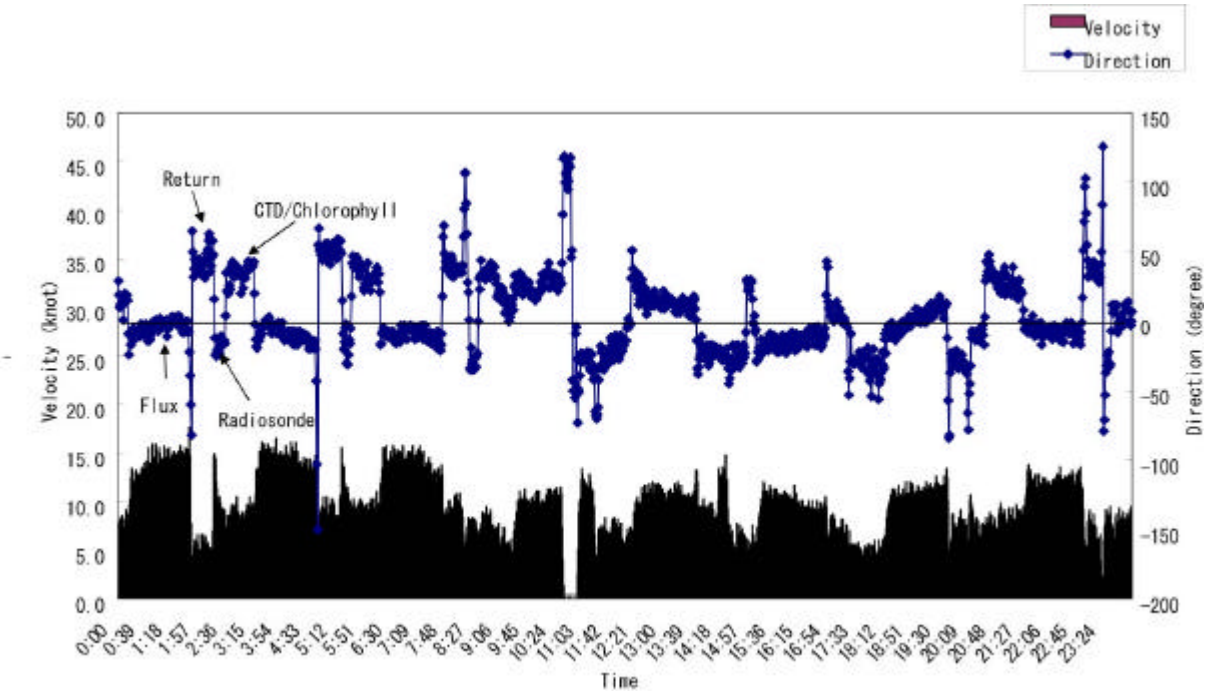

Fig.6.11-3: An example of the temporal variation of the wind relative to the ship in Dec.1, 2002.

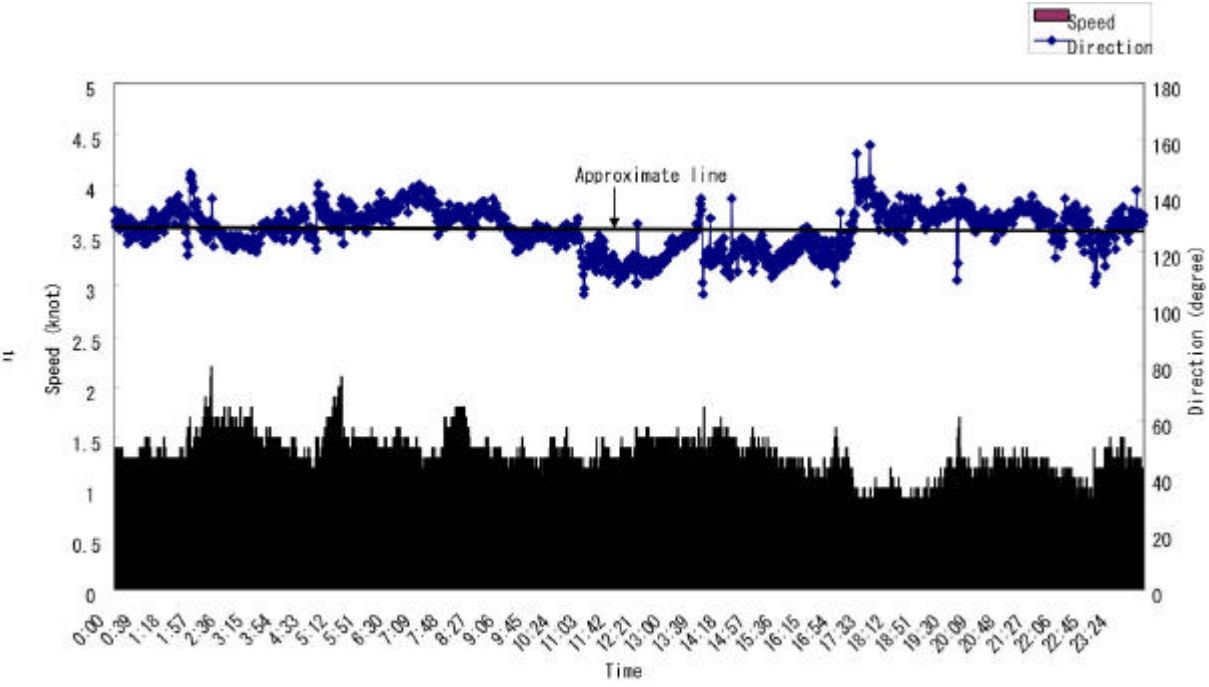

Fig.6.11-4: An example of the temporal variation of the external force by the wind and the current, in Dec.1, 2002.

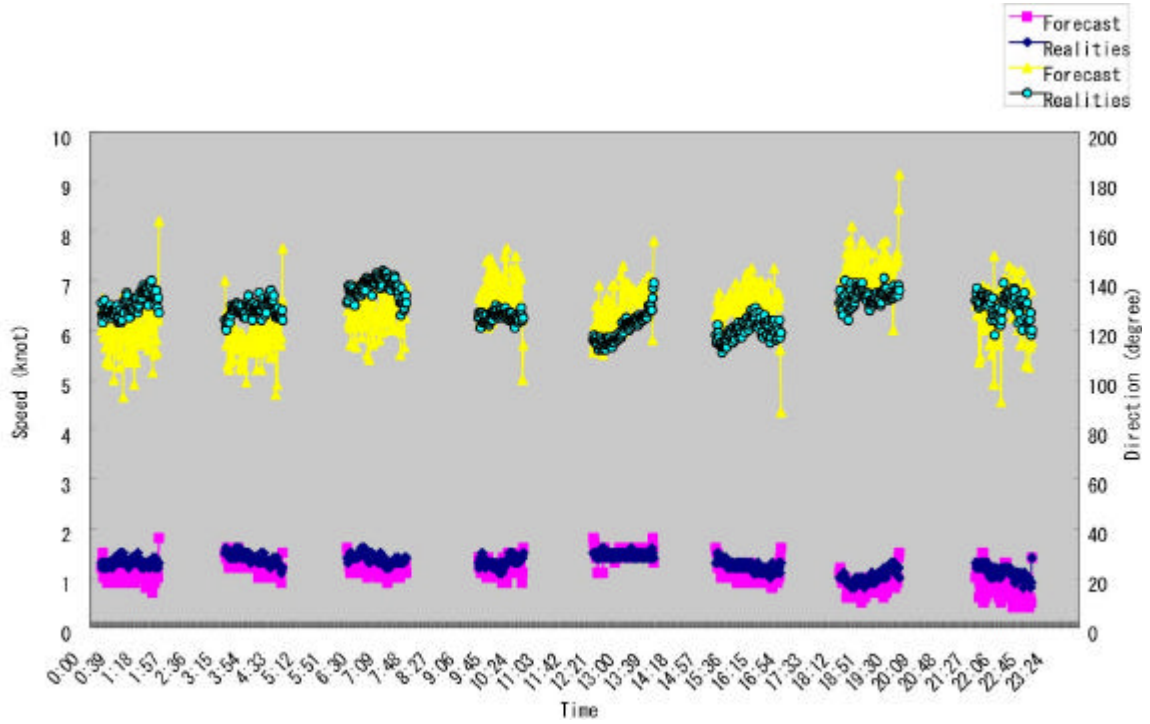

Fig.6.11-5: An example of the temporal variation of the difference between real and forecasted influence of the external force, in Dec.1, 2002.

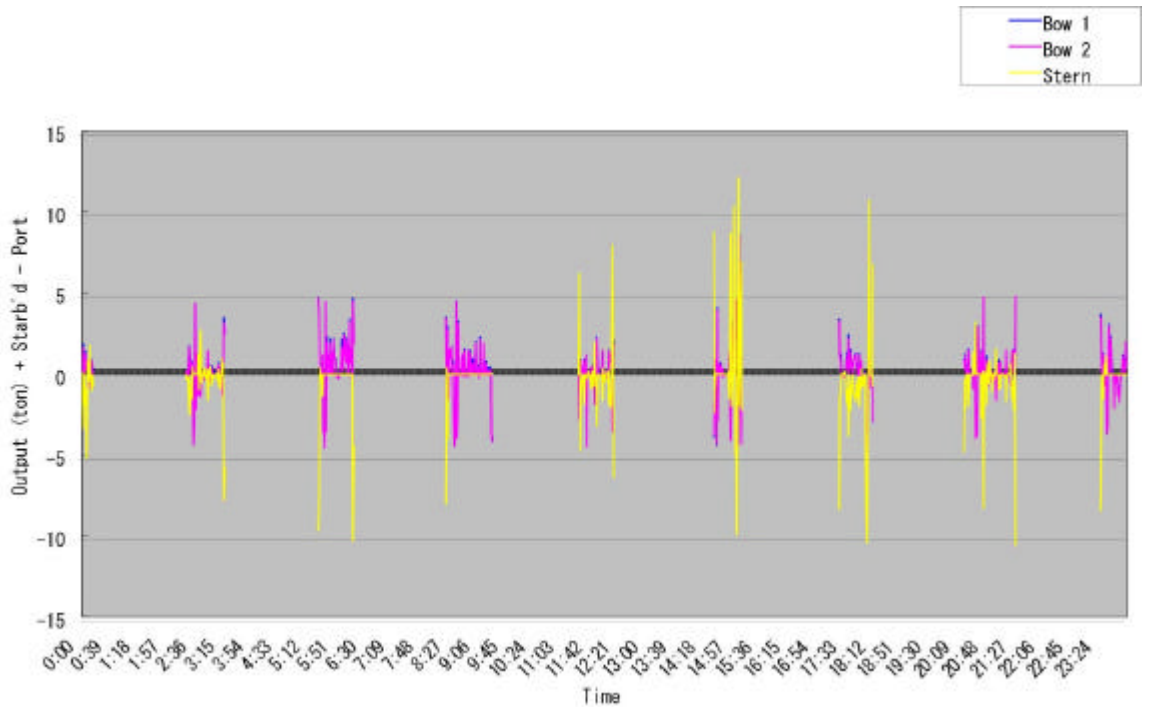

Fig.6.11-6: An example of the temporal variation of the output for side thrusters, in Dec.1, 2002.